2011

Four Market Studies for the Beef and Electric Power Industries

Huan Zhao
Iowa State University

Four Market Studies for the Beef and Electric Power Industries

by

Huan Zhao

A dissertation submitted to the graduate faculty

in partial fulfillment of the requirements for the degree of

DOCTOR OF PHILOSOPHY

Major: Economics

Program of Study Committee:

David A. Hennessy, Co-major Professor

Leigh Tesfatsion, Co-major Professor

James Bushnell

Helle Bunzel

Dermot J. Hayes

Iowa State University

Ames, Iowa

2011

DEDICATION

I would like to dedicate this thesis to my wife and to my Mom without whose support I would not have been able to complete this work. I would also like to thank my friends and family for their loving guidance and financial assistance during the writing of this work.

TABLE OF CONTENTS

LIST OF TABLES

LIST OF FIGURES

ACKNOWLEDGEMENTS

I would like to take this opportunity to express my thanks to those who helped me with various aspects of conducting research and the writing of this dissertation. First and foremost, I am greatly in debt to my major professor Dr. David Hennessy and Dr. Leigh Tesfatsion for their guidance and support throughout this research and the writing of this dissertation. Their insights and words of encouragement have inspired and kept me motivated to finish my dissertation. Look back the five years of Ph.D study, I could not achieve what I am now without their directions.

I would also like to thank my committee members for their efforts and contributions to this work: Dr. James Bushnell, Dr. Hele Bunzel, and Dr. Dermot J. Hayes.

Except the help gained from Iowa State University, I also appreciate the consistent support I get from the staff in Pacific Northwest National Lab and ISO-New England.

ABSTRACT

This dissertation targets at studying the cause and implication of empirical grounded industry facts using multiple methodologies, including analytical model, statistical model, and agent-based simulation. Basically, this dissertation investigates two main research objects, the U.S. beef industry and restructured electricity market.

Beef is the single largest sector within United States agricultural production, accounting for a fifth of farm market revenues.Unlike other animal products, only a small share of output is produced under vertically integrated arrangements. Beef production also differs from other sectors because of the long production lags and the opportunity to utilize forage from lower quality land. The sector divides between grass-based cow-calf operations during the first year of a beef animal's life and grain-based feeder operations during the months preceding slaughter. The two sub-sectors also differ in regards to financial performance. Empirical data shows that cow-calf sector has strong positive autocorrelation in returns over time while the feeding sector return is close to white noise. Using the notion of Ricardian rent this study extends existing dynamic models of beef market equilibrium to rationalize this difference. Time series data are tested where preliminary tests provide evidence in favor of the theory proposed by this study. The results are important in explaining why the cattle feeding sector is relatively immune from demand and supply-side shocks whereas cow-calf operations are more exposed.

The second part of the dissertation turns focus on the restructured electricity market. In April 2003, the U.S. Federal Energy Regulatory Commission (FERC) proposed a new market design for U.S. wholesale power markets. Core features of this design include oversight of operations by some form of Independent System Operator (ISO), a two-settlement system consisting of a day-ahead market supported by a parallel real-time market to ensure continual balancing of supply and demand for power, and management of grid congestion by means of locational marginal pricing. The restructuring of electricity market stays in the layer of wholesale market

while the retail market still remains highly regulated by the state government. To alleviate the disconnection between wholesale and retail market, ISO propels demand response program to encourage retail customers join the wholesale market which is supposed to pass wholesale market price signal to the final customers. To investigate the impact of this connecting attempt on current power system performance in terms of both market and physical operation, this dissertation conducts agent-based simulation experiments on three topics that are closely related with demand response and price-sensitive bidding behavior. Specific studied issues include: a close-loop simulation study of two-settlement market with price-sensitive customers and intelligent load serving entity(LSE thereafter), a multi-agent simulation study of demand response (DR thereafter) provider baseline inflation behavior and generator company(GenCo thereafter) investment decisions under high penetration level of DR resource with a market framework requested by new FERC Order 745, an agent-based simulation study of LSE strategic price sensitive bidding behavior under three different market clearing mechanisms. To carry out this research, a flexible simulation framework is developed independently with a major extension of the AMES wholesale power market test bed to include two-settlement system, Unit Commitment system, smart device, intelligent LSE, multi-task ISO and capacity market.

CHAPTER 1. GENERAL INTRODUCTION

1.1 Introduction

This dissertation has two major research objects: U.S. beef industry and restructured electricity industry. Both of the two commodity goods have special properties that distinguish themselves from other commodities. This dissertation incorporates these distinguishing properties into analytical or simulation models and draws conclusions leaning on these properties.

Beef production has the longest life span among all the major agricultural products. Usually it takes up to three years for a new-born calf to finally end up in beef market. This long life span forms a cycle pattern for the cattle livestock and therefore beef price. The other property of cattle industry is the limited supply of proper pasture land for the use of cattle breeding which determines supply of cow herds. On the other hand, cattle feeding is more competitive since the feeding inputs can be easily purchased from nation wide agricultural product market. These features give the cattle breeding operators market power to get the Ricardian rent which results from limited supply of scarce resource.

Electric power has also two distinct features. First, it is extremely expensive, if not impossible, to store power energy. Thus, it must keep a constant balance of supply and demand on power grid. In traditional power system operation, this balance is guaranteed through adjusting generation resource to satisfy fluctuating load, a concept well known as "load following". Second, power flow among transmission paths cannot be freely controlled due to the underlying physical law of power flow. Increase of power injection at one bus could have significant change to the power flow on other buses and branches. These two features contribute to the fact that a centralized control room is needed to monitor and coordinate supply of power on the grid. Economic Dispatch is a management tool used to dispatch power, result of which containing

locational marginal price (LMP thereafter) and dispatched generation quantity. Due to the non-storable property, electricity price has high volatility and are sensitive to real-time load fluctuation. Due to the physical power flow constraints, some transmission line may reach the capacity limit when the system achieves the most efficient power dispatch. The inability to transfer power through the congested transmission line creates price difference not only at the two ends of the congested line but across the whole power system. Therefore, high degree of volatility and separation of LMP is a common phenomenon in power market.

Except special natures of the two commodity goods, the two industries also have distinct market structure. Beef industry has two separated sectors, the upstream cow-calf sector and the downstream cattle-feeding sector. The two sectors interact through intermediate goods, calf. While the upstream operators concentrate in a few breeding lot, the downstream is more open to competition.

Power industry also has two sectors, the transmission level wholesale market and distribution level retail market. The restructure of power industry mainly refers to that of wholesale level market. In April 2003 the U.S. Federal Energy Regulatory Commission (FERC thereafter) proposed a complicated market design called the Wholesale Power Market Platform (WPMP thereafter) for common adoption by all U.S. wholesale power markets. In this power market, Generator Company(GenCo thereafter) and Load Serving Entity(LSE thereafter) are bidding into a Independent System Operator(ISO thereafter) conducted market. Retail market is still subject to regulation where fixed price contract is prevalent for retail customers. As blind to the wholesale price signal, electricity load is known for its inelasticity. Demand inelasticity and the associated "load following" concept induces GenCo to exercise market power by either withholding capacity or bidding at high price. The lack of load flexibility also hampers the adoption of intermittent renewable energy, such as wind and solar. However, the lack of demand elasticity is a result of market structure flaw rather than the nature of electricity consumption. As realizing this situation, FERC lists incorporating demand response as one of the three top initiatives.

The complexity of studying restructured energy market lies in three aspects: the complex set of market protocols, the must-be-satisfied physical constraints, and the market participants

strategic behavior. A thorough testing and simulation work is necessary to understand and evaluate the impact of market rules modification in terms of both economic efficiency and system reliability. This dissertation utilizes agent-based modeling approach to set up a virtual world that imitates market participants, market environment and the interaction between them. As the first step to set up agent-based simulation, ISO's market operation protocols are carefully examined to ensure that simulation could replicate market operation procedure used in the real world. Physical constraints and market clearing algorithm are incorporated into the model which represents the distinct natures of electricity as mentioned above. Meanwhile, market participants are modeled to seek for the best action for their own interest. Simulation results are characterized by the emerging system pattern rather than the calculated equilibrium. By conducting such agent-based simulation experiments, we can test the potential policy implication and shed light on the problem resolving method.

1.2 Organization of the Dissertation

The remainder of this dissertation is organized as follows.

Chapter 2 is devoted to the issue of beef industry return pattern. It starts with a description of observed different return patterns in the upstream and downstream sector of beef industry. An analytical model is set up to examine the dynamics of the two sectors return given a market structure with upstream sector obtaining Ricardian rent. A careful comparison of the two sectors implied return is conducted to reveal the underlying reasons of different return patterns. The conclusions implied by the analytical model is then tested using data collected from different sources. The time series data is cleaned and fit into different statistical model. The empirical work supports the implications of the analytical model.

Chapter 3 overviews the research background and methodology of the following study on restructured electricity market. In the U.S., power system has been under restructuring for more than a decade. Since then, power trading, and investment in this electricity market has experienced significant changes. Market designers are facing with new problems and challenges with the process of restructuring. Agent-based model emerges as a powerful tool to study the electricity market since it pays equal respect to both the physical constraint and market partic-

ipants behavior. This chapter explains the concept of agent-based modeling and distinguishes it from other simulation approaches. A thorough literature review shows the wide application of agent-based modeling in electricity market research.

Chapter 4 summarizes the research work of the project "integrated retail and wholesale electricity market", a joint program of Iowa State University and Pacific Northwest National Lab. The primary objective is to test the market performance with a dynamic pricing retail contract which passes wholesale market price to the retail customers. The IRW project seams two independently developed test bed, Agent-based Modeling of Electricity Systems(AMES thereafter) for transmission level system and GridLab-D for distribution level system. A smart meter device was designed to balance between utility and cost of electricity use which also takes into consideration inter-temporal physical constraints. LSE passes day-ahead price to final customer and settles itself with both day-ahead and real-time price. Intelligent LSE learns to submit bids that replicates final customer's price-sensitive behavior to minimize its loss. Simulation result suggests a robust market performance.

Chapter 5 studies the impact of FERC order 745 which requests ISO to compensate load curtail by the wholesale market price. This study targets at both the short-term and long-term effect of FERC order 745. In the short-term, DR providers have incentive to maneuver their bids to either inflate baseline estimation or enjoy free compensation. In the long-term, DR has strong incentive to participate into the market due to the double payment which in turn squeeze away the capacity revenue of conventional generators. Both of the two aspects indicate that the design of compensation method as requested by FERC order 745 might lead to significant distortion and cause social efficiency loss.

Chapter 6 turns the focus on LSE price sensitive bidding in day-ahead market. It introduces the fact that during California crisis, big utility companies avoids bidding into day-ahead market to lower their total power procurement cost. Convergence of forward market and spot market is a main concern for the system operator because of the security reason since day-ahead market collects information to commit units for next-day. To study market participant's incentive of strategic bidding, three different market structures are compared. An agent-based model incorporating unit commitment is used to test LSE strategic bidding behavior under different

market structures. The study sheds light on the complexity of electricity market which takes both financial and physical functionalities.

Chapter 7 concludes the whole dissertation. Findings and challenges of each research topic are summarized to illustrates the contribution of this dissertation to academic literature and empirical research work.

CHAPTER 2. RATIONALIZING TIME SERIES DIFFERENCES BETWEEN COW-CALF AND FEEDER RETURNS

2.1 Introduction

Beef is the single largest sector within United States agricultural production, accounting for a fifth of farm market revenues. Unlike other animal products, only a small share of output is produced under vertically integrated arrangements. The industry divides between grass-based cow-calf operations during the first year of a beef animal's life and grain-based feeder operations during the months preceding slaughter. Cow-calf sector, which produces calves that go into feedlots, is mostly pasture based. The cattle feeding sector purchases the feeder cattle from the open market, and use corn and other concentrates to finish animals for slaughter. The two sub-sectors also differ in regards to financial performance. Using data from the Livestock Marketing Information Center[1], Figure 2.1 provides time series of returns for the two sub-sectors. Casual inspection suggests the former reflects strong positive autocorrelation in returns over time while the latter may be close to white noise. This difference can be viewed as the motivation for this paper. Our investigation of the link between the upstream and downstream of cattle industry will help understand the production decision mechanism. The results are important in explaining why the cattle feeding sector is relatively immune from demand and supply-side shocks whereas cow-calf operations are more exposed, a phenomenon well observed in the beef industry[2]. It is well known that beef production differs from other sectors because of long lags in production responses. The beef industry can not respond to a price signal quickly, but

[1]The Livestock Marketing Information Center (LMIC) is a institute providing economic analysis and market projections concerning the livestock industry since 1955. Return data used here include annual return data for cow-calf operation and feeding operation, ranging from 1975 to 2007.

[2]USDA Economic Research Service has made great contribution to the understanding of different effects of feed cost on these two sectors. One good example is the research report by Stillman, Harley and Mathews in 2009, which indicates that the cow-calf operation is less affected by the current high feed cost.

(a) Initialization (b) Daily Operation

Figure 2.1: Cow/Calf and Feeding Sector's Return Series

The data used here is provided by LMIC. Both of the two returns are annual data.

rather needs years of time to adjust the breeding stock. Producers make decisions to expand or contract production before feed and product prices are known. Biological lags mean that animal products consumed today are based on production decisions made up to 2 years ago. Cow-calf operators make production decisions by choosing between calf sale for fattening and retention for breeding, that is a choice between consumption goods and capital goods.

In addition to this dynamic constraint, the cow-calf sector also differs from other production sector by the scarcity of suitable pasture for the cattle to graze on. The distribution of cow-calf operation region is illustrated in Figure 2.2. This map groups the cow-calf operation according to regions based on the survey of Agricultural Resource Management Study (ARMS). By this survey, cow-calf operators in the west and southern plains have significant cost advantages over operators in other regions due to the longer grazing season. The two regions account for 50 percent of the production of weaned calves. [3]The suitable pasture land for cow-calf operation is a scarce resource that can not be replicated.

By contrast, the feeding operation does not have such properties. It takes around 160-180 days to finish the fattening process, a much shorter time than the production of feeder cattle.

[3]See USDA statistical bulletin report number 974-3.

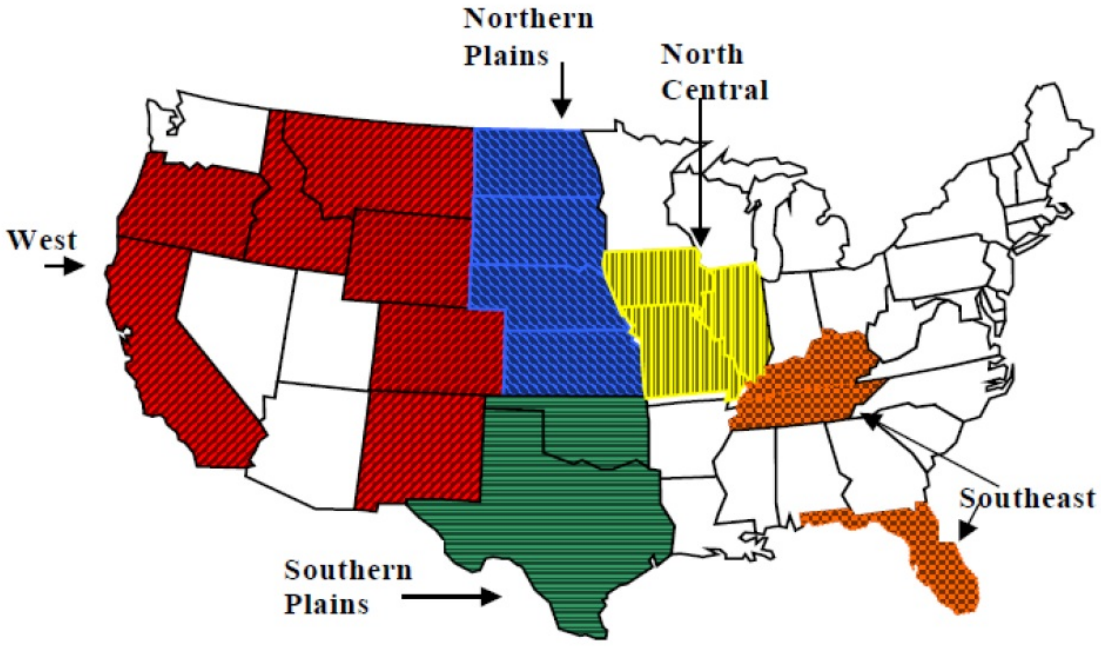

Figure 2.2: Distribution of cow-calf operation reginons in US

Except for feeder cattle, the main cost for cattle feeding is corn and other feed grain, which can be purchased freely on commodity markets. The feeder sector allows free entry and exit. Based on this fact, we assume the cow-calf sector will obtain the Ricardian rent from beef sales, be it positive or negative. The Ricardian rent is passed to cow-calf sector through the price of feeder cattle. Feeder cattle prices are affected by prices paid for fed cattle which, in turn, are affected by consumer demand for beef as reflected in retail beef prices. At the time of the feeder cattle transaction, bid for cattle feeder will drive up the feeder cattle until there is zero expected economic profit. Since the futures market for live cattle is very mature, market information is available to all the participants who utilize this finance tool to make hedging. With the assumption of full incidence pass through, we extend existing dynamic models of beef market equilibrium to rationalize the difference.

A substantial amount of progress have already been made in understanding cattle cycles. Jarvis (1974) was among the first to point out that a permanent increase of beef price might reduce the live cattle supply, and hence brought attention to how cattle investment decisions interact with biological production lags in the cattle cycle. Along the same line, Rucker et al.

(1984); Foster and Burt (1992); Rosen (1994) developed models to explain how the biological structure affect cattle supply by treating live cattle both as consumption and capital goods. Particularly, Rosen (1994) stripped away most of the details and focused on the exogenous shock's effect on the formation of cattle cycles. Rosen et al. (1994) (RMS hereafter) extended this model to a more complete biological structure, and implied clear cyclical pattern for breeding stock and live cattle price.

Heterogenous expectation also attracted scholar's attention when trying to interpret the cattle cycle. Both Baak (1999) and Chavas (2000) tested for different forms of bounded expectations and estimated the weights of operators with these expectations. Baak's study found that approximately one-third of ranchers appear to have bounded rationality in the sense that they forecast future prices based solely on time series observations. Chavas found that less than one-fifth of cattle producers appear to behave consistently with full rational expectations. But as argued in Aadland (2004), despite of these empirical evidences, rationality in expectation formation is still mostly favored by economist seeking to explain the aggregate cattle stock behavior. The evidence on heterogenous expectations is not strong enough to reverse the conclusion made under rational expectation. So, in this study, we adhere to the rational expectation formation.

So far, most of the literature about cattle cycles does not separate the cow-calf and feeder sectors in the beef supply chain. One exception is the work by Aadland and BAILEY (2001), Aadland (2004), Aadland (2005). Aadland distinguished the fed beef price from unfed beef price, and hence proposed two margin problems for cow-calf operators. Under this framework, producers will respond positively to relatively higher prices along one margin and will build up stocks along the other margin. Despite this segregation, the feeder sector was still ignored, and hence the interaction between the two sectors was not considered.

To investigate this interaction issue, our work employs the idea of Ricardian rent theory (RRT hereafter). In RRT, rent is defined as "that portion of the produce of the earth, which is paid to the landlord for the use of the original and indestructible powers of the soil" Ricardo (1821). Economic theory suggests that extra production profits resulting from high beef prices will ultimately accrue to the cow-calf operators because breeding stock as well as the suitable

pasture land is the most limiting resource in beef production. However, the RRT is quite challenged in the recent study in farmland rent and price. Kirwan () estimates that only 25 percent of the government subsidy will finally flow to the landlord. Du et al. (2007) finds little support of RRT when examining the crop price increase effect on cropland rent. They attribute the failure of RRT to the lack of mobility for tenants and inertia in leasing contract re-negotiations. However, compared with tenants, feeder cattle are easier to transport and the feeder cattle market is quite liquid, which implies the failure of RRT reasons might not exist in the cattle industry.

The paper is organized as follows. Section 2 sets up the dynamic rational expectation model including two sectors, with an explicit form of the two sectors' return derived. Section 3 tests the RRT using the live cattle futures price. Also in section 3, we have a formal test of the return's pattern, and the implications from the model. Section 4 concludes by summarizing the main findings of the paper and suggesting avenues for further research.

2.2 Theoretical Model

2.2.1 Background and Main Assumption

This paper clearly builds on the aforementioned work of Rosen (1994) and Aadland and BAILEY (2001). Before introducing the model setup, it is necessary to formally outline the environment being modeled. The separation of cattle life is a relatively recent phenomenon. Prior to the 1930s, feeding of high concentrate grains was rare and most cattle lives on the pasture or harvested forage for the whole life. Since then, the practice of finishing feeder cattle on grains has become commonplace and in more recent times (beginning in the 1960s), finishing has graviated toward organized feedlots.

Within the first six months after the calf is born, there are few decisions to make. After weaning, a calf is typically six to ten months old. If it is male, the calf will most likely be castrated and sent to feeding lot later, with only a small portion left for breeding purpose. The problem for the female calves is complicated since it is a consumption good and also a capital good. Cow-calf operators need to decide whether to retain the female calf for addition to the

breeding stock (capital good) or sell them for beef production (consumption good).

The calves for consumption will then be sold as feeder cattle in the open market. They will first go through the so called *finishing* process for four to six months. After this stage, the animal will reach the final stop, the feedlot, where they will be fed high-concentrate grains for approximately six months to be fattened for slaughter. So, generally there are two main stages for a typical beef animal's life. Roughly speaking, a beef cattle will grow up under two operations, cow-calf operation and feeding operation, with each one accounted for one year time. On the other branch, breeding cattle will be first bred when they are fifteen months old. The gestation period will last for nine months. So, it takes around two years for a calf to give birth to its offspring. Two years is also the age at which a meat animal is ready to be slaughtered.

A dynamic rational expectation model is set up to capture the essential components in the beef supply chain. The key to this model is the interaction between the two sectors through the pricing of feeder cattle. As discussed in the introduction, since breeding cattle sector faces dynamic constraint, and the suitable pasture land is inelastic as well, we will assume the cow-calf operation will obtain all the extra profit from beef production. With rational expectations of all the market participant, the feeder cattle price will be bid up when there is positive expectation concerning forward beef markets, and will be bid down when the forward beef markets are depressed.

The model is set in discrete time with decision intervals one year in length. The biology structure is assumed to be consistent with the reality. The cow-calf operators make decision when the calf is one year old. The calves reserved for retention will be added into the breeding stock while the feeder calves will be sold to the feedlot and enter the beef market in the following year. Because of separation of two sectors, there are two prices, feeder cattle price and beef price. To make the problem tractable, we assume the breeding cow has the same value before and after giving the first birth. This setup is different from Aadland and BAILEY (2001) which distinguished between fed and unfed beef price but ignores calf price. This simplification will not change the main conclusions of this paper if the fed and unfed beef is highly correlated, but will provide great convenience for the model setup.

For the market participants, we assume cow-calf operators to be forward-looking, rational agents that maximize a discounted expected future stream of profits subject to biological and market constraints. The feedlot operators have the same rational expectation as cow-calf operators, but they are take-it-or-leave-it participants that can freely enter and exit the market. We assume that operators in each type are identical and make decisions in competitive input and output markets.

Properties of market equilibrium are established by analyzing the activities of a representative cow-calf operator and a representative feedlot operator. Consistent with other animal cycle models, the present and future production possibilities are linked by a population dynamics constraint, which gives the trade off between current consumption and potential future consumption. The main difference from Rosen (1994) is that the cow-calf operators now have to make beef production decisions one year earlier by selling a fixed number of feeder calves to feedlots one year earlier.

The model is determined by a stochastic difference equation and the shocks come from three aspects. Two types of shocks originate on the supply side, the holding cost of breeding cattle, h_t, as well the finishing and marketing cost of feeder cattle, m_t. The other shock comes from the demand side, the income level shock y_t. As with Rosen (1994), we simplify the model setup by abstracting from sex and life-cycle aspects of herd management, assuming a homogeneous female population with a biologically determined constant birth rate.[4] Table 2.1 gives the connection between this model and that of Rosen (1994).

Table 2.1: Connection between this model and Rosen (1987)

	Rosen (1987)	**This Paper**
biological structure	Not clearly specified	Yearling-Cow
market structure	one layer competitive market	up-stream and down-stream industry
slaughter at period t	made at period t	decision made at period t-1
shocks	coming from demand side, holding cost and marketing cost	as Rosen (1987)

[4] As noted in Rosen (1994), p 548

2.3 Dynamic constraints:

Consider a closed economy, the growth of breeding cattle stock x_t is determined by two parts, the addition of total new born calves gx_t, and the deletion of sold calves s_t. So $gx_t - s_t$ is the net addition of calves, and they will grow to be the breeding stock in the next period. The feeder calves sold to feedlot will go through finishing and fattening, and end up in beef market in the next period. This evolution of cattle stock is shown in equation (2.1):

$$x_{t+1} = (1+g)x_t - s_t \tag{2.1}$$

with x_0 given and $s_t \geq 0, x_t \geq 0$ for all time points $t \in \{0, \infty\}$. We can solve equation (2.1) by forward substitution. From equation (2.1), we can get $x_t = \frac{s_t}{1+g} + \frac{x_{t+1}}{1+g}$.Then forward this result for one period, we can get $x_{t+1} = \frac{s_{t+1}}{1+g} + \frac{x_{t+2}}{1+g}$. Substitute x_{t+1} into the expression of x_t, we can get $x_t = \frac{s_t}{1+g} + \frac{s_{t+1}}{(1+g)^2}$. Repeat this process, we can get the following complete intertemporal constraint:

$$x_t = \sum_{\tau=0}^{\infty} s_{t+\tau}/(1+g)^{\tau+1} \tag{2.2}$$

Also given the available information of period t, take expectation to both side of equation (2.2) implies:

$$x_t = E_t \sum_{\tau=0}^{\infty} (s_{t+\tau})/(1+g)^{\tau+1} \tag{2.3}$$

2.3.1 Market Equilibrium

Market equilibrium is achieved through the dynamic decisions made by cow-calf operators as well as static decision of feedlot operators. Given the feeder cattle price and the rational expectation, the market supply and demand of feeder cattle must equate. Looking at the cow-calf operation side, cow-calf operator's profit per animal is defined as

$$\pi_t^{cc} = q_t s_t - h_t x_{t+1} \tag{2.4}$$

where q_t is the price of feeder cattle sold to feedlot, and the superscript cc stands for cow-calf. The cow-calf operator's return per cattle can be written as:

$$R_t^{cc} = q_t - h_t \tag{2.5}$$

where R is for returns and the superscript is for cow-calf. As assumed, cow-calf operators will make the reproduction decision, and they will get the Ricardian rent, which drives feedlot's expected profit to be zero. At time point t, feedlot operator purchases s_t feeder calves from cow-calf operators and sell them to the beef market in period t+1. The feedlot's return per cattle can be written as:

$$R_t^{fd} = (p_{t+1} - m_{t+1})/(1+r) - q_t \tag{2.6}$$

where p_{t+1} is the fed-cow price in the beef market, m_{t+1} is the finishing and marketing cost, so $(p_{t+1} - m_{t+1})/(1+r)$ is the discounted revenue from one cow, while q_t is the cost for purchasing a yearling. Ricardian rent theory implies that the time t expected return is 0, so from equation (2.6), we can get:

$$q_t(1+r) = E_t(p_{t+1} - m_{t+1}) \equiv p_{t+1}^* - m_{t+1}^* \tag{2.7}$$

where E_t is the expectation operator at period t, and the notation $p_{t+1}^* = E_t(p_{t+1})$ is used to be consistent with Rosen (1994). At this stage, it's necessary to sum the notation used for this model setup, as shown in Table 2.2. Under this model setup, cow-calf operators will face a dynamic problem, and maximize the sum of discounted life-time profit:

$$V_t = E_t \sum_{\tau=0}^{\infty} \pi_{t+\tau}^r/(1+r)^\tau \tag{2.8}$$

The solution to this problem is characterized by the Euler Equation that make the cow-calf operators indifferent between holding and selling, that is:

$$q_t = \frac{1}{\beta} E_t(q_{t+1} - h_{t+1}) \tag{2.9}$$

$$where \beta = \frac{1+r}{1+g} < 1 \tag{2.10}$$

Table 2.2: Notation and Definition

x	breeding stock
s	the number of yearlings sold to feedlot
q	price of yearling
p	price of fed cow
m	unit cost of finishing incurred by feedlot
y	demand shifters
h	unit holding cost of yearlings incurred by cow-calf operators
r	the market rate of interest
β	(1+r)/(1+g),the net discount rate
R^{cc}	cow-calf's net return for opreatiing cow-calf business
R^{fd}	feeders net return for finishing fed cow
g	net birth rate after accounting for natural deaths
π_t^{cc}	cow-calf's net cash flow in period t
V_t	capital value of operating the cow-calf business
E_t	expection operator, given all the information at period t
b	the fed cow supplied in beef market
$k^*_{t+\tau}$	short for $\mathrm{E}_t(\mathrm{k}_{t+\tau})$

To get an analytical solution to this problem, we suppose the demand of beef follows a linear demand function:

$$b_t = \alpha - \gamma p_t + y_t \tag{2.11}$$

where in this demand function, b_t is the demand for fed cow at period t, p_t is the price for fed cow in beef market, y_t is the demand shifter for fed cattle. As assumed, the supply of fed cow in period t comes from the sold feeder cattle in period t-1, that is, $b_t = s_{t-1}$. So we can rewrite the beef demand function in terms of feeder cattle: $s_t = \alpha - \gamma p_{t+1} + y_{t+1}$.Take expectation given all the information at time t, we can get:

$$s_t = \alpha - \gamma p^*_{t+1} + y^*_{t+1} \tag{2.12}$$

where $p^*_{t+1} \equiv E_t(p_{t+1})$, $y^*_{t+1} \equiv E_t(y_{t+1})$ are the expected beef price and demand shifter in year t+1,which is consistent with Rosen (1994)'s notation. By assumption, the feedlot makes zero expected profit from finishing operation. Substitute equation (2.7) into equation (2.12), we can get the sold amount s_t in terms of yearling's price q_t:

$$s_t = \alpha + y^*_{t+1} - \gamma[q_t(1+r) + m^*_{t+1}] \tag{2.13}$$

Using the law of expectations, equation (2.13) can be rewritten as:

$$s^*_{t+\tau} = \alpha + y^*_{t+\tau+1} - \gamma[q^*_{t+\tau}(1+r) + m^*_{t+\tau+1}] \tag{2.14}$$

With the same approach, we can rewrite the Euler equation (2.9) as:

$$q^*_{t+\tau} = \beta(q^*_{t+\tau+1} + h^*_{t+\tau+1}) \tag{2.15}$$

where the price of q at the beginning is given. Solve this by forward substitution, $q^*_{t+\tau} = \beta q^*_{t+\tau-1} + \beta h^*_{t+\tau-1} = \beta^2(q^*_{t+\tau-2} + h^*_{t+\tau-2}) + \beta h^*_{t+\tau-1}$.Repeating this process, we can get the expected future feeder cattle price in terms of current yearling price and expected holding cost. As shown in equation(2.16), it pins down the optimal path for cow-calf operator.

$$q^*_{t+\tau} = \beta^\tau q_t + \sum_{i=1}^{\tau} \beta^\tau h^*_{t+\tau-i} \tag{2.16}$$

Collecting equations, the competitive market equilibrium is described by equation (2.16), (2.14) and the intertemporal budget constraint(2.3).

2.3.2 Solving the model

To illustrate the recursive property of the model, it's convenient to express the variables in the deviation form. Equation (2.17) expresses the shocks in such a form, where the bar_expressions are "normal" values and u^j_t's are deviation from normal.

$$y_t = \overline{y} + u^y_t, m_t = \overline{m} + u^m_t, h_t = \overline{h} + u^h_t \tag{2.17}$$

Following this, define the capital notation as the deviations from the normal level:

$$X_t = x_t - \overline{x}, S_t = s_t - \overline{s}, Q_t = q_t - \overline{q} \tag{2.18}$$

With this deviation form, we can rewrite equation (2.18) as follow:[5]

[5]Please refer to Appendix A

$$
\begin{aligned}
X_t &= -\frac{\gamma(1+r)}{1+g-\beta}Q_t + \sum_{\tau=0}^{\infty} v^*_{t+\tau}/(1+g)^{\tau+1} && (2.19)\\
Q_t &= \frac{1+g-\beta}{\gamma(1+r)}[-X_t + \sum_{\tau=0}^{\infty} v^*_{t+\tau}/(1+g)^{\tau+1}] && (2.20)\\
S_t &= (1+g-\beta)X_t - (1+g-\beta)\sum_{\tau=0}^{\infty} v^*_{t+\tau}/(1+g)^{\tau+1} + u^{y*}_{t+1} - \gamma u^{m*}_{t+1}\\
X_{t+1} &= \beta X_t + (1+g-\beta)\sum_{\tau=0}^{\infty} v^*_{t+\tau}/(1+g)^{\tau+1} - u^{y*}_{t+1} + \gamma u^{m*}_{t+1}\\
\text{where} v^*_{t+\tau} &= u^{y*}_{t+\tau+1} - \gamma u^{m*}_{t+\tau+1} - \frac{(1+r)\gamma\beta u^*_{t+\tau}}{1+g-\beta}
\end{aligned}
$$

Notice that, compare with Rosen (1994)[6], the difference is that the effect of demand shifter y and feedlot's feeding cost m comes from time $t+1$, while the effect of cow-calf operator's holding cost is the same. This difference comes from the assumption change that yearling's price is determined by the expected beef price in next year. Assume that all the shocks evolves as serially correlated processes with parameter ρ_j :

$$
\begin{aligned}
u^y_{t+1} &= \rho_y u^y_t + \varepsilon^y_{t+1} && (2.21)\\
u^m_{t+1} &= \rho_m u^m_t + \varepsilon^m_{t+1}\\
u^h_{t+1} &= \rho_h u^h_t + \varepsilon^h_{t+1}
\end{aligned}
$$

where the ε's are pure noise. This implies $u^{j*}_{t+\tau} = \rho^\tau_j u^j_t$, substitute into equation(2.19), [7]we can get:

$$Q_t = \frac{1+g-\beta}{\gamma(1+r)}[-X_t + \frac{\rho_y}{1+g-\rho_y}u^y_t - \frac{\gamma\rho_m}{1+g-\rho_m}u^m_t] - \frac{\beta}{1+g-\rho_h}u^h_t \qquad (2.22)$$

$$S_t = (1+g-\beta)X_t + \frac{\rho_y(\beta-\rho_y)}{1+g-\rho_y}u^y_t - \gamma\frac{\rho_m(\beta-\rho_m)}{1+g-\rho_m}u^m_t + \frac{\beta\gamma(1+r)}{1+g-\rho_h}u^h_t \qquad (2.23)$$

$$X_{t+1} = \beta X_t - \frac{\rho_y(\beta-\rho_y)}{1+g-\rho_y}u^y_t + \gamma\frac{\rho_m(\beta-\rho_m)}{1+g-\rho_m}u^m_t - \frac{\beta\gamma(1+r)}{1+g-\rho_h}u^h_t \qquad (2.24)$$

[6]the counterpart can be found in the Appendix D.
[7]Please refer to Appendix B

Compare this solution with Rosen (1994)[8], we can see the main difference is that the effect of shock u_t^y and u_t^m is weakened through multiplying by ρ_j, while the effect of shock u_t^h is magnified through multiplying by (1+r). The reason in the first change lies in the structure of u_{t+1}^y and u_{t+1}^m. With these equations, we can back out the path for the profits which are of our interest.

2.3.3 Result

In this subsection, we will derive the main conclusions of the model. Under the assumption of Ricardian rent incidence on cow-calf operator, feedlot will earn a zero expected profit. It's easy to see the realized return of feedlot is random, and there is no recursive property. Substituting equation (2.7) into equation (2.13), we can get $q_t = \frac{1}{1+r}(\frac{\alpha+y_{t+1}^*-s_t}{\gamma} - m_{t+1}^*)$. Inserting this into the return function of feedlot (2.6), we can get:

$$\begin{aligned} R_t^{fd} &= \frac{1}{1+r}(\frac{\alpha+y_{t+1}-s_t}{\gamma} - m_{t+1}) - \\ &\quad \frac{1}{1+r}(\frac{\alpha+y_{t+1}^*-s_t}{\gamma} - m_{t+1}^*) \\ &= \frac{\varepsilon_{t+1}^y/\gamma - \varepsilon_{t+1}^m}{1+r} \end{aligned} \tag{2.25}$$

As both ε_{t+1}^y and ε_{t+1}^m are pure random variables, the profit for feedlot is also a random variable. Also, the expectation of this return is 0. This is the first conclusion of this paper:

Proposition 1. *The realized return of feedlot is random and only affected by the shock from demand shifter side and finishing feed cost.*

Then look at the returns of cow-calf operator. Follow equation (2.5), we can rewrite the returns of cow-calf operators in deviation form:

$$\begin{aligned} R_t^{cc} &= Q_t - u_t^h \\ &= \frac{1+g-\beta}{\gamma(1+r)}[-X_t + \frac{\rho_y}{1+g-\rho_y}u_t^y - \frac{\gamma\rho_m}{1+g-\rho_m}u_t^m] - \frac{1+g+\beta-\rho_h}{1+g-\rho_h}u_t^h \end{aligned} \tag{2.26}$$

[8] the counterpart can be found in the Appendix D

As X_t has recursive property as shown in equation (2.24), the return of cow-calf operator's profit also has recursive property. Also, notice that, if the correlation ρ_j is small, which means the shock is temporary, the effect from demand shifter and finishing cost can be very small, while the effect from holding cost can't be negligible.

To make this paint more clearly, we can solve the explicit form of cow-calf operator return.[9] . The recursive form for R_t^r can be written as

$$R_{t+1}^{cc} = \beta R_t^{cc} + \lambda u_t^h + \Psi_{t+1} \tag{2.27}$$

where $\lambda = \frac{(1+g+\beta-\rho_h)}{(1+g-\rho_h)}(\beta - \rho_h) + \frac{\beta(1+g-\beta)}{1+g-\rho_h}$, $\Psi_{t+1} = \frac{1+g-\beta}{\gamma(1+r)}[\frac{\rho_y}{1+g-\rho_y}\varepsilon_{t+1}^y - \frac{\gamma\rho_m}{1+g-\rho_m}\varepsilon_{t+1}^m] - \frac{(1+g+\beta-\rho_h)}{1+g-\rho_h}\varepsilon_{t+1}^h$

Equation (2.27) confirms our observations of returns of cow-calf operators, and this is our second proposition:

Proposition 2. *The return of cow-calf operation has first-order positive autocorrelation*

Examine this clear form of cow-calf operator's return, we can get two corollaries:

Corollary 1. *The deviation level of beef demand shifter and finishing feed cost does not affect the cow-calf operator's return in next period.*

This is not a surprising result following previous assumptions. As the Euler equation (2.9) states, the price for selling the yearlings this period should equal the expected payoff from holding these yearlings and selling the new yearlings in next period's market. Rewrite the Euler equation in the return form, we can get:

$$R_t^{cc} + u_t^h = \frac{1}{\beta}E_t(R_{t+1}^{cc}) \tag{2.28}$$

So we can see that the demand shifter and finishing cost has dropped out from the optimal path for cow-calf operator's return. The effect of two shocks on cow-calf operation only comes from the unexpected random term, as in Ψ_{t+1}. So, the cow-calf operation's return is largely shielded from the price fluctuation of the two shocks.

[9] Please refer to Appendix C

This result comes from the rational expectation assumption. The three shocks have auto-correlation structure as defined in (2.21). So, at the time when feeder cattle is set the part of shocks u_{t+1} coming from the correlation with current shock $\rho\mu_t$ has already been expected. This feeder cattle's price, in turn, is reflected in time t's return R_t^{cc}. So, current shock's level μ_t will have no influence on the return structure when R_t is also present.

Corollary 2. *The effect of holding cost on the return pattern can go either way, which is determined by the difference by* $\beta - \rho_h$.

From the definition of λ in equation (2.27), we can see the magnitude of λ depends on the sign of $\beta - \rho_h$. If $\beta > \rho_h$,then $\lambda > 0$, and a high level of holding cost deviation from normal level in this period can bring a high level of cow-calf operation's return. If $\beta < \rho_h$, λ can be a small positive number or even negative, which means the high holding cost induces a low cow-calf operation's return in next period. Particularly if $\beta = \rho_h$, λ is degenerated to β, the net discount rate.

This result is also intuitive as can be seen from return form of Euler equation (2.28). If the holding cost is very high in the current period, it is optimal to get a higher return in next period in order to compensate this high cost. If the next period's expected return is not high enough, cow-calf operators will sell more of feeder cattle at this time point, which will cut the supply capability in next period. This cut in supply in the next period will drive the expected return of cow-calf operation up in the next period. This compensation effect is captured by the net discount rate β. On the other hand, if the autocorrelation of holding cost is large, a high holding cost this period means a good chance for high holding cost in the next period. So it is likely that the cow-calf operators realized returns will be small due to the high cost of feed or forage cost.

2.4 Empirical Work

The work in this section is in three folds. The first one is to test Ricardian rent theory, the base of this model. The second one tests the causal observation of different return pattern. The third one examines the implication from the theoretical work.

2.4.1 Ricardian Rent Theory Test

The model is largely based on the assumption that the Ricardian rent is passed to the Cow-calf operators through the price of feeder cattle. If Ricardian theory is correct, then the increase of market expectation for fattened cattle would bid up spot feeder cattle prices. The first data source is Chicago Mercantile Exchange (CME), which provides daily data of live cattle(lc) and feeder cattle(fc). The second data source is National Agricultural Statistics Service (NASS) under United States Department of Agriculture. Data found from NASS includes the monthly data of corn's price, feed grain and hay index, Consumer Price Index. All the data are reported regularly in NASS's monthly agricultural report. The time span of all the data goes from Jan 1979 to Feb. 2009. Altogether there are 362 samples for monthly data and 30 samples for annual data. Daily data are transformed to be monthly data by taking an arithmetic average. So, for the live cattle and feeder cattle futures, monthly data are used.

We need to further transform the available data to fit the purpose. Firstly of the test, we use the nearest maturing cattle feeder future price to substitute cattle feeder's spot price P_t^{fd}, ignoring the basis between the two prices. Secondly, assume the farmers could use live cattle's futures price to lock in a certain price when the cattle is ready for slaughter. As reported by Iowa Beef Center, it typically takes 6 or 7 months for a calf to grow up to a steer. As the CME live cattle futures contracts are only settled in even months (like February, April and so on), we suppose in even month it takes 6 months for finishing while in odd months it takes 7 months so that when the fed cattle is mature there is a corresponding price. By this rule, we can get a series of live cattle future prices $F_{t,t+s}^{lc}$, the one matured when cattle are fattened. Here the upper script lc stands for live cattle while s is the time needs to fatten cattle. Thirdly, we use the monthly corn price to represent the cost for feeding. As reported by USDA[10], 90 percent of feeding cost comes from corn. A preliminary test confirms that soybean price has no significant effect in feeder cattle's price.

By the futures specifications of CME in 2009, the feeder cattle midpoint weight is 749.5 pounds while it is 1262.5 pounds for live cattle. So, we need to transform the "per animal expression" of RRT in equation (2.7) to the per pound expression. The corresponding regression

[10]Please refer to the report by Stillman, Haley, and Mathews in 2009.

Table 2.3: Unit root Test statistics for corn, live cattle and feeder cattle

	feeder cattle future q_t	Live cattle future $F^{lc}_{t,t+1}$	Corn P^{cn}_t
	Single Mean Case		
ADF	-1.71	-1.60	-3.38**
P-P	-1.98	-1.80	-2.64*
KPSS	1.23***	1.26***	0.17
	Trend Case		
ADF	-3.71**	-2.82	-3.38*
P-P	-2.78	-2.71	-2.70
KPSS	0.23***	0.27***	0.15**

Notice: the statistics for ADF, P_P and KPSS are t, adj-t and adj-LM respectively,
* rejects the hypothesis at 10% level,
** rejects the hypothesis at 5% level,
*** rejects the hypothesis at 1% leve

is shown in as follow:

$$P^{fd}_t = \beta_0 + \beta_1 F^{lc}_{t,t+1} + \beta_2 P^{cn}_t + \varepsilon_t \text{ where } \varepsilon_t \sim N(0, \sigma^2) \tag{2.29}$$

Let the half year discount rate to 5%, and take into account the death rate of feeder calves as 1.2%[11], then RRT implies $\beta_1 = \frac{1262.5}{(1+0.012)(1+0.05)*749.5} = 1.58$. The estimate of the coefficient β_1 will indicate the proportion of Ricardian rent passed to the cow-calf operator.

As summarized in Wang and Tomek (2007), the unit root is a common problem in the commodity price, especially the nominal price. Also, different unit root test approaches do not agree in many cases. To establish that the regression is not spurious, we subject the data to a detailed unit root test, and the results are listed in Table 2.8. Notice that, the hypothesis for ADF and P-P methods is the existence of unit root while the hypothesis for KPSS is that the time series is stationary. The test result shows there is strong evidence that the variables have unit root problem and are not stationary time series. Despite of this news, we could do the cointegration test to test whether the linear combination of these variables are stationary. Table 2.4 gives positive information with all the three variables having significant evidence of cointegration. So, the three variables have inherent correlation, and the regression result will not be spurious.

[11] 1.2% is the mean level of death rate in feeding process as reported by Food Link.

Table 2.4: Cointegration tests for corn, live cattle and feeder cattle

	Trace Test		Maximum Eigenvalue Test	
No. of CE(s)	trace stat	Prob	Max-Eig stat	Prob
None	55.6	0.000	31.8	0.001
At most 1	23.8	0.002	19.6	0.006
At most 2	4.2	0.039	4.2	0.039

Notice: the test result is obtained using Eviews 5

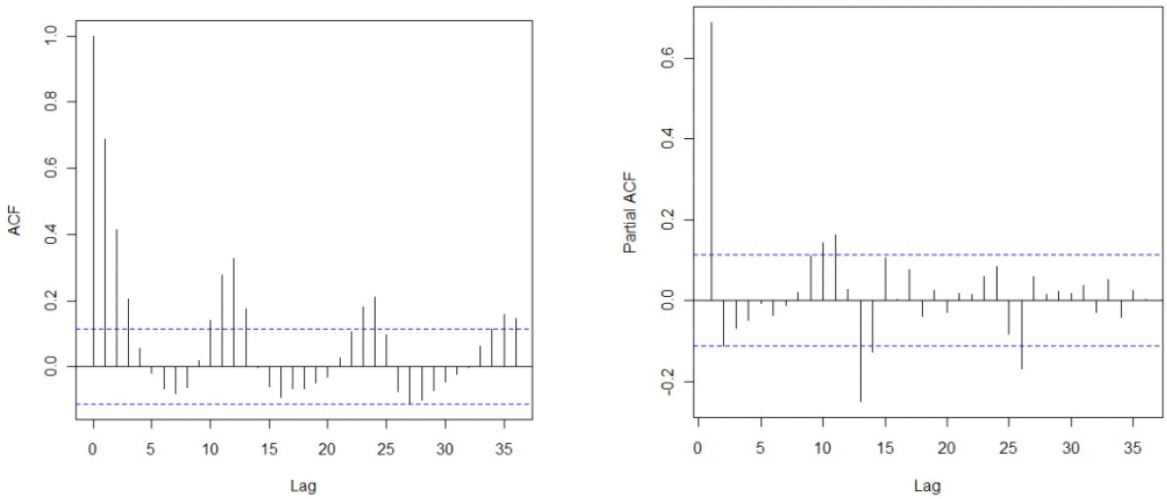

(a) ACF (b) PACF

Figure 2.3: ACF and PACF for the OLS residual

Using OLS to estimate (2.29) could give us a flavor of how the model works. Figure 2.5 presents the ACF and PACF of the OLS residual. From this ACF figure, we can see there is strong seasonal effect with a seasonal lag of 12 months. This seasonal effect is commonly observed in agricultural commodities, which is largely affected by the weather and timing. The PACF figure suggests that the residual has strong AR(1) correlation, as the PACF cuts off from lag 1. This result is consistent with the theoretical work. Since the feeder cattle is the main revenue source for cow-calf operations, the cow-calf return's AR(1) structure implies the feeder cattle price may also have AR(1) structure. To specify the model correctly, we need to remove the seasonal and AR(1) correlation from the residual. A two step FGLS method is employed to remove this correlation. In the first step,we run the SARMA model over the OLS residual,

Table 2.5: FGLS estimate of coefficients in regression (2.29

Coefficient	β_0	β_1	β_2
Estimate	-0.004	1.35***	-6.43***
Std. err	0.59	0.04	0.51
P value	0.993	0.000	0.000
Adj R^2	0.75	D-W stat	2.05

Notice: the test result is obtained using Eviews 5

with the SARMA structure shown as follow:

$$(1 - \Phi_1 L^{12})(1 - \theta_1 L)\omega_t = \varepsilon_t$$

With the coefficient estimates $\widehat{\Phi_1}$ and $\widehat{\theta_1}$, we can transform the regressors in equation (2.29) . The new regressors y_t is defined as $y_t = (1-\widehat{\Phi_1}L^{12})(1-\widehat{\theta_1}L)x_t$, where x_t is the original regressor. Then run OLS over this new regressors to get the estimate of β. Referring to Greene(2007), there is no gain by iterating this process. As can be seen in Table 2.5, the D-W test is close 2, implying that the residual has no correlation problem. Figure 2.4 compares OLS and FGLS residual diagnosis, it is clear that FGLS approach has removed the residual correlation problem from OLS estimation.

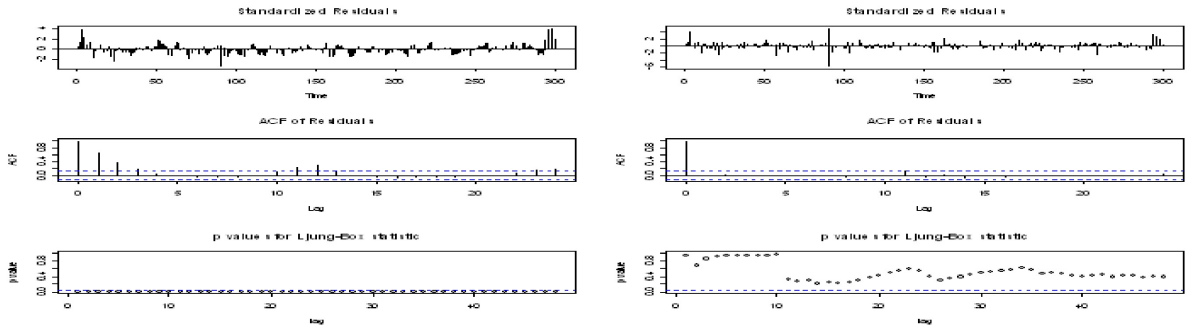

(a) OLS (b) FGLS

Figure 2.4: Comparsion of OLS and FGLS residual diagnosis [a]

[a]The diagnosis is done using R 2.8.2

Table 2.5 lists the estimate for β using FGLS. Especially, the estimate for β_1 is 1.35, and the 5% level confidence interval for β_1 is [1.25,1.45]. Compared with the ideal value of 1.58,

Table 2.6: Mean zero test result

Sample mean	-10.01
Sample std.dev	60.52
t-statistic	-0.95
P-value	0.34

the estimate value of 1.35 suggests that **85.4%** of the increase of future live cattle's price will transfer to the current feeder cattle. The confidence level for this estimate ranges from 78.1% to 90.6%. In another word, about **85.4%** of the Ricardian rent is passed to the cow-calf operation. Compared with the 25% pass through ratio in the crop subsidy, 85.4% is significantly large. This indicates that the Ricardian rent incidence on cow-calf operators is a plausible assumption.

2.4.2 Different Return Patterns for Cow-calf And Feeding Sectors

Feedlot Return

This subsection will seek to verify the casual observation from figure 1 that feedlot have random return while cow-calf operations have positive autocorrelation. This is also the main conclusion of our model.

The RRT implies that the feeding lot should have zero expected profit. If the market participants have rational expectation, the realized return should be consistent with this expectation, that is, the realized return has a zero mean. The t-test result in Table 2.6 indicates that we can't reject the zero mean hypothesis of feeding sector's return. So, the feeding sector does not earn a significant positive profit over the last thirty years.

If the market forms rational expectations, the realized return to feedlot should be pure white noise, without any correlation pattern. A complete correlogram can illustrate this test result well, which is summarized in Table 2.7. For the lags up to 10, there is no autocorrelation or partial autocorrelation is significantly different from 0, and the corresponding p-values fail to reject the null hypothesis. So, we can say feeding sector's return is just a series of random variable, without clue to show any correlation.

Cow-calf Return

Table 2.7: Corrlogram of feeding sector's return

Lag	Autocorrelation	Partial Autocorrelation	P-values
1	0.039	0.039	0.812
2	0.021	0.019	0.964
3	0.065	0.064	0.971
4	-0.001	-0.006	0.994
5	0.030	0.028	0.998
6	0.116	0.110	0.991
7	0.029	0.021	0.996
8	0.059	0.051	0.998
9	0.079	0.063	0.998
10	0.139	0.134	0.993

As talked before, the cow-calf sector should have positively correlated returns. We can test this property by fitting an ARMA structure to the data. Before running any regression, we need to make sure this time series is stationary. A test for unit root in cow-calf return is listed in Table 2.8. It shows that the unit root hypothesis is rejected at a 5% level for both of the two test methods. So, it is safe to run a regression over the undifferenced data.

Table 2.8: Unit root test for cow-calf return

Test Method	ADF test	PP test
Test Statistics	-2.187	-2.255
p value	0.029	0.025
1% Critical Value*	-2.637	-2.636
5% Critical Value	-1.952	-1.951
10% Critical Value	-1.621	-1.611

As shown in the model, cow-calf sector's return has first order positive autocorrelation. We will use several models to fit the data, and test the AR(1) coefficient respectively. Suppose the most general model has the following form, with β_i as the AR(i) coefficient and γ_i as the MA(i) coefficient:

$$R_t^1 = \beta_0 c + \beta_1 R_{t-1}^1 + \beta_2 R_{t-2}^1 + \beta_3 R_{t-3}^1 + \gamma_1 \varepsilon_{t-1} + \varepsilon_t \tag{2.30}$$

The test result is summarized in Table 2.9 with several criterion listed to compare the performance of these models.

Table 2.9: Comparison performance of different models (2.29)

	AR(1)	AR(2)	AR(3)	ARMA(1,1)	ARMA(2,1)
β_0	5.24(7.98)	7.05(7.75)	7.81(8.21)	16.42(27.61)	18.71(19.59)
β_1	0.74**(0.11)	0.95**(0.17)	0.91**(0.19)	0.64**(0.17)	1.14*(0.43)
β_2	NA	-0.31(0.17)	-0.24(0.26)	NA	-0.46(0.33)
β_3	NA	NA	-0.07(0.20)	NA	NA
γ_1	NA	NA	NA	0.29(0.22)	-0.23(0.48)
F-test	40.18**	21.48**	11.89**	21.92**	14.03**
AIC	10.53	10.46	10.55	10.52	10.51
S-C	10.62	10.60	10.73	10.65	10.70
D-W	1.53	2.05	1.98	1.92	1.98

* significant at 10% level
** significant at 5% level

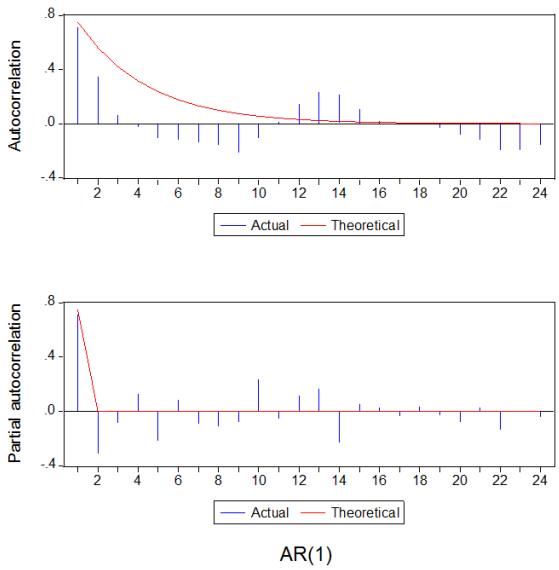

(a) AR(1)

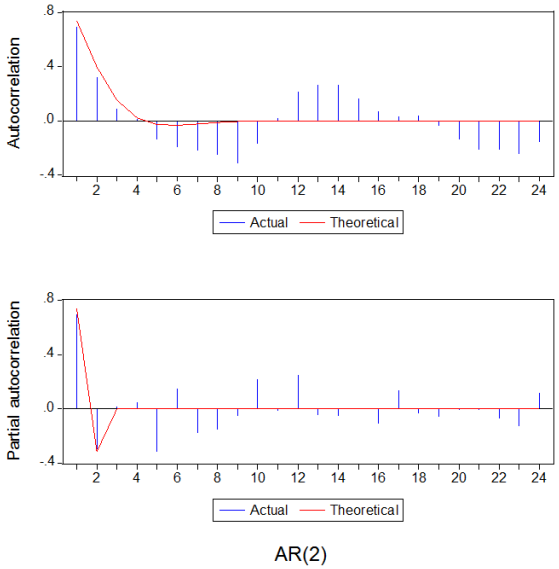

(b) AR(2)

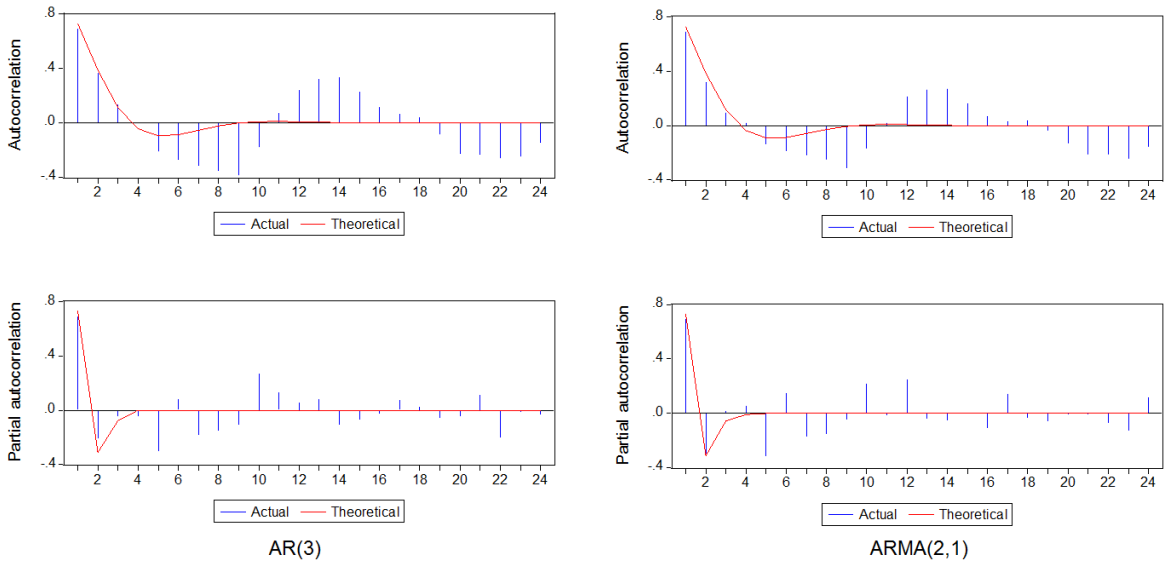

(c) AR(3)

(d) ARMA(2,1)

Figure 2.5: ACF and PACF for the OLS residual

Firstly, notice that β_1 is the only parameter that is significant through different models. This strongly suggests that the first order correlation is significant, which is consistent with the theoretical analysis. Secondly, both the AIC and S-C criterion shows that AR(2) model best fits the data. Also, the S-C criterion suggests that AR(1) model is the second best model to fit the data. But the D-W test indicates that the residual term of AR(1) model still has some correlation not explained by the model. Another approach to compare the performance of different model is to look at the AC and PAC graphs, which are listed in Figure 2.5. The pattern of AC and PAC also suggest that a higher order of autocorrelation term is preferable than the AR(1) model. In a word, the data suggest that cow-calf sector's returns have strong first order correlation, but higher order correlation is still possible. And it helps to explain the data better.

So, this section's empirical work verifies the casual observation about the different return pattern. It also provides strong support for the theoretical model.

2.4.3 Calibration and Test of Model Implication

This section will calibrate the parameters used in the model, which, in turn, will confirm the model setup.

Cattle Holding Cost Correlation

The data used to calibrate cow-calf sector's holding cost correlation comes from USDA Economic research service (http://www.ers.usda.gov/Data). Among the listed cost items, only the total feeding cost is consistently surveyed from 1982 to 2007. So, we are going to use this total feeding cost as a substitute of the cattle holding cost. Including time trend, we can get a AR(1) estimation as follow[12].

$$h_t = \underset{(24.37^{***})}{61.54} + \underset{(0.19^{**})}{0.45}\, h_{t-1} + \underset{(1.48^{***})}{11.67}\, t + \varepsilon_t$$

Cattle Feeding Cost Correlation

As we have talked before, the main grain used for feeding cattle is corn. We can use the historical corn price as a candidate to estimate cattle feeding cost correlation. The data used here come from USDA NASS agricultural price report, covering annual data from 1949 to 1999. Also including time trend, we can get an estimation as follow:

$$f_t = \underset{(0.0023^{***})}{0.0094} + \underset{(0.10^{***})}{0.48} f_{t-1} - \underset{(0.000^{**})}{0.001}\, t + \varepsilon_t$$

Demand Shifter Correlation

Different from the previous two cost variables, the demand shifter can not be observed directly. Instead, we will employ the FGLS approach to estimate the correlation of demand shifter. Follow equation (2.11), if the demand shifter y_t has AR(1) correlation structure, then the regression of equation (2.11) will have serial correlation problem. Using the two steps FGLS, we will run the OLS regression first, and then run the AR(1) auxiliary regression to the OLS residual in the last step. This auxiliary regression will have asymptotically efficient estimate of the demand shifter correlation ρ_y, and there is no gain to iterate the two steps. So, we will use the estimator of the auxiliary regression as the estimate for ρ_y.

[12]The numbers in parenthesis are the standard errors of estimates, this expression will be used for the rest of this section.

The data we employ includes annual steer whole sale value and annual steer slaughter quantity, covering from 1970 to 2005. The data can also be found in USDA Economic research service. (http://www.ers.usda.gov/Data/). Run OLS to estimate demand function, and then fit residuals into AR(1) model.

$$\begin{aligned} b_t &= \underset{3.49}{208.2^{***}} - \underset{0.02}{0.21^{***}} p_t + y_t \\ \text{with} y_t &= \underset{0.10}{0.16^{*}} y_{t-1} + \varepsilon_t \end{aligned}$$

Other Parameter

Chavas (1999) estimates the expected birth rate for calf as 1, which means that the breeding cow will give birth to one calf. The mean death rate is 0.08, which is also reported in his work. Then, we can get a net birth rate to be $g = 1 - 0.08 = 0.92$. Take the annual discount rate r as constant 10%, we can get an estimate of $\beta = \frac{1}{1+0.92} = 0.58$. In sum, the calibration for the parameters used in the model is listed in Table 2.10.

Table 2.10: Calibration of parameter value

Parameter	ρ_h	ρ_f	ρ_d	β
Estimate	0.45	0.48	0.16	0.58
Ste err	0.19	0.10	0.1	

Test of Corollary 1

The theoretical model shows that cow-calf operation return only relies on the maintain cost of breeding stock, but it is not directly related with the feeding cost or demand shifter. We collected corn's price, which is the main feeding cost, to test this inference. Based on previous work, we will use both AR(1) and AR(2) model to test corn's effect on the cow-calf sector's return, which are presented in the two equations of (2.31) respectively.

$$\begin{aligned} R_t^1 &= \beta_1 R_{t-1}^1 + \alpha C_t + \varepsilon_t \\ R_t^1 &= \beta_1 R_{t-1}^1 + \beta_2 R_{t-2}^1 + \alpha C_t + \varepsilon_t \end{aligned} \tag{2.31}$$

So, the hypothesis to test is:

$H_0: \quad \alpha = 0$

H_1 : *otherwise* The test result is summarized in Table 2.11. It indicates that in both models, the corn price effect is not significant. The AIC and S-C criterions are not better but worse off over the original models. Also, the corn's price does not explain the residual term's correlation in AR(1) model, which is reflected in the D-W test. So we can conclude that the corn price, which is a indicator of feeding cost, does not affect cow/calf sector's return.

Table 2.11: Test of corn's effect on cow-calf operation return

Model	AR(1)	AR(2)
α	-25.223(23.62)	-11.60(25.88)
Result	Can't reject	Can't reject
AIC	10.53	10.52
S-C	10.62	10.70
D-W	1.53	2.02

2.5 Conclusion

This paper seeks to explain the differences in return patterns of the upstream and downstream operators in the beef supply chain. Under the assumption that the Ricardian rent incidence is on the cow-calf operators, we set up a rational expectation dynamic model to investigate the interaction between cow-calf operators and feeding operators. The model shows that the cow-calf operators, who make production decision, will get positively correlated returns to maximize the whole life profit. With free entry and exit, the feeding operators can not affect the production decisions, and end up with pure random returns, which are only affected by random shocks. The model also suggests that feeding operation provides a cushion for cow-calf operators from the demand shifter and finishing feed cost. The empirical study shows that 85.4% of the Ricardian rent will go through to the upstream sector, giving strong support to the model's validity. The key parameters are calibrated through real world data, which also adds credit to the model specification. We believe it is the first time in literature to explicitly discuss the relationship between the two sectors of beef industry under the dynamic rational expectation framework.

We have four remarks about future possible extensions to the present study. Firstly, the

empirical study suggest that there is an AR(2) component in the cow-calf operator returns. This AR(2) structure can give rise to the cow-calf return cycles, which can not be explained by the current theoretical work. This requires to extend the model to a more complete biology structure, such as that of RMS (1994). Secondly, in addition to the calf retention decisions, cow-calf operators also need to make cull decisions of breeding cow. But our model did not distinguish fed beef price from unfed beef price, so we can not analyze this double decisions problem explicitly. Aadland (2001) has shown there will be a different effect from the classic conclusion as in RMS (1994) when considering this price differences. Thirdly, compare the integrated industry and two-layer industry, we can find that the main difference is that the cow-calf operators have to make production decisions one year earlier. In the integrated industry, the operators can delay to make the feeding decisions until there is more clear information about market demand or feeding cost. So, one can investigate whether this real option value is significant to justify the integration of the two sectors. Fourthly, the beef industry was affected by exogenous shocks, for example, Oprah Winfrey's comment about mad beef disease caused beef price plummet in 1996 although this effect disappeared quickly. By the setting of this model, such unexpected and uncorrelated shocks will affect the of down-stream sector profit but have little impact on the up-stream sector. Such case study on the different effects can be done in the future.

CHAPTER 3. ELECTRIC POWER MARKETS: HISTORICAL BACKGROUND AND METHODOLOGICAL TOOLS

3.1 Overview of Electricity Market Restructuring

3.1.1 Electricity Market Restructuring and Current Status

As the 21st century begins, the United States, like many other industrialized nations, is in the midst of a revolution in the electricity business. An industry dominated by monopoly utility companies, regulated from top to bottom by the states and the federal government, is seeing competition and deregulation in the generation and sale of electric power. As mentioned in Brennan et al. (2001), promoting competition has become associated with rules, regulations, institutions, and in some cases divestitures designed to ensure that the power markets operate efficiently and competitively. For that reason, the process of enacting and implementing laws and policies to bring more competition to electric power markets has come to be known as restructuring.

The propelling forces for market restructuring comes from high electricity price as a result of bad stranded investment decisions where suppliers could get guaranteed rate of return. As pointed out by Borenstein and Bushnell (2000), in a market-based environment, firms that do not have the security of a guaranteed rate of return on their investments will be more prudent in their capital expenditures and the way they manage risk. The promise of electricity restructuring is that a competitive market in power will lead to a more efficient electricity industry. Opening markets to competition generally gives firms better incentives to control costs, introduce innovations, and seek new ways to serve consumers. Competition will also allow those savings to be passed on to consumers. But ensuring that markets achieve their goals requires attention to make sure that competition works well where it can, and that

price regulation promotes efficiency where monopoly is inevitable. In this sense, electricity restructuring is far different from deregulation. One example for regulation in the restructured electricity market is the price caps which is necessary due to the lack of significant scale of real-time responsiveness demand.

In the U.S., the electricity restructuring is promoted and managed by FERC. In 1996, FERC issued Orders 888 and 889 to guide the formation of ISOs. In 2003, FERC published the White Paper Federal Energy Regulatory Commission (2003) for common adoption by North American wholesale power markets, referred to below as the Wholesale Power Market Platform (WPMP). The White Paper recommends standards for market design which contains several core features:central oversight by an independent system operator (ISO); a two-settlement system consisting of a day-ahead market supported by a parallel real-time market to ensure continual balancing of supply and demand for power; and management of grid congestion by means of locational marginal pricing (LMP). As depicted in Fig 3.1,versions of the WPMP design have been implemented (or adopted for implementation) in energy regions encompassing over 50% of U.S. generating capacity. These energy regions include the Midwest (MISO), New England (ISONE), New York (NYISO), the Mid-Atlantic States (PJM), California (CAISO), the Southwest (SPP), and Texas (ERCOT).

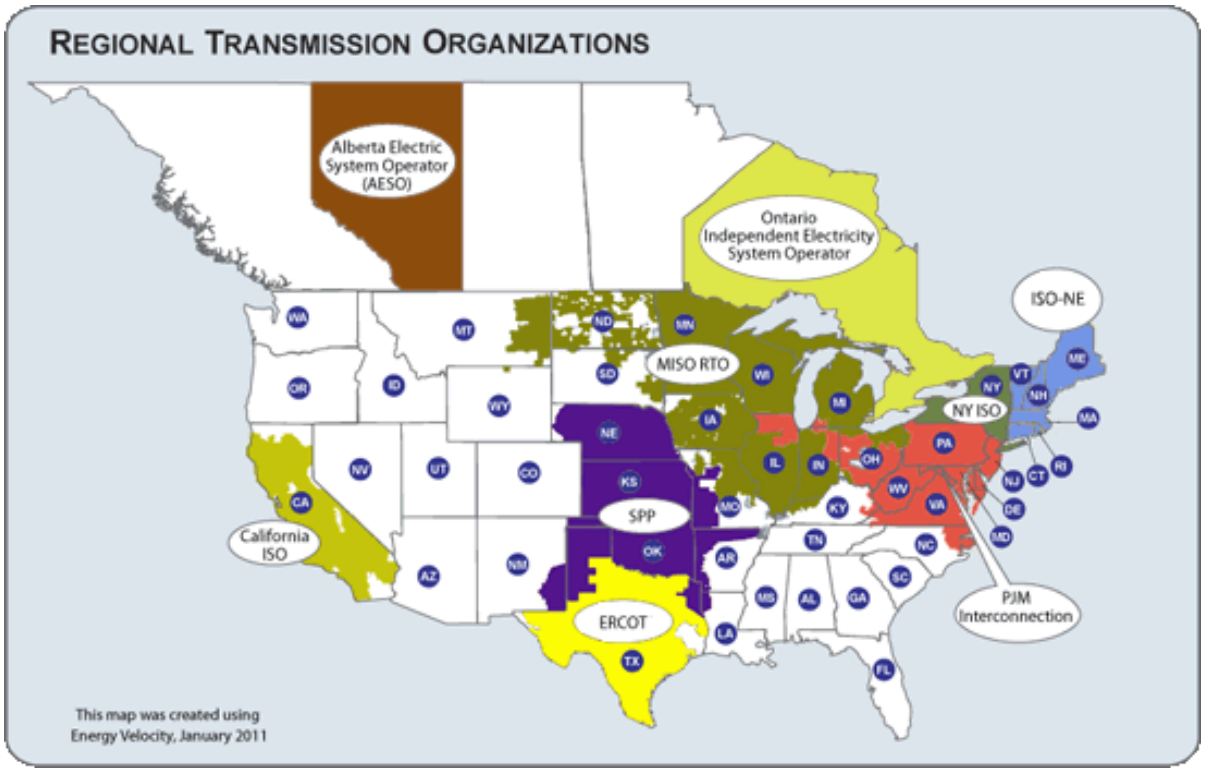

Figure 3.1: North American energy regions that have adopted FERCs wholesale power market design

Source: FERC Market Oversight

3.1.2 Market Operation

A typical timeline for the wholesale market operation is shown in Figure 3.2, as summarized by Botterud and Wang (2010). The procedures and timeline are based on the current rules in the MISO market. However, other markets are operated in a similar way, following FERC recommended market operation standard. The main steps in the market operations, including determination of reserve requirements, day-ahead (DA) operations, reliability-assessment commitment(RAC), and real-time (RT) operations.

In a typical day D, LSEs and GenCos bid into the day-ahead market before 11 am. ISO collects and evaluates all the bids and offers. ISO then runs security constrained unit com-

mitment(SCUC) to solve for the unit commitment decisions for operation day D+1. Unit commitment is a plan decision that can not be changed in the real-time operation because generation units can not be instantly turned on. Because of this limited ramping rate, ISO needs to ramp generation units before the operation hour to keep enough resource on line to serve load and meet reserve requirement. Given the unit commitment decisions are made, ISO runs security constrained economic dispatch (SCED) to solve for the shadow price of transmission line capacity, locational marginal price of local bus, cleared price-sensitive demand of LSE bids, cleared power output of GenCo offers. Since the whole procedure solves both the binary unit commitment variables and continuous power dispatch variables, this problem is known as mixed-integer-programming(MIP). The cleared price and quantity are then posted used for DA market settlement.

What follows day-ahead unit commitment(DA UC) is the reliability assessment commitment process. The RAC process provides input into the operation of the Real-Time Energy and Operating Reserve Market to ensure that sufficient Resources are available and on-line to meet the demand and Operating Reserve requirements within the Market Footprint.The RAC process also employs a SCUC algorithm to minimize the cost of committing the required capacity to meet forecasted demand. The difference between RAC and DA UC is that DA UC is based on the ***demand bids*** of LSE but RAC relies on the ***load forecast*** provided by load balance authority (LBA). In a word, the market participant settles their cost and revenue through the result of DA market, but the actual unit commitment and production follows the order of RAC. Because LSEs do not have the right incentive to bid all their load to the day-ahead market, ISO needs to make load forecast to guarantee there are sufficient generation resource on-line. By doing that, ISO separates the ***financial hedging function*** and ***physical scheduling function***.

When it goes to real-time operation in day D+1, ISO has few things to do with changing unit commitment which is a plan decision made in day-ahead operation. ISO clears real-time market using SCED every 5 minutes and post the ex-post price for RT market settlement. Another difference between DA and RT market is that in DA market, LSE submits price-sensitive bids which reflects demand elasticity. In the RT market, ISO only dispatch generation resource to

serve the realized power consumption, which has no demand elasticity.

After day D+1, market are settled using both the DA and RT market information. LSE is charged for the cleared demand at day-ahead price and load deviation at real-time price. GenCo are settled in the same way. The extra cost incurred due to difference between DA UC and RAC decisions are settled out of the market, which usually takes the form of uplift payment.

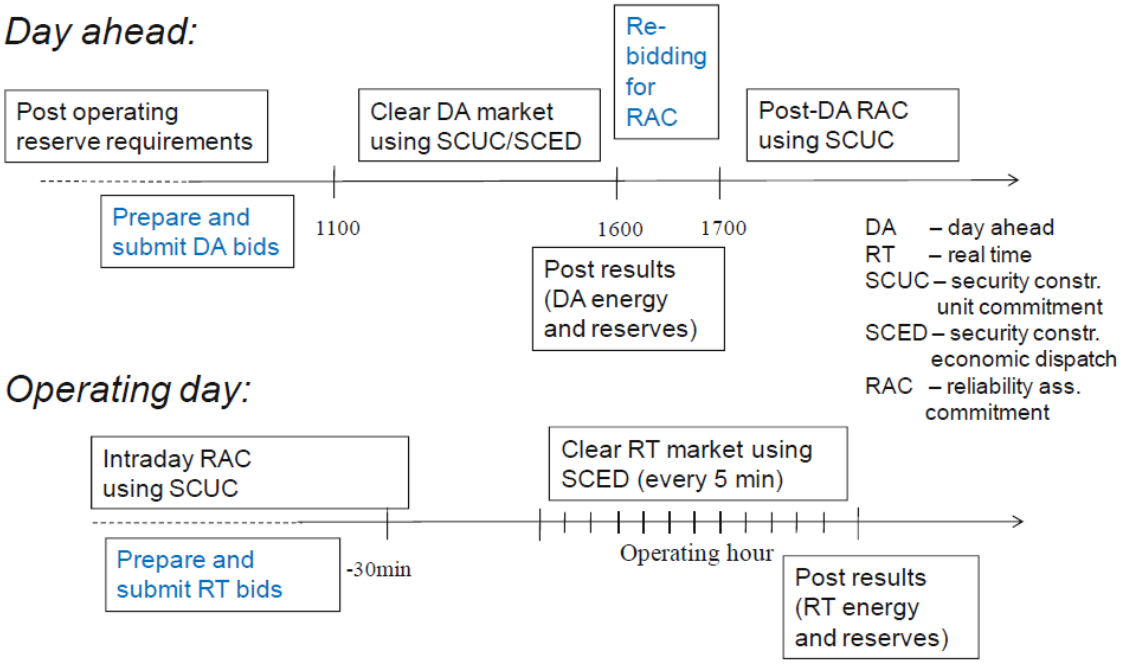

Figure 3.2: Market Operation Line for MISO

3.1.3 Electric Choice

ERCOT is chosen as our empirical benchmark for modeling retail competition because ERCOT has moved further than any other U.S. energy region towards the integrated restructuring of its retail and wholesale power market operations, as stated in Kiesling and Kleit (2009). Moreover, ERCOT is vigorously pursuing implementation of smart grid initiatives such as smart metering. For example, in December 2009 ERCOT launched a new system of wholesale settlement for its advanced metered customers based on their 15-minute electricity

usage ERC (2009).

One important theme of electricity market reform in ERCOT has been the divestment of traditional utility operations. Specifically, Chapter 25 of the *Public Utility Commission of Texas (PUCT)* now requires that each electric utility shall separate its business activities and related costs into separate units handling generation, transmission, and distribution. [1]

The result has been that retail competition in ERCOT is now realized through the separation of physical power flows from the financial contracting for power purchases and sales. As depicted in Fig. 3.3, power flow operations are managed by *Transmission and/or Distribution Utilities (TDUs)* whereas financial contracts are provided by *LSEs*.

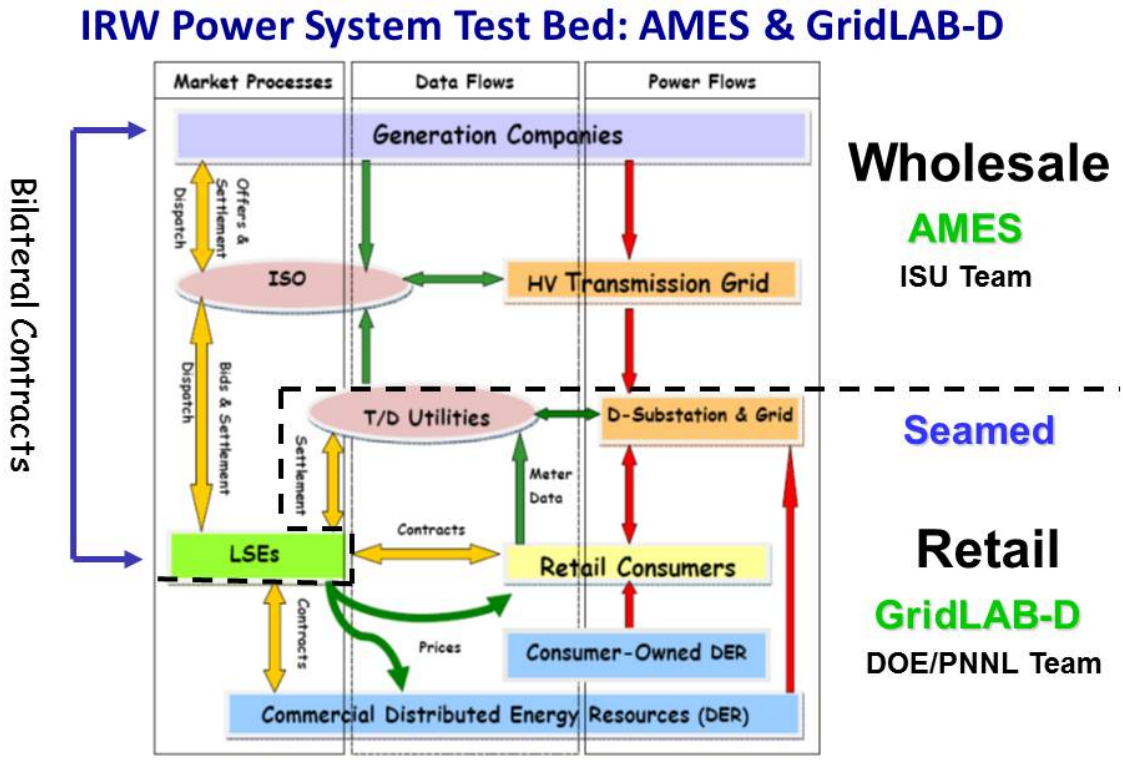

Figure 3.3: IRW Power System Test Bed: AMES & GridLAB-D

[1] more details can be found in PUC () operation manual.

More precisely, LSEs purchase bulk power from the wholesale market and resell it to retail customers through various financial contracts. LSEs are not responsible for infrastructure construction and maintenance, but compete for retail customers. Customers can switch financial contracts or LSEs without power usage interference.

Fig. 3.4 depicts the entities involved in ERCOT electric retail operation in greater detail. LSEs represent either *Competitive Retailers (CRs)*, which are the only organizations authorized to sell electricity to retail customers who have customer choice, or *Non Opt-In Entities (NOIEs)*, which are represented by wholesale delivery points. LSEs forecast their customer load and negotiate privately with other market participants, such as power marketers, to buy energy.

The CRs in ERCOT are further subdivided into *Retail Electric Providers (REPs)* and *Opt-In Entities (OIEs)*. Entry barriers for REPs in ERCOT are quite low. As reported in PUC (2009), by June 2008, 85 REPs were providing electric service to customers. These REPs were offering as many as 96 different products in various territories, including 13 REPs which were offering, between them, 23 different renewable energy options.

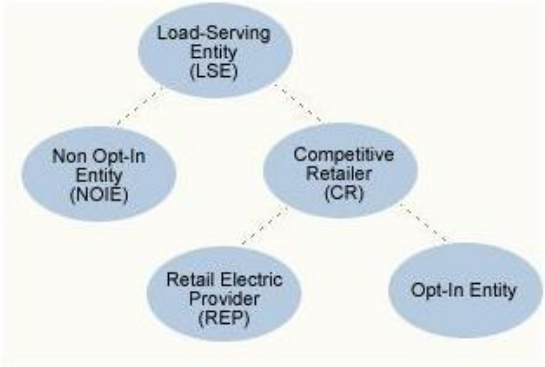

Figure 3.4: Retail Entities in ERCOT

Electric service switching can be done smoothly with this business separation structure. CRs interact directly with ERCOT when submitting switching requests, where customers choose a new CR. ERCOT processes the switching requests by working with TDUs to obtain the initial and final meter reads, confirming switches with customers, and confirming the switch with the relevant CRs once the switch is approved. The rules for REP operation are evolving to deal

with the ripple effect of REP's bankruptcy. For example, ERCOT is currently in the process of finalizing its REP rules on disclosure and billing terms.

Various types of customer service contracts flourish in ERCOT's retail market. Indeed, ERCOT provides over 96 different types of contracts for its retail customers. These contracts are primarily differentiated in terms of the type of rate structure that is offered to meet different customer needs. For example, customers can choose among *fixed-rate (FR)* contracts, *time-of-use (TOU)* contracts, and *real-time-pricing (RTP)* contracts.

3.2 Overview of Agent-Based Computational Model

3.2.1 Introduction of Agent-Based Model

Before goes to the detail of agent-based model, it is useful to look at a example of agent-based model(ABM). The study in Schelling (1971) is a good illustration of agent-based modeling. Household modeled in this experiment chooses to move when they observe there is not enough surrounding neighbors with the same color as them. When simulation reaches a stopping point, where households no longer wish to move, there is always a pattern of clusters of adjacent households of the same color. Figure 3.5 shows this pattern of clusters compared with the demographics distribution. This experiment mimics the behavior of household, and the emerging pattern could be used to explain the observed segregation.

(a) Actual (b) Simulated

Figure 3.5: Comparison of Actual Demographics and Simulated Result

As a general form of this example, agent-based model represents complex system that consists of **interacting, autonomous** components. A complex adaptive system has the additional capability for agents to adapt at the individual or population levels. Investigations into complex systems could be used to identify universal principles and emergent phenomenons of such systems. Following Macal and M.J. (2010), a typical agent-based model has three components:

1. A set of agents, their attributes and behaviors.

2. A set of agent relationships and methods of interaction: An underlying topology of connectedness defines how and with whom agents interact.

3. The agents environment: Agents interact with their environment in addition to other agents.

A typical agent structure is illustrated in Figure 3.6. In an agent-based model, everything associated with an agent is either an agent attribute or an agent method that operates on the agent.

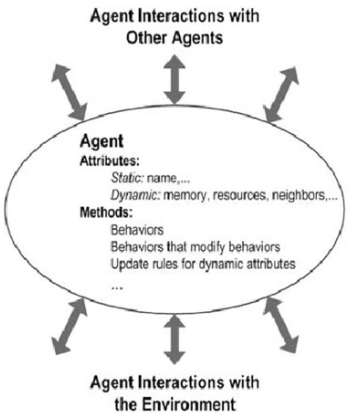

Figure 3.6: Typical Agent

3.2.2 Analytical Model v.s. Agent-Based Model

Like other mathematically intensive sciences, economics is becoming increasingly computerized. Despite the extent of the computation, however, there is very little true simulation. Simple computation is a form of theory articulation, whereas agent-based simulation is analogous to an experimental procedure. In another word, computation mimics the mathematical model while agent-based simulation mimics the true economic process. The computer has been seen as a legitimate tool in economics only when traditional analytical solutions cannot be derived. But agent-based simulation is usually shun by economist because the "bottom-up" approach cannot link the assumption and conclusions, while the traditional mathematical model could improve economic understanding by analytical deriving from a set of fundamental economic axioms. (Lehtinen and Kuorikoski (2007))

Although saying that, agent-based model has some attractive properties that could help economists to understand economic process. LeBaron et al. (1999) conducts an agent-based simulation of a simple financial market that produces interesting results that have proved to be hard to derive from an analytical equilibrium model. LeBaron et al. (1999) first derive analytically a general form of linear rational expectations equilibrium under the assumption of homogeneity of risk aversion and normal prices and dividends. The homogeneity assumption allows the use of a representative agent, which makes the analytical solution possible. An

agent-based simulation experiment is conducted to mimic stock trading behavior and system dynamics. The main simulation result is that if learning is slow, the resulting long run behavior of the market is similar to the rational expectations equilibrium benchmark. If the learning is fast, the market does not settle into any stable equilibrium, but exhibits many of the puzzling empirical features of real markets. The result highlights how important market phenomena can crucially depend on features such as learning dynamics and heterogeneity, which make the situation difficult or impossible to model analytically.

The simplicity and analytical tractability of equilibrium models nearly always rest on assumptions that are known to be highly unrealistic (perfect rationality and different kinds of homogeneity). The computation ability of agent-based modeling could help alleviate strong assumption and models some distinct features of the research object. It may not be appropriate to completely substitute analytical model with agent-based simulation, but the latter could be used as complement tools to test, validate analytical model or explain puzzles that analytical model cannot answer. Agent-based model is especially useful for the study of complex system with heterogenous agents and non-linear interactions among agents.

3.2.3 Application of Agent-Based Model in Electricity Market Research

Electricity market has been one of the most fertile grounds for agent-based simulation, mostly because electricity market research involves complicated market protocols, physical constraints, market inefficiencies and therefore potential market power. Agent-based model appears to be a strong research tools to study the dynamics of the market with the capability of dealing with high non-linear interactions and heterogeneous market participants.In recent years, more and more researchers have developed different kinds of agent-based models to simulate electricity markets. In Weidlich and Veit (2008), and Zhou et al. (2007), surveys about agent-based simulation of wholesale electricity markets give a lot insights of agent-based modeling application. In Zhou, Z. , Chan,W. and Chow, J. (2007), there are four agent-based electricity market simulation tools are mentioned:

1. Simulator for electric power industry agents (SEPIA), is developed by Honeywell Tech-

nology Center and the University of Minnesota. Generation companies, consumers and transmission operator are modeled as agents. Generation company agents can use both a Q-learning module and a genetic classifier learning module to make decisions. As one of the earliest agent-based simulator for power markets, it is a good example. And it contains two learning methods. But it lacks ISO agent, and has some practical limitations of model, both restrict its usage.

2. Electricity market complex adaptive systems (EMCAS), is developed by center for energy, environmental and economic systems analysis at the Argonne national lab. Generation companies (GenCos), transmission companies operators (ISOs) or regional transmission organizations (RTOs), demand companies (DemCos), consumers, and regula12 tors are modeled as agents. An EMCAS simulation runs over six decision levels, ranging from hourly dispatching to long-term planning. At each decision level, agents make certain decisions, including determining electricity consumption (customer agents), unit commitment (generation companies), bilateral contracting (generation and demand companies), and unit dispatch (ISO/RTO agent). EMCAS is used by regulatory institutions interested in market design and consumer impact issues, transmission companies and market operators interested in system and market performance, and generation companies for strategic company issues.

3. Short-term electricity market simulator-real time (STEMS-RT), is developed by Electric Power Research Institute (EPRI). STEMS-RT has features: agents rely on mathematical programming for bidding decisions and the latest techniques and strategies for bidding and realistic market rules can be added and their effects can be tested.

4. National electricity market simulation system (NEMSIM), is developed particularly for the Australia National Electricity Market (NEM). Interestingly, the latest NEM model is a modified and extended version of the Agent-Based Modeling of Electricity System (AMES) model.

3.2.4 Learning Algorithm

Learning algorithm plays a key rule in modeling adaptive agent. With certain learning ability, agent could learn from past experience and pick the best action for his own interest. Learning algorithm can be as simple as a sentence of code to define a rule of thumb. It can also be complicated as genetic learning which is a learn to learn process that can generate new learning method along the process. With these learning algorithms, versatile agents can be created to replicate the learning behavior of real economic process. The emergent system pattern resulted from agents with learning ability is more meaningful to capture the real world situation since humans are believed to continuously adjust his own action to adapt to the changing environment. The ignorance of individual participant's adaptiveness may cause misleading theory.For example, *Lucas Critique* states that macroeconomic theory should have solid microfoundation since individual decision maker could change its behavior when the policy changes and that will, in turn, change the economic structure. The theory that ignores this adaptiveness relies heavily on the historical data and will not be able to make good forecast within a changed economic environment. In this sense, agent-based model, by modeling micro-level adaptive decision maker, helps economist to understand the economic structure change and make better predict of a policy experiment.

As summarized in Li (2009), a key aspect of learning for agents is the amount of information (look-back,look-current, and look-ahead) that agents employ. The general learning process can be expressed as: at beginning, an agent is at a state in a general environment. When a stimulus occurs, the agent reacts to this stimulus by choosing a particular action (response). The agent then observes an outcome, and it uses this outcome to either weaken or strengthen the association between the state and the action in the future. Many different kinds of learning algorithms have been developed to focus on the information that will be used to update agent's belief. Li (2009) enumerates five widely used learning algorithm in the field of artificial intelligence(AI), including Reinforcement Learning, Stochastic Reactive Roth-Erev Algorithm, Q-Learning, Genetic Algorithm. The distinguishing features of each learning algorithm is the amount of information that one agent utilizes to strengthen or weaken the association between

state and action choice probability.

The other important concept of learning algorithm is the definition of state. Depending on this criteria, the learning algorithm can be categorized as stateless, exogenous-state, and rival-action-state learning. Some of the reinforcement learning algorithms are stateless learning which means that agent can not distinguish the environment that he is living in. Agent takes every game round as the same, and only updates its belief of the value of a specific action.

Q-learning, as a special form of reinforcement learning, takes exogenous environment variable as the state. As summarized by Yu (2007), Q-learning allows agents to learn how to act in a controlled Markovian domain with unknown transition functions. The environment is Markovian in the sense that state transition probabilities from state x to state y only depends on x , y and the action a taken by the agent, and not on other historical information. The learning works by successively updating the belief of the value of a state-action pair, $Q(x, a)$, which is known as the Q-value. This Q-value is the expected discounted reward for taking action a at state x and the following optimal decision rule thereafter. It is proved in Watkins (1989) that once these estimated converged to the correct Q-values, the optimal action in any states is the one with the highest Q-value.

Fictitious-play is another kind of learning algorithm which is firstly introduced by Brown (1951). The fictitious play differs from Q-learning in that it takes the opponent's strategy, instead of exogenous environment variable, as the state. The target for a fictitious player is to find the best strategy at each state. In it, each player presumes that her/his opponents are playing stationary (or possibly mixed) strategies. At each round, each player thus best responds to the empirical frequency of play of his opponent. The opponent's strategy may be conditioned on the fictitious player's last move. If at any time period all the players play a Nash equilibrium, then they will do so for all subsequent rounds. Berger (2007) also points out that the original idea of fictitious play is for players to update strategies alternatingly. Berger (2007) then uses original form of Brown (1951) to present a simple and intuitive proof of convergence in the case of nondegenerate ordinal potential games.

Both the Q-learning and fictitious-play are implemented in the simulation framework. The detailed description of these two learning algorithms realization can be found in the following

chapters.

3.2.5 Brief Overview of the Simulation Framework

To fulfill the task of investigating demand response impact on power market, a simulation framework is independently developed in the environment of Matlab. This simulation framework inherits and extends the function of AMES test bed (Li (2009)) and includes stub function that mimics the function of another test bed GridLAB-D [2]. This framework extends AMES to include two-settlement wholesale market, unit commitment process, demand response bidding, state-based learning algorithm, price responsive smart meter. This framework contains modules of *ISO, PowerGrid, ClearHouse, GenCo, LSE, Load, Learning, and DRProvider*. A brief description of each modules function is provided below.

3.2.5.1 Module of *ISO*

The module *ISO* is set up following MISO business practice manual. The market process follows the one described in section 3.1.2. In each day, ISO runs two-settlement market simultaneously. For the day-ahead-market, ISO collects 24 consecutive hourly day-ahead bids and offers from module of *LSE* and *GenCo* respectively. ISO then calls the function of day-ahead market in the module of *ClearHouse*. Depending on the needs, ISO can clear the market using either single DCOPF algorithm or combined Unit Commitment and DCOPF algorithm. After the market is cleared, ISO publishes cleared price and quantity result. For the real-time market, to reduce the computation load, real-time market is cleared every hour, instead of ever 5 minutes as used in the real-time market operation. Differently from day-ahead market, ISO uses the real-time load generated from the module *Load* rather than the load bids submitted by module *LSE*. Day-ahead supply offers are rolled over to the real-time market, *i.e.*, day-ahead and real-time market have the same supply offers. After collect all the real-time market information, ISO calls the function of realtime-market in the module of *ClearHouse*. In the real-time-market function, there is only one DCOPF algorithm. After the market is cleared, all the cleared result will be published.

[2] details of which can be found in chapter 3

Different from AMES, the market settlement process is made by the module of *ISO* instead of *GenCo*. After the two markets are cleared, the hourly cleared price and quantity are public information to all the agents. Using this data, ISO calculates and posts the actual payments paid by *LSE* and compensation received by *GenCo*.

Another task of ISO is to incorporate Demand Response into daily market operation. *ISO* takes the price-sensitive offers from module*DRProvider* and add that data into *ClearHouse*. As an institutional requirement, ISO needs to calculate a threshold price that forms the price floor of DR bids. To fulfill this task, ISO collects all the supply offers from module *GenCo*, and form an aggregated supply function. Aggregated supply function is then fit into exponential function and the threshold price is then calculated using Net-Benefit criteria. [3]

3.2.5.2 Module of *PowerGrid*

Throughout the simulation, it is assumed that the power grid topology does not change. Given the location of generation bus, load bus and branch reactance, powerflow on the transmission grid is then calculated using the DC approximation, which is known as state estimation. The algorithm employed in the module PowerGrid is swing-bus-free, which means that the powerflow calculation does not rely on the assumption of a specific swing bus. A detailed description of this algorithm can be found in the Appendix.

The benchmark power grid is a 5-bus transmission grid with branch reactances, locations of LSEs and GenCos, and initial hour-0 LSE fixed demand levels adopted from Lally (2002). The true parameter values of LSE load profile, GenCo supply function, and transmission grid reactances can be found in table B.1 of Li (2009).

3.2.5.3 Module of *ClearHouse*

The module *ClearHouse* is used to clear the market by maximizing social benefit subject to physical constraints. The social benefit contains three parts, supplier surplus, consumer surplus, and ISO surplus. *ClearHouse* contains three functions, day-ahead-market, real-time-market and unit-commitment. The first two functions employ the built-in solver "quadprog"

[3] Details of DR bids can be found in Chapter 5

to solve the quadratic DC Optimal Power Flow problem. The last one calls a commercial solver "CPLEX" to solve the Mixed Integer Programming problem. [4]

3.2.5.4 Module of *GenCo*

The module *GenCo* mimics generator company behavior in the power market. Everyday, GenCo submits supply offers to ISO and receive the cleared information from ISO after the market is cleared. Supply offer has three parts, marginal supply function, generation capacity limit and ramping cost. The marginal supply function is formulated as

$$MC_i(p_{Gi}) = a_i + 2b_i p_{Gi} (\$/MWh) \tag{3.1}$$

which is defined over an operating capacity interval of

$$Cap_i^L \leq p_{Gi} \leq Cap_i^U \tag{3.2}$$

The inter-temporal ramping cost is formulated as

$$RC_{i,t}^{up} = c^{up} \tag{3.3}$$

$$RC_{i,t}^{dn} = c^{dn} \tag{3.4}$$

where $RC_{i,t}^{up}$ is the ramping up cost and $RC_{i,t}^{dn}$ is the ramping down cost. Throughout this dissertation, it is supposed that GenCo submitted DA offers will roll over to the RT market, *i.e.*, supply functions in DA and RT market are the same. But due to the load forecast error, GenCo RT actual generated power p_{Gi}^{RT*} can be different from DA dispatched amount p_{Gi}^{DA*}. The net earning of GenCo for supply power in day D+1 hour H is:

$$NE_i(H, D) = LMP_{k(i)}^{DA} * p_{Gi}^{DA*} + LMP_{ki}^{RT} * p_{Gi}^{RT*} - VCost(p_{Gi}^{RT*})(\$/h) \tag{3.5}$$

where $VCost(p_{gi}^{RT*})$ is the variable cost which can be avoided in the daily operation. The unavoided cost, also known as sunk cost, can be compensated from daily net earning.

[4] Details of DCOPF can be found in the appendix and the description of Unit Commitment can be found in chapter 6

3.2.5.5 Module of *LSE*

Following the market rules, LSE only participates in the DA market. For each day D, the demand bid reported by LSE j for each hour H of the day-ahead market in day $D+1$ consists of a fixed demand bid $p^F_{Lj}(H)$ and a price-sensitive demand bid function:

$$D_{jH}(p^S_{Lj}) = c_j(H) - 2d_j(H)p^S_{Lj}(H)(\$/MWh) \tag{3.6}$$

defined over a purchase capacity interval

$$0 \leq p^S_{Lj}(H) \leq SLMax_j(H)(MW) \tag{3.7}$$

where p_{Lj} denotes the bids of real power for LSE j. LSE could have learning ability in terms of choosing different combinations of $\{c_j, d_j, SLMax_j\}$.

3.2.5.6 Module of *Load*

The module *Load* is designed to generate real-time load. It has two modes for the user to choose from.

- passive mode.

  In this mode, real-time load is set the same as the sum of day-ahead fixed load p^F_{Lj} and cleared price-sensitive load:

  $$p^{RT*}_{Lj}(H) = p^F_{Lj} + p^{S*}_{Lj} \tag{3.8}$$

  This mode can be used to compare the clearing result of DA and RT market.

- smart-meter mode.

  This mode models the load equipped with smart meter device that can make optimized power consumption decisions that balance between cost and utility of electricity consumption. [5].

[5] Details can be found in chapter 4

3.2.5.7 Module of *Learning*

There are two learning methods adopted in the *learning* module. Other modules, such as *LSE* and *DRProvider*, are allowed to call this module. By doing that, we can model adaptive intelligent agents that could learn from the past experience.

- Q Learning.

  Q-Learning which is one kind of reinforce learning algorithm that depends on the observed state. Agents with Q-Learning ability are allowed to choose the action that maximize its own objective function, either net earning or utility. This learning module updates the value belief of the {state, action} pair chosen in a experiment cycle. [6]

- Fictitious-Play.

  Fictitious-Play is different from reinforce learning in that it takes the opponent's action, instead of the observed environment variable, as state variable. A sequential Fictitious-Play algorithm is implemented which means that one agent picks the action that maximize its objective function given all other opponents' action unchanged. The system will reach an equilibrium when no one has the intention to change action. [7]

3.2.5.8 Module of *DRProvider*

The module *DRProvider* models the behavior of DR providers that participate in the wholesale market. Module *DRProvider* has similar bidding functionality as module *LSE*. The bids of *LSE* also contain two parts, the fixed demand and price-sensitive demand, as defined in equation 3.6. Different from *LSE*, *DRProvider* could control the real-time consumption, which mainly refers to the real-time load curtail. In this sense, *DRProvider* is a combination of module *LSE* and *Load*.

To run a simulation, not all the modules are needed. For example, the simplest simulation could only involve the module *ISO*, *LSE*,*GenCo*, and *ClearHouse*, with one-settlement system.

[6] Details can be found in chapter 4
[7] Details can be found in chapter 6

This framework is also flexible to add new modules or functions depending on the research purpose. The following three chapters conduct three specific experiment on this framework, emphasizing on different aspect of demand response program.

CHAPTER 4. SIMULATION RESULTS for TWO SETTLEMENT ELECTRIC POWER MARKETS WITH DYNAMIC-PRICING CONTRACTS

THE increasing demand for energy along with growing environmental concerns have created the need for a modern power grid with the capacity to integrate the renewable energy resources at large scale. In this paradigm shift, demand response and dynamic pricing are often advocated as means of mitigating the uncertainty of the renewables and improving the systems efficiency with respect to economic and environmental metrics. Studies, like Li and Tesfatsion (009a), argues that generators have strong incentive to exercise market power by withholding capacity or increasing supply offers when facing a low demand elasticity. The potential benefit of introducing more flexible retail contracts has been examined by Borenstein et al. (2002). They argue in favor of real-time pricing, characterized by passing a price, that best reflects the wholesale prices, to the end customers. They conclude that real-time pricing delivers the most benefit in the sense of reducing the peak and flattening the load curve.

There are also extensive literatures that compare dynamic pricing with the fixed-price contract which is still the most dominant form of retail electricity contract. Borenstein and Holland (2005) claims that fixed-price contract not only lead to the prices and investment that are not first-best, it even fails to achieve the constrained second-best optimum. They also argue that the increase of RTP customer proportion will hurt the existing RTP customer's benefit. Joskow and Tirole (2006) pushes this argument forward by analyzing different scenarios depending on the advanced metering availability and LSE retail contract tariff. A more diversified conclusions regarding the efficiency loss of different scenarios are drawn from this analysis.

However, this real-time, price-based coupling between supply and demand creates new challenges. Firstly, the bill risk is transferred from LSE to the final customer, who pays the

volatile wholesale market price now. A customer with RTP contract could find itself consuming a large quantity of power on the day that prices skyrocket, resulting in a high monthly bill. Borenstein (2006) measured this risk using empirical industrial customer data and claimed this risk can be mostly hedged off through simple forward contract. The other problem of potential large-scale RTP customer is the information asymmetry between the customers and the system operators. Indeed, real-time pricing under information asymmetry leads to increased uncertainty due to the uncertainty in consumer behavior, preferences, private valuation for electricity, and consequently, unpredictable reactions to real-time prices. The high penetration level of RTP customer may increase the load volatility and hurt power grid operation if these uncertainties can not be fully removed. Roozbehani et al. (2011) give a mathematical prove that the system will be stable when the demand elasticity of price is lower than the supply elasticity given the assumption that retail customer take a stationary price forecast method.

In this study, both the problems of risk transfer and system volatility will be carefully examined. The simulation model is set up using the simulation framework as discussed in chapter 3. Most of the previous studies only look at the open-loop problem, either only the effect of RTP on retail customer's behavior or only the effect of load responsiveness on system operation. This study will bring the two pieces of a ring together and make a close-loop study.

Particularly, the model simulates how the load customers equipped with smart meter response to the ex-ante, or day-ahead price. LSEs respond to final load customers' action and bid into wholesale market. LSE behaves for its best profit by collecting information from past bidding record and corresponding payoff. The model finally close the loop by forming a new price for the next day and passing it to the load customers. The mode for passing ex-post price to final customers is also examined using a simplified load and network model. Both of the simulations designed to pass ex-ante and ex-post price illustrate the system dynamics that agents interact with the environment signal and other agents.

4.1 Overview of the Integration of Retail and Wholesale Project

As argued in the general introduction chapter, restructured power market is a complicated research object that involves the issue of power engineering, law, economics and IT commu-

nication. the complexity of the market characteristics suggest the need for an integrated restructuring of both retail and wholesale power markets. Rather than use actual systems as test beds, however, we are developing an agent-based test bed that seams together two previously developed agent-based test beds:

- AMES IA2 (2011), an open-source software platform developed by a team of researchers at Iowa State University for the study of strategic trading in ISO-operated restructured wholesale power markets with congestion managed by LMP.
- GridLAB-D PNL (2011), an open-source software platform developed by the U.S. Department of Energy at Pacific Northwest National Laboratory (PNNL) for the study of power distribution systems for end-use customers with power loads arising from a variety of modeled appliances and equipment.

The task of the IRW project includes the following:

1. Extension of AMES to include a fully operational two-settlement system (real-time and day-ahead markets)
2. Development of the IRW Power System Test Bed: Seaming of AMES (wholesale) and GridLAB-D (retail) test beds
3. Development of an initial test case: A household resident with an intelligent HVAC system
4. Modeling and implementation Load Forecast Function to LSE
5. Design and running of experiments to study IRW system performance under alternative household electricity contracts
6. Development of an experimental lab set-up and an analytical model of distributed photovoltaic (PV) generation for IRW power system analysis
7. IRW system impacts of reactive power support by distributed PV generation
8. Preparation of IRW Power System Test Bed for open source release

All these itemized tasks aim at preparing a test bed that is capable of testing the effect of bringing on-line the price-responsive load customers with the assistance of smart grid technology. The first test case is developed using the seamed test bed as illustrated in Fig(4.1). In this test case, wholesale market has the same setup as that in AMES, details of which can be found in Li and Tesfatsion (2009). The difference from AMES setup is that LSE has more empirical grounded load information. As shown in Fig(4.1), each LSE serves households whose power consumption behavior is extensively modeled in the GridLab-D. The interface of the two test bed is developed in MySQL. The communication between the two test beds include physical power flow, price series, and real-time load meter information.

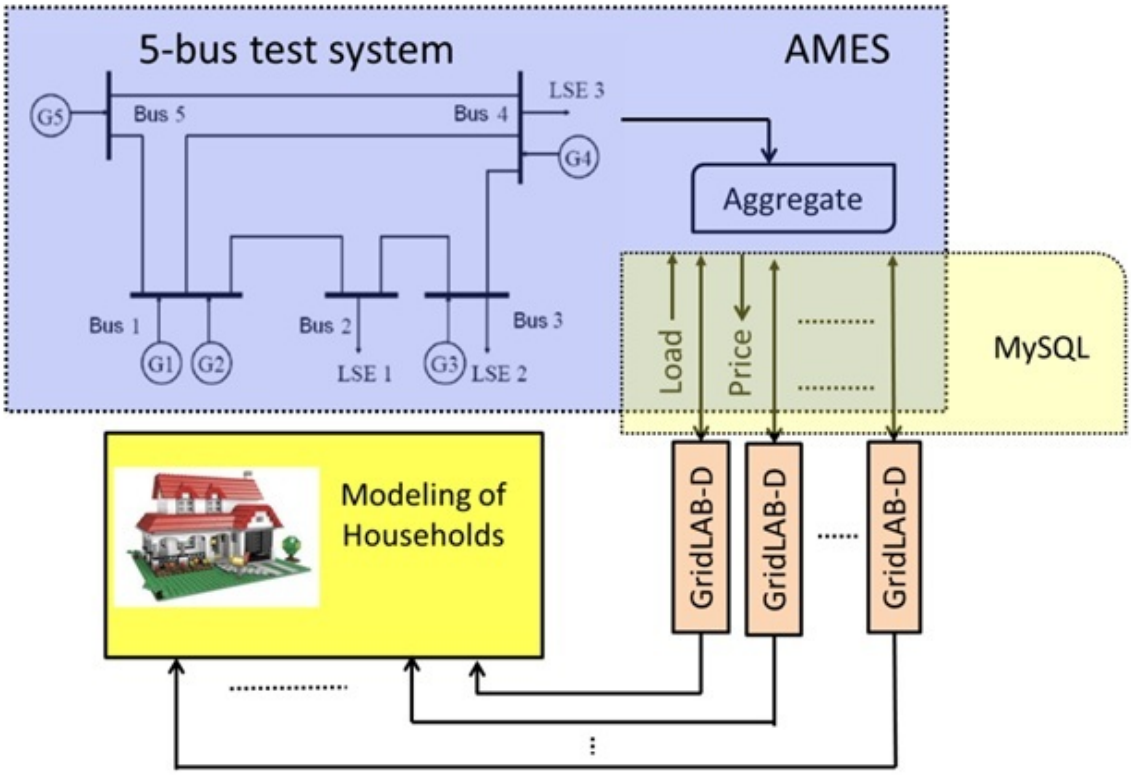

Figure 4.1: Overview of the IRW Project

There are two key questions in seaming the two test beds. The first one being asked is how load customers respond to the dynamic pricing, *i.e.*, what is the best response of load

customers to maximize its utility. The second question is what is LSE best strategy to bid into wholesale market. Keep in mind, day-ahead market is cleared using LSE's demand bid while real-time market is cleared using load customer's actual load consumption. The following two sections are dedicated to answer these two questions in order to finish the puzzle of seaming.

4.2 Smart Meter Design

This section tries to design a smart meter that can control the work sequence of HVAC, on behalf of final customers, to maximize final customer's net surplus. After setting customer's preference parameters, the smart meter will be able to automatically control HVAC responding to the dynamic price. This smart meter does not need to change the function mechanism of HVAC but only make a little modification for the run-time control. This convenient characteristic makes it cheaper and easier to be widely adopted.

4.2.1 Model Setup

Suppose the state equations defining the change in the average inside temperature of home h over periods 1 through T take the following form: For each $t = 1, \ldots, T$,

$$m_t^h \;=\; S_t(e_t, w_t, m_{t-1}^h) \quad , \tag{4.1}$$

where the initial average inside home temperature from "period 0" is exogenously given at the beginning of period 1:

$$m_0^h \;=\; \overline{m}_0^h \quad . \tag{4.2}$$

Suppose the *total cost* accessed on the home h resident in period t by the LSE, conditional on a given energy usage, price, and contract type, is given by the following function:

$$C_t(e_t, \mathrm{LMP}_{tk}, R^h) = [\mathrm{LMP}_{tk} e_t + \tau_t e_t + F_t] \tag{4.3}$$

Let the *instantaneous utility* attained by the home h resident during period t, conditional on a given home temperature, energy usage, price, and retail contract, be measured by a function u_t defined as follows:

$$u_t(m_t^h, e_t, \mathrm{LMP}_{tk}, R^h) = \Big[v_t(m_t^h) - \alpha_t C_t(e_t, \mathrm{LMP}_{tk}, R^h)\Big] \tag{4.4}$$

Let the *total utility* attained by the home h resident over periods 1 through T, conditional on a given home temperature vector $\mathbf{m}^h$, energy usage vector $\mathbf{e}$, price vector $\mathbf{p}$, and retail contract R^h, be measured by a function U_T defined as follows:

$$U_T(\mathbf{m}^h, \mathbf{e}, \mathbf{p}, R^h) \;=\; \Sigma_{t=1}^{T} \left[u_t(m_t^h, e_t, \mathrm{LMP}_{tk}, R^h)\beta^t \right] \tag{4.5}$$

Let the expected value of (4.5), conditional on (4.1) and (4.2), be denoted by

$$E\left[U_T(\mathbf{m}^h, \mathbf{e}, \mathbf{p}, R^h)\right] = \int_W \left[U_T(\mathbf{m}^h, \mathbf{p}, \mathbf{e}, R^h)\right] f(w)dw \tag{4.6}$$

Putting this all together, now consider the following optimization problem:

$$\max_{\mathbf{e}} E\left[U_T(\mathbf{m}^h, \mathbf{e}, \mathbf{p}, R^h)\right] \tag{4.7}$$

subject to

$$m_t^h \;=\; S_t(e_t, w_t, m_{t-1}^h) \quad , t = 1, \ldots, T \quad ; \tag{4.8}$$

$$m_0^h \;=\; \overline{m}_0^h \quad . \tag{4.9}$$

Let

$$\mathbf{A}^h \;=\; (\mathbf{u}, \beta, T, R^h) \tag{4.10}$$

denote an attribute vector consisting of the home h resident's vector $\mathbf{u}$ of instantaneous utility functions $\mathrm{u}_t(\cdot)$, time-preference discount factor β, planning horizon T, and contract type R^h. Then any solution to this expected utility maximization problem will have the following form: For each $t = 1, \ldots, T$,

$$\mathbf{e}_t^{\mathrm{opt}} \;=\; G_t^{\mathrm{opt}}(\mathbf{p}, \overline{m}_0^h, f(\cdot), \mathbf{A}^h) \tag{4.11}$$

How can a smart meter be constructively designed to generate a sequence of HVAC energy usages that satisfactorily approximate the optimal solution (4.11) for the home h resident?

Suppose the comfort function $\mathrm{v}_t(\cdot)$ for the home h resident in each period t is the same for all t and can be approximated by a concave continuous piecewise-linear "tent function" $\mathrm{v}(\cdot)$ whose graph in the temp-u plane consists of an upward slopping line segment L_1 and a downward sloping line segment L_2 that meet at a kink point corresponding to the home h resident's most preferred temperature setting, $\mathrm{BestTemp}^h$. Let $\mathrm{vMax} \equiv v(\mathrm{BestTemp}^h)$. Also,

suppose the slope of L_1 is $a > 0$ and the slope of L_2 is $-b < 0$ for each period t. Finally, suppose the opportunity cost measures α_t for the home h resident take on a constant value α for each period t. Then the home h attribute vector (4.10) can be approximated by

$$\mathbf{X}^h = (a, b, \text{BestTemp}^h, \text{vMax}, \alpha, \beta, T, R^h) \tag{4.12}$$

The "only" remaining task is then to design the smart meter to generate a satisfactory approximation to (4.11) having the following form: For each $t = 1, \ldots, T$,

$$e_t^* = G_t^*(\mathbf{p}, \overline{m}_0^h, f(\cdot), \mathbf{X}^h) \tag{4.13}$$

4.2.2 Numerical Solution and Implementation

As discussed in the above, the smart meter design problem will be a stochastic dynamic problem with finite time horizon. This finite time horizon dynamic problem can be solved by backward induction. Backward induction divides a multi-period optimization problem into a sequence of one-time period optimization problem, which greatly reduces computation load. There are two crucial steps in the backward induction method, the last period optimization and Bellman equation. In the specific smart meter design problem, the last period optimization problem is given as follow:

$$\begin{aligned} & V_0(m_{T-1}^h, \omega_T, p_T) \\ =& \max_{e_T}[v_T(m_T^h) - \alpha_T C_T(e_T, LMP_{Tk}, R^h)] \\ =& \max_{e_T}[v_T(S_T(e_T, \omega_T, m_{T-1}^h)) - \alpha_T C_T(e_T, p_T)] \end{aligned} \tag{4.14}$$

where V_0 is the value function with 0 period to go. The state transition function (4.1) can be retrieved from equation (1) and (2) in the ETP model. Notice that the current problem is only a planning problem, and it assumes that the smart meter could control power usage at time t. Therefore, we can drop other equations in ETP model which capture the air conditioner's power control function. Instead, the heat flux created by air conditioner is express as follow:

$$Q_{HVAC,T} = 3.413 \cdot COP \cdot e_T \tag{4.15}$$

Then, the solution of last period's optimization problem is featured by the first-order condition

$$v_T'(m_T^h) \cdot S_T'(e_T) = \alpha_T \cdot p_T \tag{4.16}$$

where p_T is the retail price charged on final customers. Equation (4.16) states that in the optimal condition, benefit of cooling house temperature is equal with the associated cost. At the last hour of a day, the smart meter will not pay respect to the inter-temporal problem.

The Bellman equation captures the inter-temporal relationship. For example, with one period to go the Bellman equation has the form as:

$$\begin{aligned} & V_1(m^h_{T-2}, \omega_{T-1}, p_{T-1}) \\ =& \max_{e_{T-1}} \ [u_{T-1}(m^h_{T-1}, e_{T-1}, p_{T-1}) + \\ & \beta \int_{\omega_T} V_0(m_{T-1}, \omega_T, p_T) dQ(\omega_T, \omega_{T-1})] \end{aligned} \tag{4.17}$$

The first order condition for equation(4.17) is as follow:

$$\begin{aligned} & v'_{T-1}(m^h_{T-1}) \cdot S'_{T-1}(e_{T-1}) \\ =& \alpha_{T-1} \cdot p_{T-1} + V'_0(m^h_{T-1}) \cdot S'_T(m^h_{T-1}) \cdot S'_{T-1}(e_{T-1}) \end{aligned} \tag{4.18}$$

Compare the optimal condition for Bellman Equation (4.18) with optimal condition for the last period problem (4.16), we can see that the marginal benefit of extra energy consumption should be equal with the marginal cost as well as the effect on next period's value function. Solving equation (4.17) enables us to obtain the explicit form of policy function $e^*_{T-1}(m_{T-2}, \omega_{T-1}, V_0, Q)$ and the value function $V_1(m^h_{T-2}, \omega_{T-1}, p_{T-1})$. Iterating this process and we can get a solution for the smart meter's dynamic problem, which is featured by a series of policy function with the form of equation (4.13).

Notice that, this planning problem may be viewed as the best solution with the assumption that the smart meter could control directly the electric power of air conditioner. The granularity of each period must be small enough so that the concept of energy consumption e_t in this model could approximate the power concept in ETP model which is based on continuous time. The small time step will increase computation work to solve this dynamic problem. Also, this planning method does not pay respect to traditional air conditioner's functionality. Air conditioner works under bang-bang control mechanism, which means that energy consumption is automatically determined after the thermal stat is set. This control mechanism is reflected in equations (3),(4), and (5) in the ETP model.

There is an easy way to incorporate ETP model's result into smart meter's dynamic problem and cohere to the function of thermal stat. This method assumes that smart meter receives price signal, outdoor temperature distribution, current indoor temperature, and combines those data with consumer's preference parameters to solve optimization problem and calculate the optimal setting points. After the thermal stat is set to these optimal points, the following work will be handed over to the traditional air conditioner.

To make this method work easily, it assumes that the setting points are the temperature that consumers care about. That is to say, the setting points are the variable m_T we used in the above dynamic problem model. If the indoor temperature is mainly controlled by the air conditioner, the setting point will be a good approximation of the average indoor temperature. Under the situation when $e_T = 0$, the indoor temperature changes slowly and the setting point may not be a good approximation of indoor temperature. In the implementation, we can correct this error by comparing the final temperature at each period with the setting point. If there is a big difference, we will say this temperature setting is infeasible, and mark the energy consumption to be infinite, which will exclude this archer from the dynamic problem.

Given this assumption, the model is greatly simplified. Firstly, if we assume the outdoor temperature does not change within one hour, then the model granularity is as long as one hour. This is because the final customer will receive a price signal at each hour. Within each hour, the state variables do not change. So, the computation work is largely reduced. Secondly, we can use the simulation result from ETP model directly. Given the two setting points in adjacent hours,$m_t and m_{t+1}$, ETP model could calculate the energy consumption e_t. This is the right information we need to solve this dynamic problem. Thirdly, this method will rely on current air conditioner functionality and does not require further work to rebuild air conditioner.

4.3 Wholesale Market Design

This section illustrates the wholesale market design. The experiment continues to rely on the 5-bus test as used in Ames, as shown in Fig(4.2). Although simple the five bus net work could represent many outstanding characteristic of meshed power grid, such as the transmission line congestion, generator capacity limit, power flow path. So, this network is widely adopted by

the researchers to conduct experiments on the power market issues. The detailed information of the parameter settings, including generator location, generator cost, branch reactance, can be found in the table [B.1] of Li (2009).

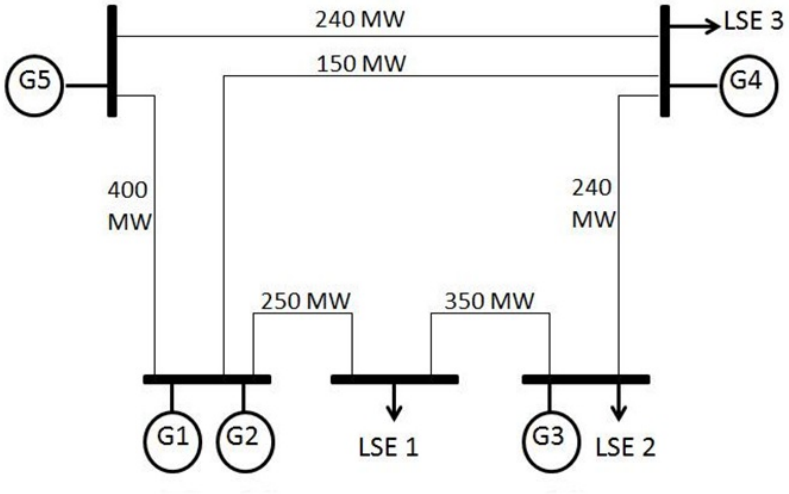

Figure 4.2: Grid Topology

The load profile is a little different from that used in AMES 5-bus test case. In this study, the HVAC energy consumption profile is firstly generated before smart meter is installed. A portion of fixed load is replaced by the fixed HVAC energy consumption while this part of load is allowed to respond to varying price. The load profile and LMP, known as benchmark case, is illustrated in Fig(4.3).

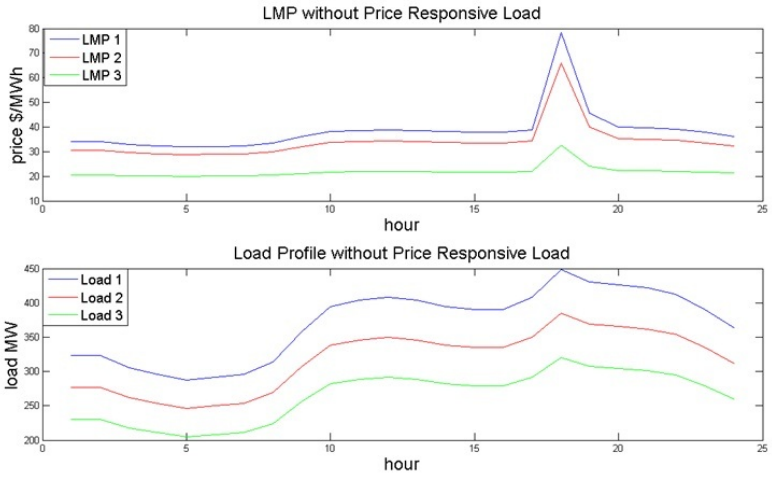

Figure 4.3: Benchmark Outcomes: LMP and Fixed Load Profiles for Traditional HVAC Case

4.4 Smart Meter Control and LSE Operation

In this section, we will test the function smart meter as being installed on the HVAC so that it can respond to the day-ahead price. The loop will not be close until next section. The HVAC with smart meter is responding to the LMP as shown in Figure(4.3). Figure(4.4) shows the result of the dynamic programming control. There are five scenarios shown on this graph, where the first three is the energy consumption of a smart HVAC to respond to the three load bus LMPs respectively. The fourth one is a fictitious case for HVAC to respond to a flat-price of 30 $\$/MWh$. The last one is energy consumption when the consumer only fix the temperature setting at 70 degrees without considering the opportunity cost of using this energy. From this figure, it is clear that with the assistance of smart meter, users use less energy at the peak hour when the cost to cool down the building is high.

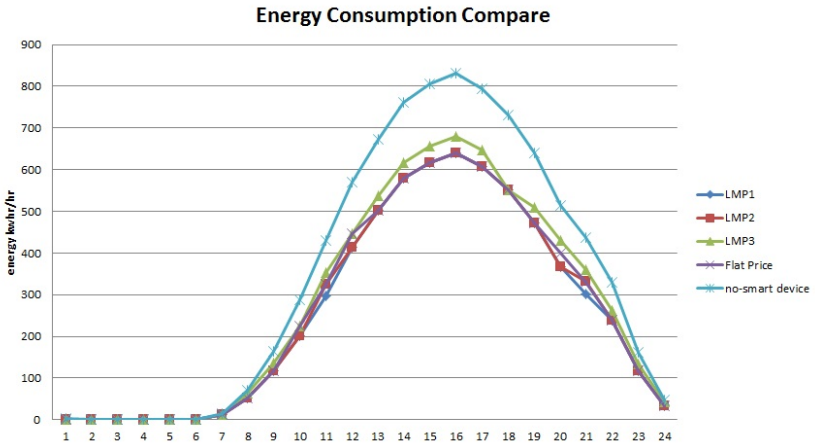

Figure 4.4: Energy Consumption under Dynamic Pricing

Figure(4.5) shows the control of indoor temperature as compared with outdoor temperature under the flat price of 30 $\$/MWh$. As shown in the above, the indoor temperature reflect the control sequence as a result of the optimal energy consumption decisions. From this figure, it is clear that consumers are willing to sacrifice some comfort at the hours when outdoor temperature is very high. Figure (4.6) compares the indoor temperature control sequence under different LMP. This figure shows that when customers under the cheapest price is the last one to increase the indoor temperature and the indoor temperature only stays in the upper bound when the lmp reaches peak at hour 18.

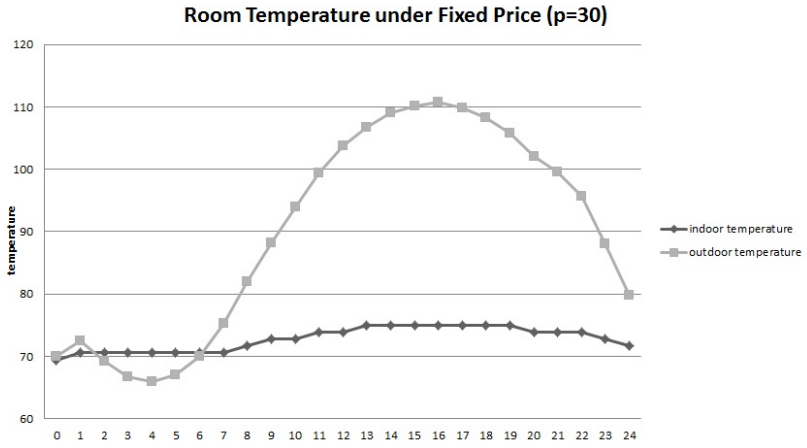

Figure 4.5: Room Temperature

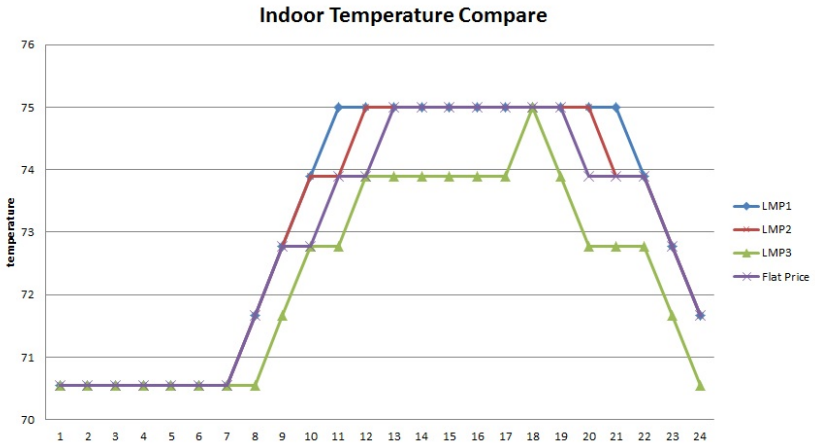

Figure 4.6: Indoor Temperature Control

We will turn the focus on LSE's behavior when facing price responsive smart HVAC load. Firstly, we close the loop by assuming that LSE does not forecast the price-responsiveness of smart HVAC demand but continue to bid the fixed load profile into day-ahead market. Figure(4.7) shows the comparison of day-ahead and real-time LMP. As it appears, there is a peak in day-ahead market while this peak is shaved in real-time market. This is not a surprising result given LSE still bid into the market the fixed load. The high demand of electricity at the peak hour creates a price spike. Final customers, in turn, respond to the price spike by cutting its load consumption which shaved the price spike.

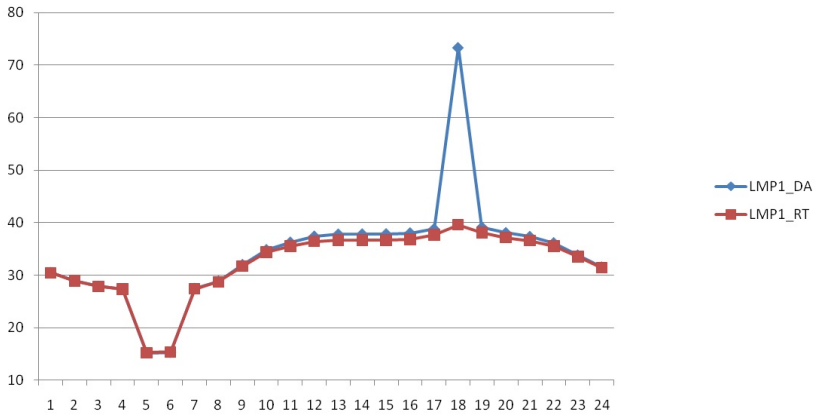

Figure 4.7: Day-Ahead vs. Real-Time LMPs at Bus 1 When LSEs Ignore Price-Responsiveness of Smart HVAC Demand

LSE profit is defined in equation 4.19. Final customers pay at the day-ahead price P_{DA} for the quantity of actual consumption Q_{RT}. LSE, instead, pays ISO the procurement cost for the cleared amount Q_{DA} at day-ahead price P_{DA}, adjusted by the real-time deviation Q_{DA} at price P_{RT}. The typical day operation profit for the three LSE agents are listed in Table(4.1). This is not a coincidence that all the LSEs experiences a financial loss for the daily operation. Go back to Figure(4.7), we can see that LSE purchases power at high day-ahead LMP but sells back at low real-time LMP. It is more clear to reinspect equation(4.20). LSE's profit is a negative product of price deviation and quantity deviation. Given the market setup, price deviation is caused by load deviation, and they have a positive correlation $corr(\triangle P, \triangle Q) > 0$. So, LSE will end up with a financial loss if it fails to forecast the load customers consumption pattern.

$$\pi = P_{DA} \cdot Q_{RT} - (P_{DA} \cdot Q_{DA} + P_{RT} \cdot (Q_{RT} - Q_{DA})) \tag{4.19}$$

$$= -(P_{RT} - P_{DA}) \cdot (Q_{RT} - Q_{DA}) \tag{4.20}$$

Table 4.1: LSE Profit with Dynamic Pricing Customers

LSE 1	**LSE 2**	**LSE 3**
-1582	-2665	-555.7

4.5 LSE with Learning Behavior

As discussed above, LSE has an incentive to forecast final customers energy consumption behavior to avoid financial loss. But the relevant parameters, such as house thermal features and people's preferences, are private information which neither LSE nor ISO has the right to access to. LSE can only learn from the historical data to try to capture final customer's new load profile. The complexity to make load forecast is significantly enlarged when there the consumer is charged at dynamic price. This is because conventional load forecast only predict a fixed load level at a specific time point. With the passing of LMP, LSE needs to make a

forecast of load at both a time point and price level. On the other hand, LSE can only observe the past realized load level at a specific price level. This historical data has little help for LSE to retrieve a demand curve. A recent paper Centolella (2010) points out the necessity to develop new forecast tools to integrate dynamic pricing customers into current power market operation. But so far, there is no well designed load forecast tools available for the industry use.

This study is not targeted at developing a forecast tool for LSE to use but check LSE's bidding behavior given a new market environment. LSEs are allowed to choose from an action set for the day-ahead bidding. LSE does not have access to final customers private information and it can not make a forecast based on load generation mechanism. Instead, LSE learns from its daily operation profit. LSE tunes up demand bidding to reach a better chance of high profit. I will firstly show the Q-learning algorithm and then goes to the simulation result.

4.5.1 Q Learning Algorithm

This section starts with a detailed introduction of Q-Learning algorithm and parameters used for this experiment. By the procedure of Q-Learning, in the n^{th} step the agent observes the current system state x_n , selects an action a_n, receives an immediate payoff r_n, and observes the next system state y_n. The agent then updates its Q-value estimates using a learning parameter α_n and a discount factor γ as follows:

$$
\begin{aligned}
&\text{If } x = x_n, \text{ and } a = a_n \\
&Q_n(x,a) = (1-\alpha_n)Q_{n-1}(x,a) + \alpha_n[r_n + \gamma V_{n-1}(y_n)] \\
&\text{Otherwise,} \\
&Q_n(x,a) = Q_{n-1}(x,a) \\
&where V_{n-1}(y) \equiv \max_b\{y,b\}
\end{aligned}
\tag{4.21}
$$

LSE then chooses next step's action according to the probability as defined in the follow:

$$
p_D(x,a) = e^{Q(x,a)/T_D} / \sum_{b \in AD_i} e^{Q(x,b)/T_D} \tag{4.22}
$$

By this algorithm, each agent only updates the Q-value for the action a taken in state of x. It takes three parts of information to update the Q-value, the last step Q-value $Q_n(x, a)$, current reward r_n, and future expectation $V_{n-1}(y_n)$.

The learning parameter α for a state-action pair (x, a) is set to be $\alpha = 1/T^{\omega}_{x,a}$, where $T_{x,a}$ is the number of times that action a has been taken in state x. By this setting, agent gives more weight to the information for the pair x, a when there are few historical information. The weight will gradually decrease as the agent acquires more information of that pair.

The temperature parameter T_D is given by: $1/T_D = K \times (D)^{\beta}$, where $K > 0$ and $beta < 0$ are constants and D is the number of steps that have currently been simulated. At the beginning stage of simulation, $1/T_D$ is small implying that the choice probability $p_D(x, a)$ is close to uniform distribution so that agent could have chance to explore the action space. As the simulation goes by, $1/T_D$ increases and the agent assigns high probability to the action with high Q-value. By doing this, the agent could explore the action space first and finally exploit to the action that has the best payoff.

Coming down to this experiment, it is assumed that there are two states for every LSE, a hot day and a cool day. The states corresponds to outdoor temperature, which is illustrated in Figure(4.8). At the beginning of each day, the state of weather is randomly generated which is then observed by both the LSE and smart HVAC.

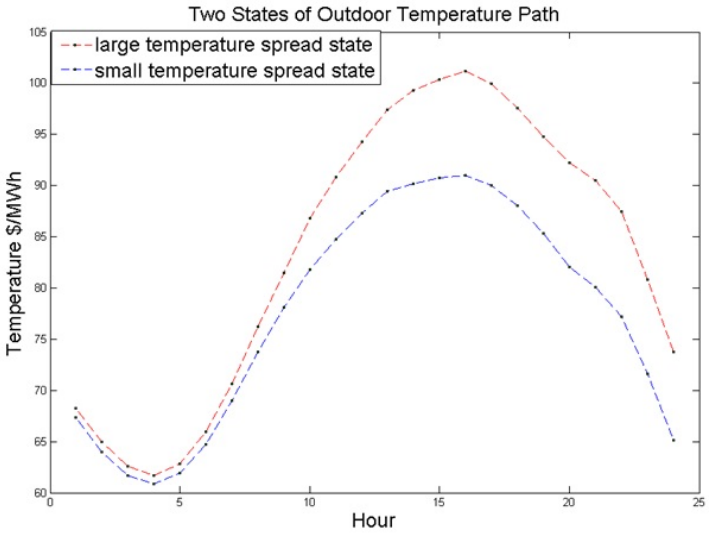

Figure 4.8: Two States of Outdoor Temperature Path

4.5.2 Simulation Result

The experiment is designed as depicted in flow chart(4.9). At the beginning of this experiment, smart HVAC is introduced to replace conventional HVAC. At each day, LSE observes the state of weather and chooses a bidding curve. The dashed box represents a learning cycle, which includes both day-ahead and real-time operation. After the learning cycle, LSE calculates its daily profit for serving final customers followed by updating belief of taking this bidding curve. The simulation will stop when reaching the maximum iteration.

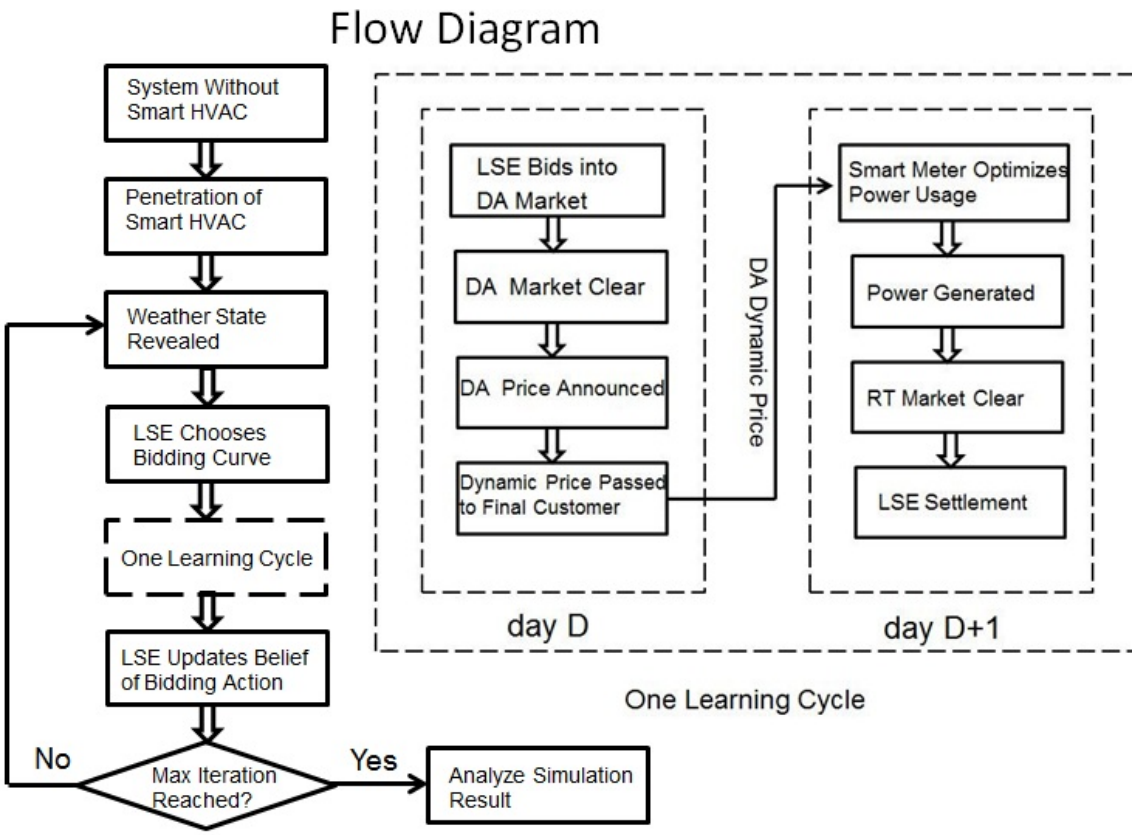

Figure 4.9: Flow Chart of Experiment

Figure(4.10) to Figure(4.12) illustrates the simulation result. Figure(4.10) shows LSEs' daily average profit through the experiment. We can see at the early stage, LSEs are testing different bidding curves and get a negative profit. Thereafter, LSE learn to give up bad performed bidding curve and stick with well performed bidding curve. Gradually, all the three LSEs start to increase their daily profit and finally approaches to 0. Figure(4.11) tells similar story. There is a clear decreasing trend in LSE load deviation. Less load deviation translates into higher profit level. In the end of simulation, all the three LSEs have learned to make bidding curve to minimize load deviation. Figure(4.12) compares the two-settlement price at the day D=1 and day D=100. In day D=1 there is a big deviation of the two prices as a result of the significant load deviation. At day D=100, the two markets almost merge together which represent an efficient market.

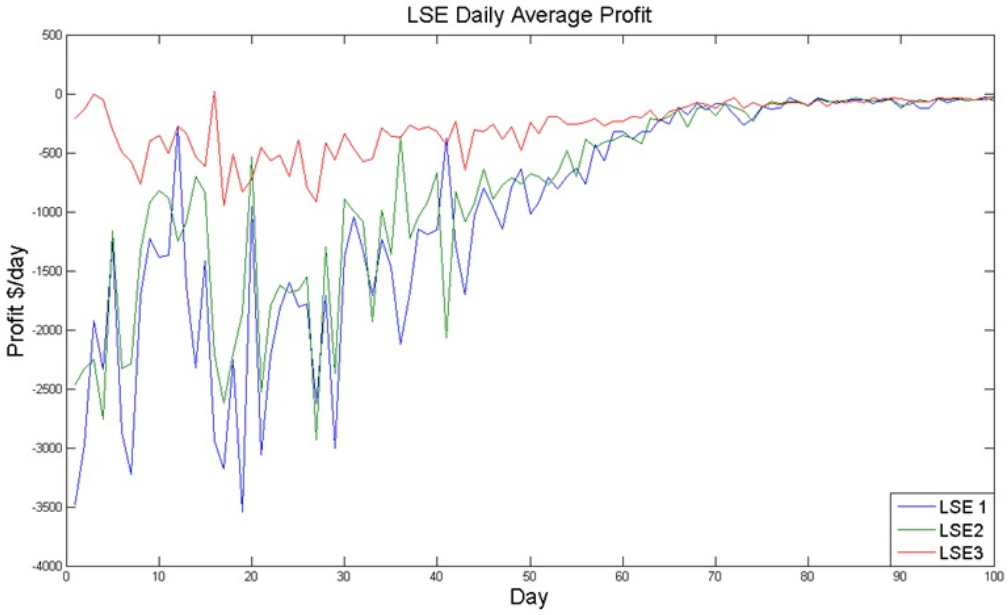

Figure 4.10: LSE Daily Average Profit

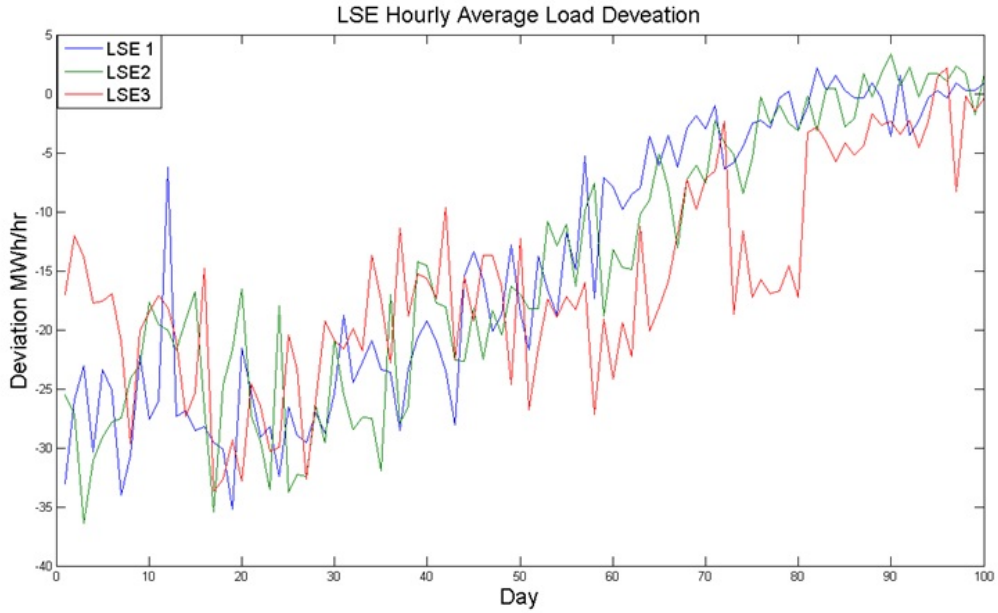

Figure 4.11: LSE Hourly Average Load Deviation

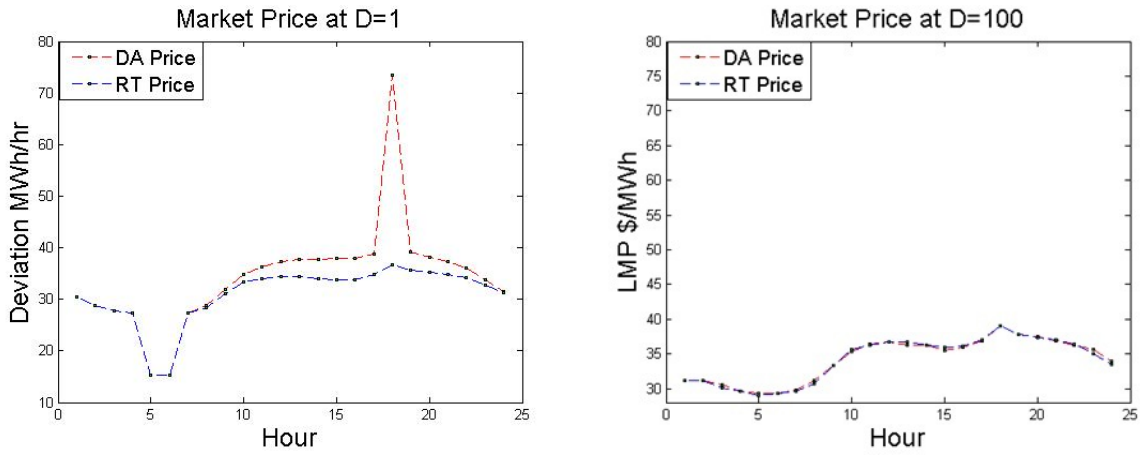

(a) Two Settlement Market at D=1

(b) Two Settlement Market at D=100

Figure 4.12: Market Performance Comparison

4.6 ex-post price passing

In the previous section, we have investigated the market operation with passing day-ahead price to final customers. As pointed out by Roozbehani et al. (2011), load customers can response to both ex-ante and ex-post wholesale market price. The mode of passing ex-ante price is the same as the idea of passing day-ahead price. The market can also charge load customers ex-post price, which is cleared after actual load is realized. This ex-post price can be interpreted as real-time price. Load customers do not observe the price charged for the consumption. Instead, they need to make a prediction of the real-time price. Compared with the ex-ante price case where LSE lacks of load responsiveness information, passing ex-post price to final customer lead customers lack of price information at the consumption hour. Many concerns have been given to the possible high system volatility due to this asymmetric information problem.

Roozbehani et al. (2011) has proved that the market is stable if the demand elasticity of price is lower than the supply elasticity. The assumption of this theory is that load customers have stationary price forecast method. If load customers believe the best forecast for tomorrow's price is today's price, a martingale style price forecast, then the market prices evolvement can

be captured by Figure(4.14). The day 1's price p_1 is higher than the true price p^*. Load customer will consume at a low level d_2 at day 2, which will cause a low price p_2. This process will continue until the price and quantity converges to the true level. If demand elasticity is lower than supply elasticity, this process will converge and vice versa.

There

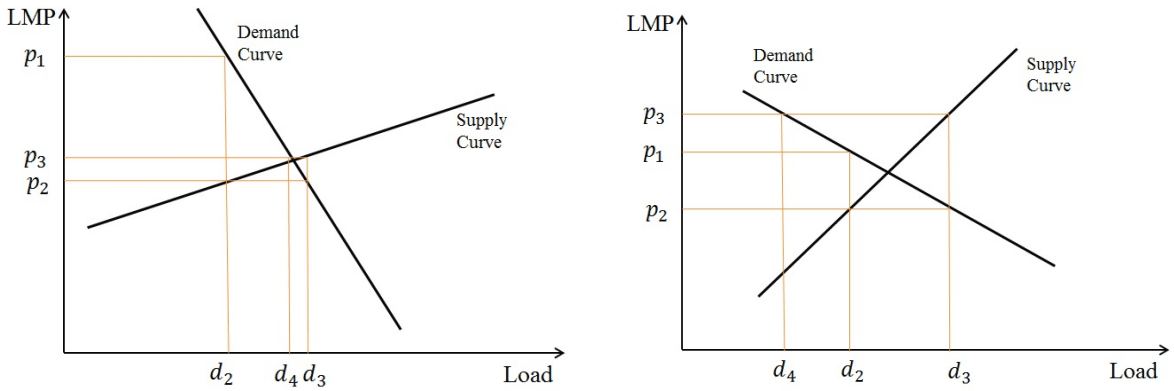

(a) Low Demand Elasticity of Price

(b) High Demand Elasticity of Price

Figure 4.13: Market Price Evolve with Martingale Load Forecast

However, the assumption that load customers stick with one price method is too strong. If customer find one forecast method performs badly, the good chance is that they will abandon it. As inspired by LeBaron et al. (1999), I propose an artificial world that each customers can choose from several price forecast method. They will stick with the well performed methods and abandon those badly performed ones. During this process, each customer's action can affect the other load customer's payoff and therefore their belief of current action. Because of this highly non-linear relationship, it is very natural to employ agent-based model to study the system volatility problem.

4.6.1 Model Setup

I will continue to use the simulation framework to conduct this experiment. As the main focus is on load customers interaction and system outcome, the network and suppliers information is simplified away. So, in this system, there is no transmission line congestion and all

the customers are located at the same bus, paying for the same LMP.

Supply curve is supposed to be a linear curve:

$$S(p_t) = \beta \times p_t \tag{4.23}$$

For a typical customer i, the load demand contains fixed load $d_{fix,t,i}$ and price-sensitive load $d_{ps,t,i}$:

$$d_{t,i} = \mu_1 \times d_{fix,t,i} + \mu_2 \times (1 + \delta_{t,i,0}) \times d_{ps,t,i}(\hat{p}_{t,i}) + \delta_{t,i,1} \tag{4.24}$$

where μ_1 and μ_2 are the weight assigned to fixed load and price-sensitive load. $\delta_{t,i,0}$ and $\delta_{t,i,1}$ are the white noise to load curve. $\hat{p}_{t,i}$ is customer i's forecast of price at t. The price-sensitive load is assumed to be linear:

$$d_{ps,t,i}(\hat{p}_{t,i}) = -\alpha/N \times \hat{p}_{t,i} \tag{4.25}$$

The market is cleared at demand equals supply:

$$\sum_{i}^{N} d_{t,i} = \beta \times p_t \tag{4.26}$$

In order to compare with the conclusions in Roozbehani et al. (2011), the demand elasticity is set to be larger than supply elasticity, with $\alpha = 3$, and $\beta = 6$.

4.6.2 Price Forecast Method

This study tries to evaluate market robustness under the circumstance that ex-post price is passed to load customers. Load customers must forecast the actual price to make a consumption decision. Customers may hold different opinions about the operation hour's price. Their collective action, in turn, affects actual outcome of price. Therefore, price forecast is an important factors for the emergent behaviors of all the agents. In this section, four methods of price forecast are provided for load customers to choose from.

1. Mean Value, which is set at the true market price p^*

$$\hat{p}_{t,i} = \bar{p}; \tag{4.27}$$

2. Martingale

$$\hat{p}_{t,i} = p_{t-1}; \tag{4.28}$$

3. Moving Average

$$\hat{p}_{t,i} = 1/2 \times (p_{t-1} + p_{t-2}); \tag{4.29}$$

4. Mean Reverse

$$\hat{p}_{t,i} = \bar{p} - (p_{t-1} - \bar{p}) \tag{4.30}$$

Figure 4.14 shows the market price when there is only one forecast methods adopted by the load customers. In this figure, only method 1 is stable as we expected. Method 2 and four are diverging and method 3 is oscillating.

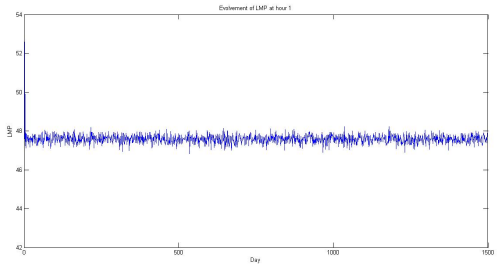

(a) Price Forecast Method 1 Only

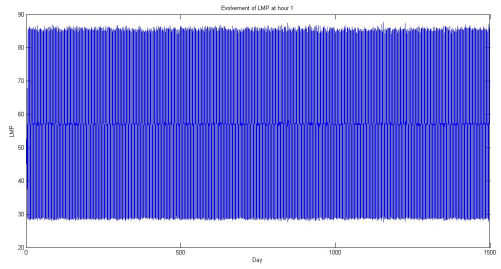

(b) Price Forecast Method 2 Only

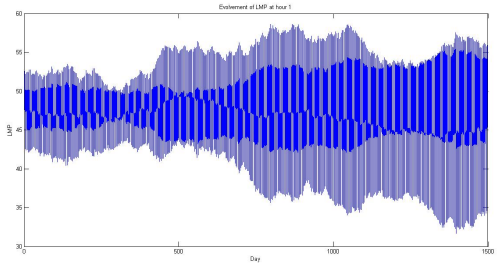

(c) Price Forecast Method 3 Only

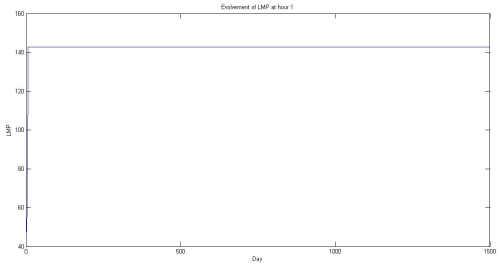

(d) Price Forecast Method 4 Only

Figure 4.14: Market Price Evolve with One Price Forecast Method Only

4.6.3 Emergent Behavior with Adaptive Load Agent

This study targets to investigate the collective of load agents given that they have to make a forecast of future price. The uncertainty of price signal could give rise to severe price volatility which hurts system stability and increase operation cost dramatically. The agent-simulation model endows load agents ability to learn from historical price, a result of interaction of all the load agents. Each agent takes different forecast methods to avoid bad consumption decisions as a result of bad price forecast. The price pattern emerged from this interaction sheds light on how robust the market is. Also, severity of price volatility is tested under different scenarios which may give clue to find key factors affecting system stability.

The simulation starts with a basic scenario, with all four price forecast methods provided to load agents. There are 20 agents living on the same bus interacting in this game. Figure 4.15 shows the simulation result with realized ex-post price. Market price is very volatile in the beginning stages and converges quickly. The price volatility in the later stage is caused by the white noise.

Figure 4.16 shows how agents choose their actions. In the beginning stages, all the four actions are taken by load agents. But agents gradually converge to action 1 after day 500. Forecast method 1, by it self, is an unbiased forecast method given everyone use it. During the learning process, forecast method 1 is not guaranteed to have unbiased forecast. But it does outperform other forecast methods and finally be adopted by all the load agents.

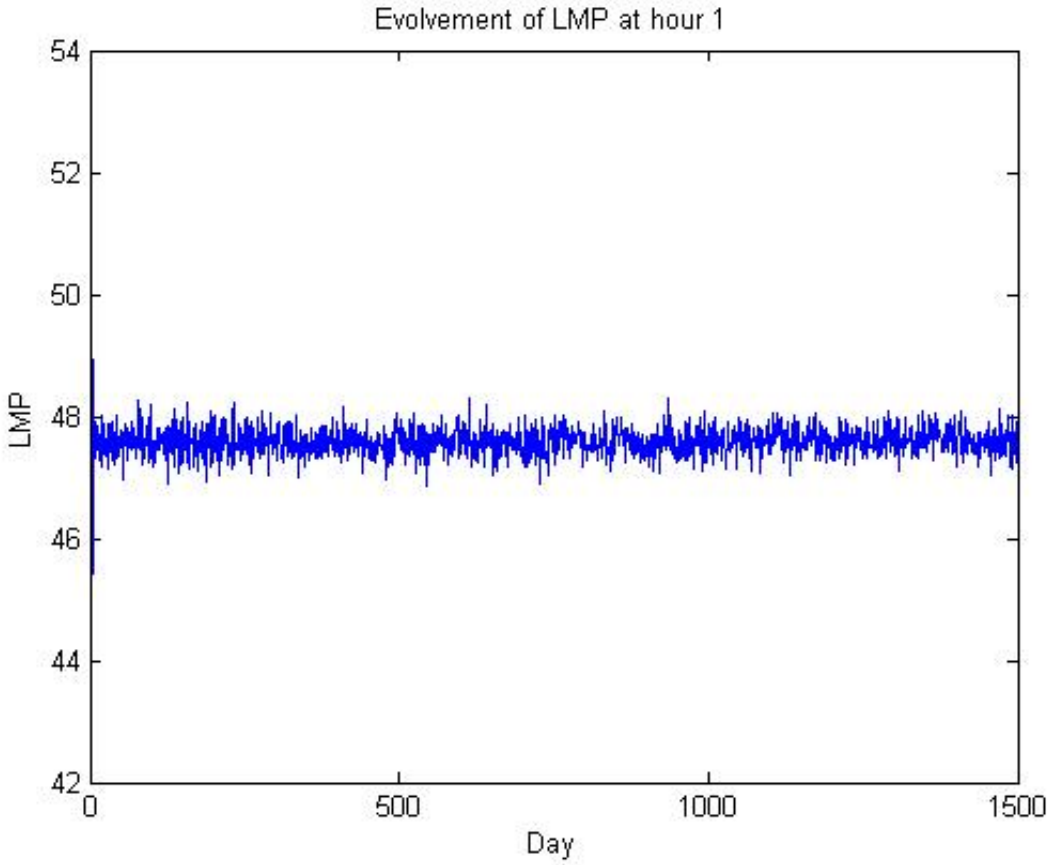

Figure 4.15: LMP at hour 1

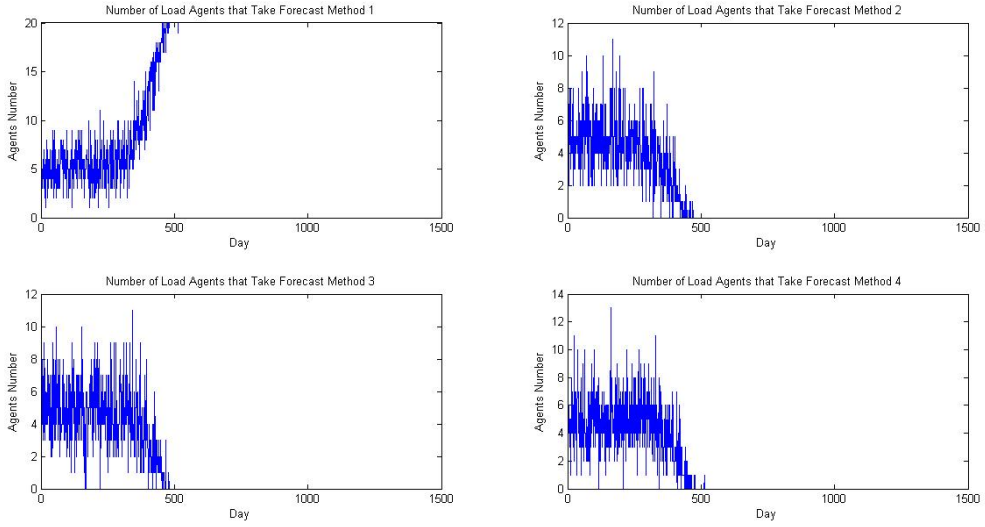

Figure 4.16: Price Forecast Methods Taken by Load Agents

4.6.4 Emergent Behavior with Wrong Mean Expectation

In the last subsection, it shown that the right belief leads the market to the right result. It may be a too strong assumption of right mean value since a single agent should not have the ability to forecast the right mean value as endowed by the model designer. In this subsection, the mean value is set to deviate the correct mean. Other simulation parameters keep the same.

Figure 4.17 shows the simulation result with a wrong belief of mean. It is clearly that in this market, the price is much more volatile than that in the correct mean-value scenario. Figure 4.18 shows that it takes a longer time for load consumers action to converge. During this learning process, mean-value method does not outperform other methods. Even if every agent has that belief, the market will not end up with the believed price. Instead, the moving-average method becomes the best one that all agents converge to. As shown on Figure 4.14c, if all the agents converge to this method, the system price will oscillate. This result appears to be a higher volatility than the basic scenario.

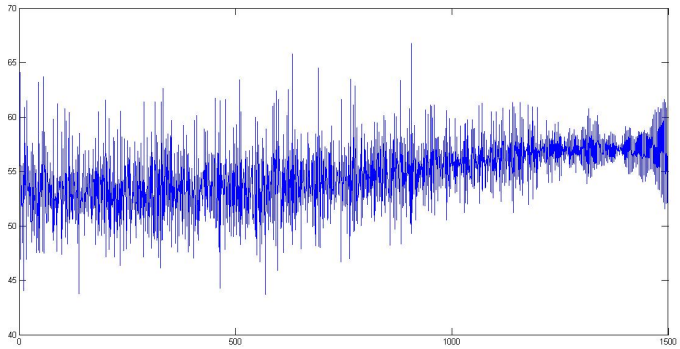

Figure 4.17: LMP at hour 1 with Wrong Expected Price Mean

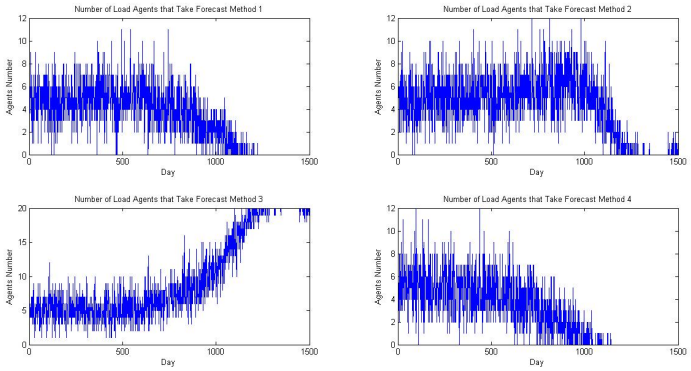

Figure 4.18: Price Forecast Methods Taken by Load Agents with Wrong Expected Price Mean

4.6.5 Effect of Agent Numbers on Emergent Behavior

In this subsection, the effect of agent number on system pattern is investigated. Similar as the subsection 4.6.4, the mean-value is set to be a wrong one. Other parameters are kept unchanged.

Firstly, the agent number is increased to 100, result of which is shown on Figure 4.19 and 4.20. Compared with the case on Figure 4.17, load agents reach an agreement at a much earlier stage of the simulation.

Secondly, the agent number is reduced to 5, result of which is shown on Figure 4.19 and 4.20. When the load agent number is small, they fail to reach an agreement and the resulting

price is very volatile.

These two cases indicate that the number of agents has a nontrivial impact on system volatility. If the agents number is small, one agent's behavior change has a significant impact on the market price and hence other agents' belief. When there are many load agents, the population sticking with one forecast method is more stable. The emergent price has a clearer pattern for the agents to follow.

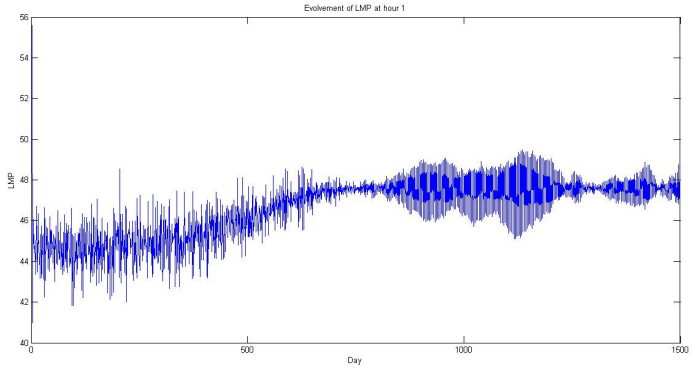

Figure 4.19: LMP at hour 1 with 100 Load Agents

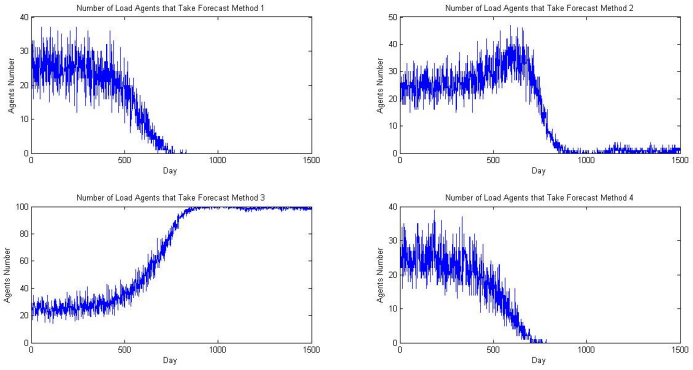

Figure 4.20: Price Forecast Methods Taken by 100 Load Agents

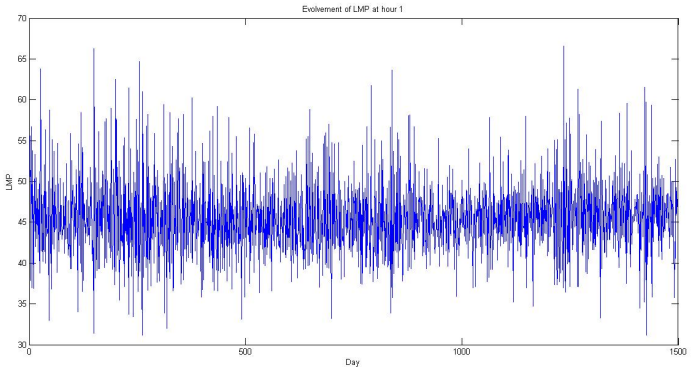

Figure 4.21: LMP at hour 1 with 5 Load Agents

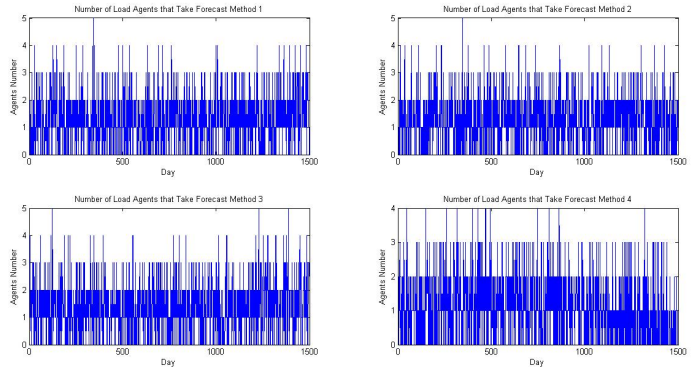

Figure 4.22: Price Forecast Methods Taken by 5 Load Agents

4.6.6 Effect of Available Price Forecast Methods on Emergent Behavior

As already talked in the above subsections, right mean-value forecast method outperform other forecast methods. After the mean is set at a wrong one, moving average becomes a better forecast method than other three. In this subsection, I will test the effect of available price forecast methods on the market price volatility. Number of agents are kept as 20.

Firstly, the best performed right-mean forecast method is removed. Simulation results are shown on Figure 4.23 and 4.24. Not surprisingly, mean-average forecast method wins just like that in the case of Figure 4.17. But the price volatility is much less in the learning stage because the wrong mean forecast method adds extra noise to the market price.

Secondly, the mean-average forecast method is removed from forecast toolbox. Simulation results are shown on Figure 4.25 and 4.26. The results show that load agents do not stick with any particular method. Instead, both of the methods are chosen by the customers. In fact, the martingale and mean-reverse are totaly two opposite forecast methods. Both of them lead to a diverge market when used alone. If agents lean to one forecast method, the other one will win over. Finally, the population of load agents choosing each forecast method keeps at a stable level. Combination of the two forecast methods keep market price volatility at a moderate level.

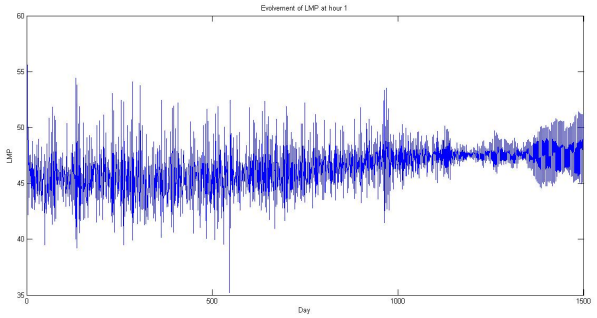

Figure 4.23: LMP at hour 1 with Price Forecast Method 2,3,4 Only

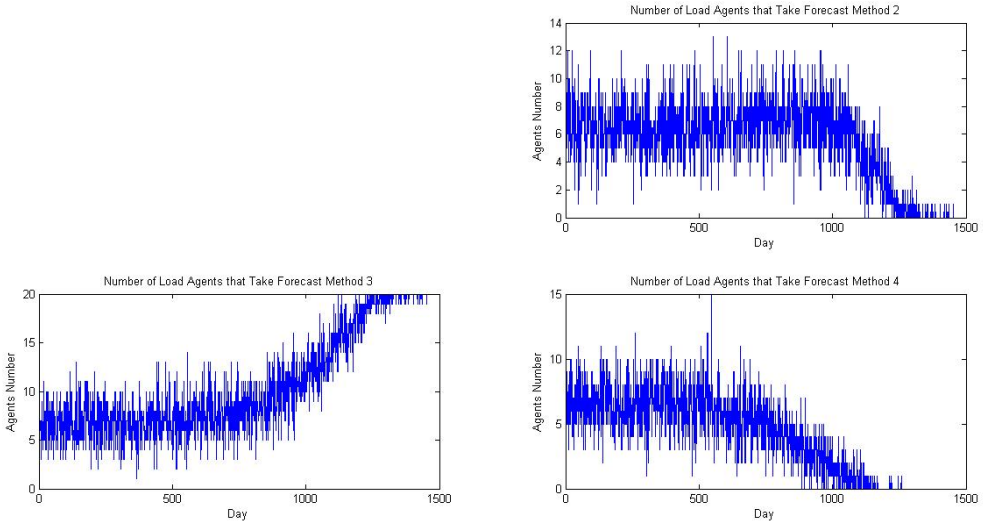

Figure 4.24: Price Forecast Methods Taken Load Agents with Price Forecast Method 2,3,4 Only

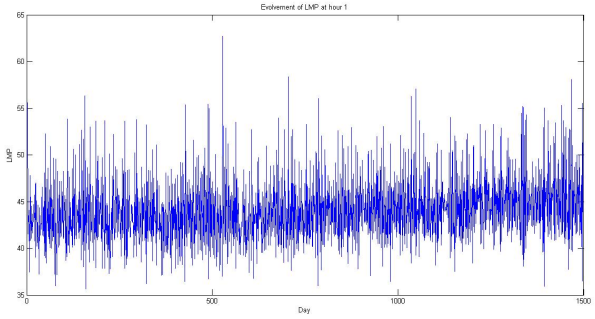

Figure 4.25: LMP at hour 1 with Price Forecast Method 2,4 Only

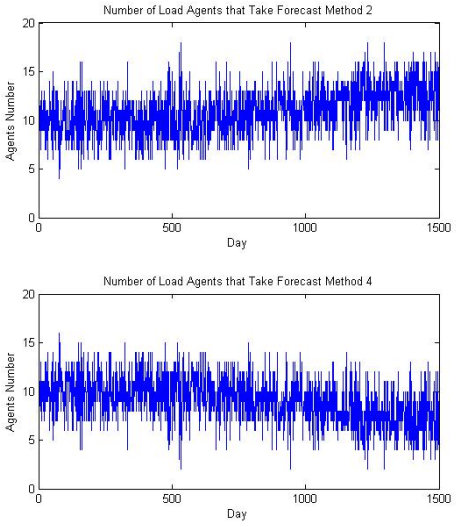

Figure 4.26: Price Forecast Methods Taken Load Agents with Price Forecast Method 2,4 Only

4.7 Conclusions

This Chapter investigates the issues of introducing dynamic price to retail load customers. Under current market structure, wholesale market price is calculated after load is realized. It creates a time delay to pass real-time price to load customers. One proposed approach is to pass day-ahead market price to load customers, which is generated in the day-ahead market. The other approach is to pass real-time market to load customers. Both of the two approaches are subject to information uncertainty problem.This study tries to assess the application of the two dynamic pricing approaches.

The contribution of this study lies in four folds:

- A seamed retail and wholesale test bed that provides flexible environment for simulation.
- Design of smart control device accommodating for dynamic price and customer preference.
- Development of LSE learning ability to perform in a day-ahead price passing market structure

- Evaluation of market volatility with heterogenous load customers.

CHAPTER 5. SHORT TERM AND LONG TERM ASSESSMENT OF A NEWLY PROPOSED PRICE RESPONSIVE DEMAND PROGRAM

On March 15, 2011, the Federal Energy Regulatory Commission (FERC) issued its final rule on demand response compensation in FER (). The Final Rule requires ISOs or RTOs that have tariff provision permitting demand response resources to participate as a resource in the energy market by reducing consumption of electric energy from their expected levels in response to price signals must:

- Pay demand response resources the full LMP when these resources have the capability to balance supply and demand and when payment is cost-effective as determined by a net benefits test accepted by the Commission
- Allocate the costs proportionally to all entities that purchase from the relevant energy market in the area(s) where the demand response reduces the market price for energy

The price responsive demand (PRD) program is an alternative approach to encourage final customers to respond to wholesale market operation condition. As specified by FER (), the qualified DR resource will be paid for the load curtailment effort based on the difference of their actual load and estimated baseline. There are many institutional barriers to apply dynamic pricing approach which charges final customers the marginal wholesale cost directly. The root of these problems come from the disconnection between wholesale and retail markets. The wholesale market is run by ISOs or RTOs and comply with FERC orders. However, the retail level is regulated by state government and lack of the incentive of dynamic retail prices. The other barrier to pass by dynamic price is the lack of market incentives to invest in enabling technologies that would allow electric customers and aggregators of retail customers to see and respond to changes in marginal cost of providing electric services as those costs change. It

must justify the cost investing on the smart devices before retail customers will be willing to take dynamic price contract. Due to these barriers, FERC order 745 compromises to over-compensate final customers to encourage participation of demand response. Per the request of FERC order, ISOs and RTOs must comply with new market rules to take the bids of demand response and compensate for the load curtailment action.

The subsidy of PRD customers, as any other subsidy policies, creates distortion and leads to efficiency loss. Market Surveillance Committee of the California ISO issued a final opinion on economic issues raised by FERC Order 745, Bushnell et al. (2011) . In this document, the market surveillance committee explains the drawback of PRD program and predicts the potential damage to market operation. It proves again that, a bad designed reform can be worse than no reform.

Using the simulation framework, an agent-based simulation is conducted to study final customers behavior in response to the new market rules. The study will follow the new market rules as specified by ISOs to comply with FERC order. Both the short-run and long-run issues have been tested. In the short fun, DR providers are allowed to bid into wholesale markets and they may have incentives to maneuver their bids to get the maximum payment. In the long run, generators capacity revenues are transferred to DR providers, which may end up with replacing cheap generation resource with inefficient DR resource.

5.1 FERC Order 745 and ISOs compliance

In this section, three of the most outstanding features of the FERC order are discussed. The net benefit test is the underlying justification for PRD program. Only when the load customers total payment is reduced could the demand PRD bids be cleared. That, indeed, defines a floor price for the PRD bidding. Baseline Estimation is the ISOs task to comply with FERC order. It is the benchmark to determine the quantity of load curtailment and therefore the payment rewarded to this action. The third feature of FERC order is that it pays final customers wholesale price LMP for load reduction. As will be discussed below, this payment includes a saved retail price and extra payment of wholesale price, which is known as double payment.

5.1.1 Net-Benefit Test

Net-Benefit Test is to guarantee the reduced energy payment of load customers is no less than the payment to the dispatched demand-response resources.[1] Figure 5.1 illustrates the layout of Net Benefit Test. Without demand response, market is cleared at price of P_0 and load of L_0. After taking DR bids, market is cleared at price of L_T and load of P_T. Compared with the no-DR case, load customers save a payment of $(P_0 - P_T) \times L_T$, the area of square B. DR providers get paid of cleared price of P_T, with a payment of $P_T \times (L_0 - L_T)$.

Net Benefit Test determines a threshold price P_T as the floor price for DR bids. By definition, at the point of threshold price the load payment reduction $\delta P_T \times Q_T$ equals the payment to DR: $\Delta Q_T \times P_T$.

$$\Delta P_T \times Q_T = \Delta Q_T \times P_T \tag{5.1}$$

$$\frac{\Delta Q_T / Q_T}{\Delta P_T / P_T} = 1 \tag{5.2}$$

Therefore, Net-Benefit Test implies that the threshold price should have an elasticity of 1. This threshold price only depends on the aggregated supply curve. The ISO will determine and publish a system-wide Net-Benefits Test threshold price at least once per month.

5.1.2 Baseline Estimation

As discussed above, baseline is the tag attached to each DR provider with which the actual consumption will be compared to determine the real-time load reduction. ISOs objective of the baseline methodology is to develop an accurate estimate of what the DR provider's load would have been, but for any financial incentive to reduce load.

For each 5-minute interval, ISO calculates the mean of a DR provider's load from the most recent prior ten non-price responsive days of the same day type. But Frequent load reductions reduce the population of non-price responsive load intervals from which to draw the baseline sample. If the number of available non-price responsive intervals falls below the minimum sample size needed to ensure baseline accuracy, the ISO will include loads from price-responsive intervals in the baseline sample.The tentative solution will ensure the baseline

[1] See footnote 162 of the Order 745

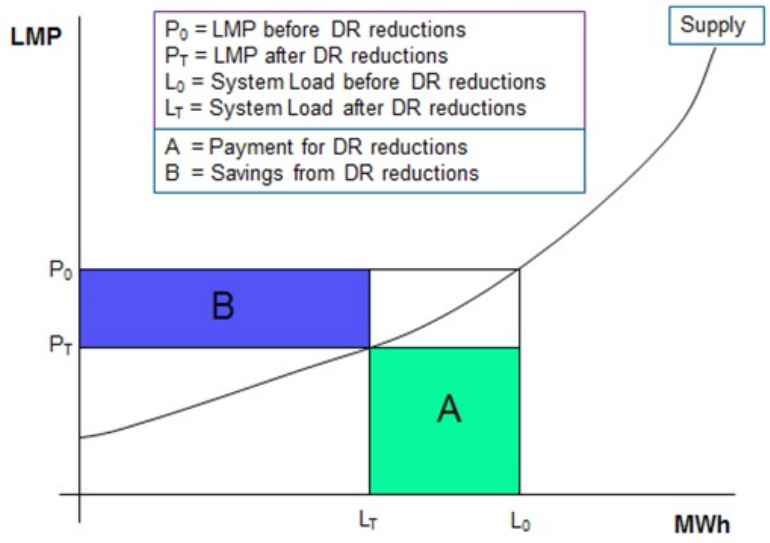

Figure 5.1: Illustration of Net Benefit Test

Graph is from ISO New England Committee and Working Group Meeting Material.

is calculated using a sample of contemporary load data that represents the DR provider's normal load.

The concept of baseline integrity price(BIP) is introduced as a criteria to take price-responsive days metered load to make baseline estimation. Actual metered loads will be included in the daily baseline calculation if the actual metered loads are from a day in which the offer price is less than or equal to the BIP, the LMP in an interval is less than or equal to the BIP, and the DR provider was scheduled to reduce load in that interval.

In sum, ISOs rules of baseline estimation contains three parts:

- 90/10 Baseline Rolling Update Rules:

$$BL_{d+1} = 90\% \cdot BL_d + 10\% \cdot P_d \cdot \mathbf{I}_{BIP}(LMP_d) \tag{5.3}$$

- Baseline Integrity Price (BIP) BIP balances data quality and data frequency

$$\mathbf{I}_{BIP} = \begin{cases} 1, & \text{if } LMP_d < BIP; \\ 0, & \text{if } LMP_d \geq BIP. \end{cases} \tag{5.4}$$

- Two-Hour Adjustment

$$BL'(t^*) = BL(t^*) + [P(t-2) - BL(t-2)] \tag{5.5}$$

5.1.3 Pay LMP to Load Reduction

If DR providers bids get cleared, they will be compensated at wholesale price LMP for each MW of load reduction. Of course, for the curtailed MW of power, the customer does not need to pay for retail price r. For a load customer who joins the PRD program, the opportunity cost for using each MW of power equals the incurred price r plus the foregone payment LMP. This payment subsidy changes load customer incentive to consume. Bushnell et al. (2011) gives a good example to illustrate the effect of price distortion. A distributed generator can get a higher payment when is located behind a meter than in front because the behind-meter generator can get paid both from serving final load customer and DR compensation payment of LMP.

5.2 Short Term Behavior Test

As discussed above, DR providers load reduction quantity is determined by the difference of actual electricity consumption and an estimated baseline. Baseline is designed to capture the load customers electricity consumption be it not interfered by the DR compensation. As pointed out by Bushnell et al. (2009), it is impossible to observe this counterfactual consumption level, because we cannot measure something that did not happen.

On one hand, it is impossible to have an accurate estimate of the counterfactual consumption level. Even the best economic or statistical models of a customers hourly electricity consumption behavior as function of hourly prices and all observable customer and weather characteristics are only able to explain a small fraction of the variation in that customers consumption of electricity across hours of the year. Therefore, when the actual consumption is low, for example family goes on vacation, the load customers could still be awarded for a phantom "load reduction" which is not consumed anyway.

On the other hand, load customers could learn from baseline estimation rules and takes actions to get extra payment. For example, if load customers have an actual high consumption level, they would like to avoid bidding into the DR market to avoid the penalty for consuming higher than baseline. Without paying for potential penalty, these load customers could get a

higher baseline estimate. When their consumption level is low, they would like to bid all their possible reduction ability to get paid by DR program.

Realizing the importance of accurate baseline estimation, FERC directed ISOs "to develop appropriate revisions and modifications, if necessary, to ensure that their baselines remain accurate and that they can verify that demand response resources have performed".[2] ISOs are developing new rules to adjust baseline estimation, rules in section 5.1.2 as an example. KEMA (2011) uses historical data to show that symmetric baseline adjustment works better than no-adjustment. But this study uses the realized historical data but ignores load customers reaction to these rules change. So, it is not convincing to fully implement them in the real market operation.

To make a better evaluation of current baseline estimation rules, as proposed to be adopted by ISOs, an agent-based model is set up in this section to investigate how the load customers will react to the new rules.

5.2.1 Experiment Design

To focus on the baseline inflation problem, this experiment extend the simulation framework, as mentioned in previous sections, to include the behavior of "DR Prividers". Features of this experiment is listed as follow:

- One Settlement Market The simulation framework is simplified to have one settlement market. DR Providers, LSE, and GenCo bid into this market and get cleared. Their actual consumption or production follows the dispatch result. So, in this model setup, there is no consumption or generation deviation problem. Because of this one-settlement setup, there is no Two-Hour adjustment, which could cause moral hazard problem. In this study, each agent's behavior can only be reflected through their bidding behavior into the market.

- Grid Topology and Market Environment The 5-bus testcase grid is used for this experiment, with the same parameters, including transmission line capacity, bus-to-bus

[2]FERC order 745 at page 94

admittance, load profile, generation capacity and generation cost. So, the market would reach the same dispatch result if there were no demand response.

- LSE and GenCo Both LSE and GenCo are modeled as truth tellers that bid their true load profile and generation cost into the market.

- ISO ISO's is in charge of clearing supply and demand, as well as implementing rules for accommodating demand response. These rules include making net-benefit test and announcing threshold price, adjusting BIP price, updating DR Providers' baseline.

- DR Provider In this experiment, DR providers are modeled as agent that has load consumption and could bid into the market. In another word, DR providers bid for the same entity that have real load service. In this sense, DR providers are modeled differently from the LSE agents in the dynamic pricing studies since LSE does not have the full information of its serving load.

  In this experiment, there are three DR Providers locating at three load buses respectively. DR Providers's state is defined as the electricity consumption without the interference of demand response program. The states are simplified to have only low and high states, with $S_i^{low} = 2.5MW$, $S_i^{high} = 7.5MW$ for $i = 1, 2, 3$. The three DR Providers' states transition follows a Markov Chain process, which means the states only depend on the states in last period. And the three DR Providers' states are generated independently so that DR providers' states are necessarily to be the same at one period.

$$\begin{pmatrix} S_{i,t+1}^{low} \\ S_{i,t+1}^{high} \end{pmatrix} = \begin{pmatrix} 0.9 & 0.1 \\ 0.1 & 0.9 \end{pmatrix} \times \begin{pmatrix} S_{i,t}^{low} \\ S_{i,t}^{high} \end{pmatrix} \tag{5.6}$$

  DR Providers's action is to bid into energy market. The DR bids are taken by ISO the same as generators' offers, which take the form of

$$p_i = TP + a_i * q_i \quad where\, 0 \leq q_i \leq S_i^b \tag{5.7}$$

  where TP is the threshold price derived form net-benefit test, which implies that DR bids can not be lower than threshold price. S_i^b is DR Providers' bids of load curtailment limit.

Also, suppose the true total load reduction cost has the linear form within the actual load consumption S_i

$$C_i = \quad c_i * q_i \quad \textit{when } q_i \leq S_i \tag{5.8}$$

$$C_i = \quad \inf \quad \textit{when } q_i > S_i \tag{5.9}$$

In this study, it is assumed that all the DR providers have the same load reduction cost and supply offer curve slope, *i.e.*, $c_i = c$ and $a_i = a$. Particularly, the value of the two parameters are $a = 10$, $c = 20$, and .The strategic variable for DR Provider is the load curtailment limit $S_i^b = \alpha_i^b \times S_i$. To discretize choice space, it is assumed that DR provider can only choose from four actions, from lowest bids to the highest bids:

$$\alpha_i^b \in \{0,\ 0.3,\ 0.6,\ 1\} \tag{5.10}$$

After the market is cleared, each DR provider receives a signal of the cleared load reduction q_i^*. The DR provider's actual load consumption l_i equals $BL_i - q_i^*$ sot that DR provider can fulfill its commitment to curtail load. The actual load reservation value C_i^* equals $(S_i - l_i) \times c$. The DR provider's reward for joining PRD program r_i^* is $p_i^* \times q_i^* - C_i^*$.

At each day, after the market is cleared, DR Provider i updates its belief of the state-action pair $\{S_i, S_i^b\}$. PR Providers adopt the Q-learning algorithms as discussed before.

- Flow Diagram The experiment runs as follow:

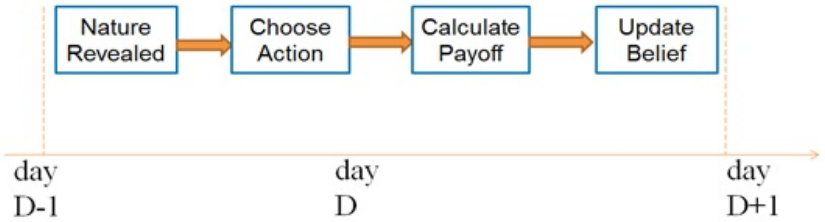

Figure 5.2: Experiment Design

5.2.2 Simulation Result

This simulation tries to evaluate the baseline estimation rules as adopted or will be adopted by the ISOs and the impact on load customer's behavior. As discussed in section 5.1.2, BIP is used to adjust baseline estimation. If BIP is set very low, days qualified for baseline update will shrink and ISO do not have enough new information to update baseline estimation. If BIP is set too high, then for some of the event days, the actual usage deviates far away from the actual non-interfered load which will under estimate DR Provider's baseline. So, ISO is seeking a proper BIP to balance between data availability and data quality.

Figure 5.3 shows the LMPs at the three buses without penetration of demand response program. At $BIP = 30$, it is higher than LMPs on bus 3 but lower that on bus 1 and 2 for most of the time. With this BIP, DR Provider 3's baseline will be updated for most of the time while DR Provider 1's baseline will not change.

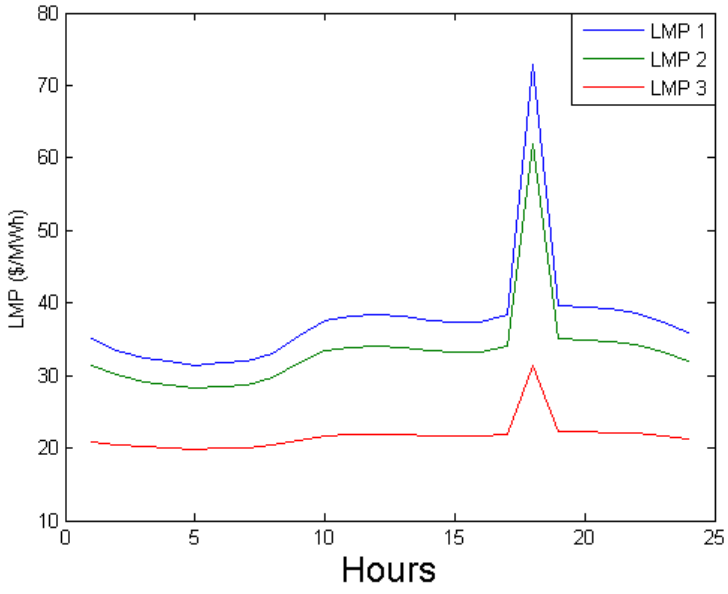

Figure 5.3: LMPs without Demand Response

Table 5.1 shows DR Provider's choice probability at low $BIP = 30$. The result shows that DR Provider 1 has incentive to bid in the full load capacity at both low and high state. DR Provider 2 has incentive to bid the full load capacity at low state but avoid bidding into the

market at high load state. DR Provider 3 has similar action as Provider 2.

As discussed above, if get dispatched a DR Provider receives payment of $(BL_i - l_i) \times p_i^*$ from ISO, and incurs a load reservation value of $(S_i - l_i) \times c$. Therefore DR Provider has incentive to send a higher bids when the actual load state S_i is lower than BL_i. In the simulation result, DR Provider 2 and DR Provider 3 bid their full capacity at low state but withhold from bidding into the market at high state. By this strategy, they can get free reward when the actual load level is low. When their actual load is high, it is best for them not to bid into the market.

At the same time, the electricity price LMP also matters. If LMP is much higher than load reservation value, it is still worthwhile to curtail load even if the estimated baseline is less than the actual load state and DR Provider's load reduction is not fully compensated. DR Provider 1's action falls into this scenario. It bids all the capacity into market at both high and low states.

Figure 5.4 shows ISO's baseline estimation for the three DR Providers. At off-peak hour, LMPs at bus 1 and 2 are higher than BIP, so their baselines are not updated and keep at the original level. LMP at bus 3 is lower than BIP, and DR Provider 3's baseline estimate keeps changing. Because baseline is updated when DR Provider 3 curtailed its load, baseline estimation can be lower than its baseline. For this reason, DR Provider 3's action at low state does not converge to one action. It still tries lower DR bids at low state for the benefit to raise baseline estimation. At peak hour, all the three LMPs are higher than BIP so that their baselines are not updated. Therefore, all of the three do not have the incentive to withhold their load capacity.

The simulation result with $BIP = 60$ is illustrated in Table 5.3 and Figure 5.5. The main difference between Table 5.3 and 5.1 is that DR Provider 1 changes its action at high state to withhold bidding. The reason can be found on Figure 5.5 where baseline estimation for all the three agents start to change. Baseline estimation for DR Provider 1 is lower than the starting point. So, it is not worthwhile to bid full capacity into the market which requires higher load reservation value.

Another difference is that DR Provider 3 converges to the action $\alpha = 0.6$, a moderate high states. It has the same reason as stated above. Because the LMP at bus 3 is the lowest and

baseline is updated at each day, it is not the best to bid all the capacity into the market which may end up with a very low baseline estimation.

Table 5.1: Agent Choice Probability with BIP=30

Submitted Capacity	$\alpha = \mathbf{0}$	$\alpha = \mathbf{0.3}$	$\alpha = \mathbf{0.6}$	$\alpha = \mathbf{1}$
DR Provider 1, low state	0.0	0.0	0.0	1.0
DR Provider 1, high state	0.0	0.0	0.0	1.0
DR Provider 2, low state	0.0	0.0	0.0	1.0
DR Provider 2, high state	1.0	0.0	0.0	0.0
DR Provider 3, low state	0.0	0.53	0.0	0.47
DR Provider 3, high state	1.0	0.0	0.0	0.0

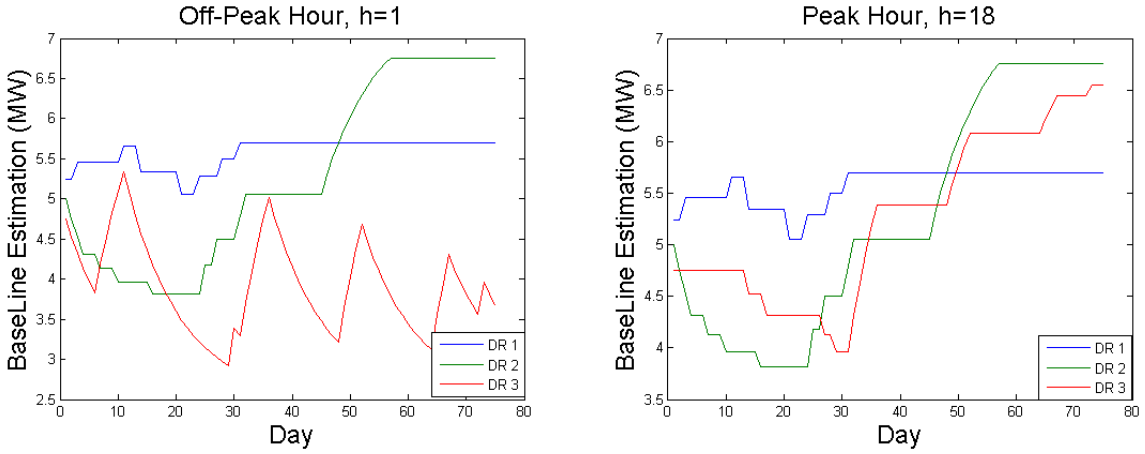

(a) Off-Peak Hour, h=1

(b) Peak Hour, h=18

Figure 5.4: Daily Baseline Estimation with BIP=30

Table 5.2: Agent Choice Probability with BIP=60

Submitted Capacity	$\alpha = \mathbf{0}$	$\alpha = \mathbf{0.3}$	$\alpha = \mathbf{0.6}$	$\alpha = \mathbf{1}$
DR 1, low state	0.0	0.0	0.0	1.0
DR 1, high state	1.0	0.0	0.0	0.0
DR 2, low state	0.0	0.0	0.0	1.0
DR 2, high state	1.0	0.0	0.0	0.0
DR 3, low state	0.0	1.0	0	0
DR 3, high state	1.0	0.0	0.0	0.0

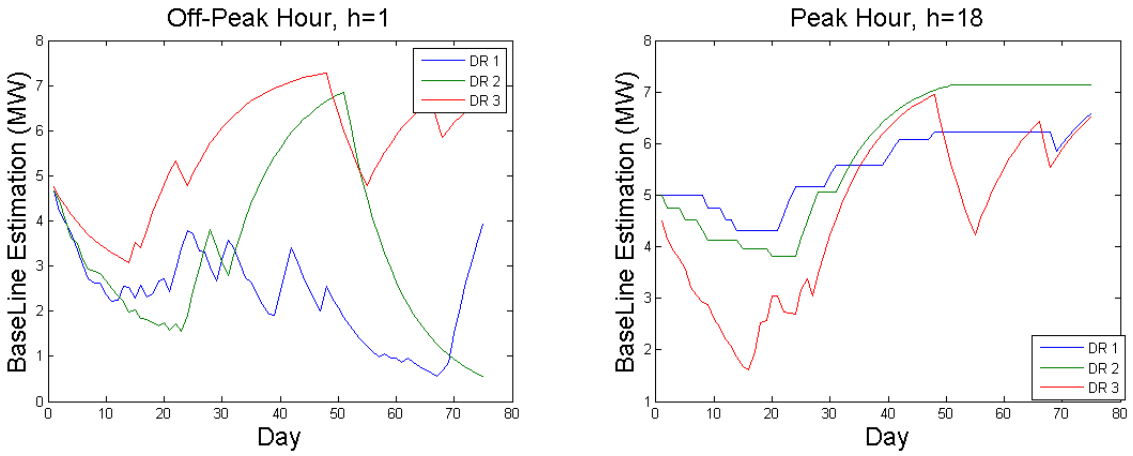

(a) Off-Peak Hour, h=1

(b) Peak Hour, h=18

Figure 5.5: Daily Baseline Estimation with BIP=60

Table 5.3: Agent Choice Probability with BIP=0

Submitted Capacity	$\alpha = \mathbf{0}$	$\alpha = \mathbf{0.3}$	$\alpha = \mathbf{0.6}$	$\alpha = \mathbf{1}$
DR 1, low state	0.0	0.0	0.0	1.0
DR 1, high state	0.0	0.0	0.0	1.0
DR 2, low state	0.0	0.0	0.0	1.0
DR 2, high state	0.0	0.0	0.0	1.0
DR 3, low state	0.0	0	0.0	1.0
DR 3, high state	1.0	0.0	0.0	0.0

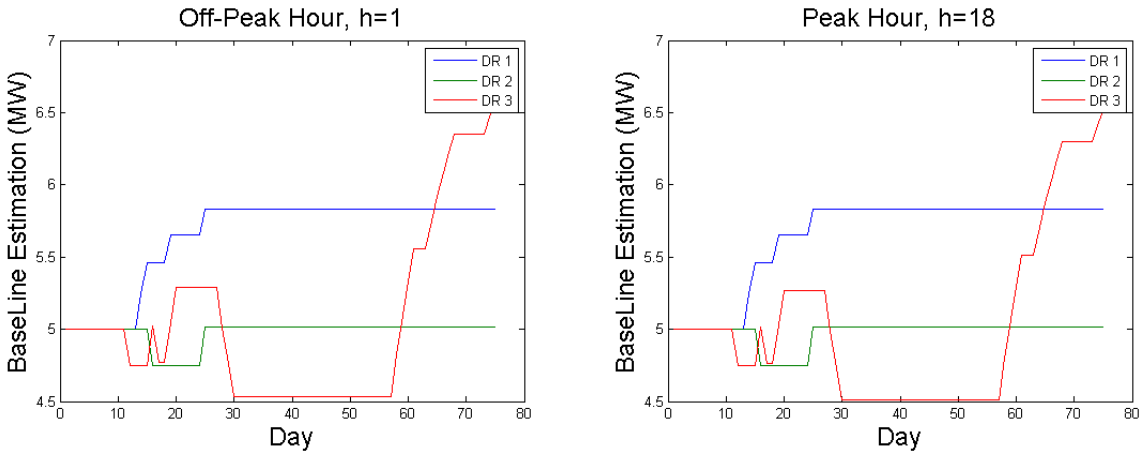

(a) Off-Peak Hour, h=1

(b) Peak Hour,h=18

Figure 5.6: Daily Baseline Estimation with BIP=0

5.3 Long Term Behavior Test

In the last section, I studied the short-term behavior of DR Providers following the market rules adopted in ISOs. In this section, I will turn the focus on the long-term effect of introducing the PRD program as requested by FERC order. A major concern of the FERC ordered PRD

program is the double payment issue. If a DR agent is dispatched in the energy market, it will be paid by wholesale price LMP and also save retail payment of r. So, DR providers, in fact, has a stronger incentive to join the market.

PRD program, by the definition, is a wealth transfer from supplier to consumers. Because of the load curtailment, price peaks are likely to be shaved. However, price peak is the main revenue source for the peak unit because most of peak units can only be dispatched at the peak hour. The portion of LMP that exceeds its marginal cost will compensate peak unit's fixed cost, which is known as capacity revenue. The wealth transfer from supplier to consumers affect all the generators. The inframarginal generators, assuming their dispatch time is not changes, gain less revenue during the operation hour since LMP are kept lower than before. It is even worse for marginal generators since there are chances that they lose the position of marginal units. The loss of capacity revenue leads to less investment in the new capacity.

But this wealth transfer should not be a problem if the new technology is paid the correct price. The more efficient technology finally replaces more expensive and inefficient technologies. Joskow (2006) points out the introduction of demand response will solve the "missing money" problems of energy market. "Missing money" problem is caused by the fact that energy market price can only reflect the marginal cost of marginal units. The fixed cost of the marginal units can not be compensated from energy market. Joskow (2006) also shows that given the generation capacities are in the optimum level, all generators lose money to compensate fixed cost to the same extent of marginal generators. Demand response, being viewed as a new generation technology, has very high marginal cost but zeros fixed cost as compared with conventional generation technology. Therefore, demand response will be dispatched as a marginal generator when the system experiences a stress of meeting demand. Given the zero fixed cost of demand response, all the generators will get fully compensated from energy market.

But as in the requested PRD program, DR Providers get double paid which gives them a wrong signal to joint the market. Firstly, it will increase the opportunity cost for load customers to use electricity, which may cause inefficiently load curtailment. The over participation of demand response will squeeze off the capacity revenues of the conventional generation units.

As discussed in the report by Bushnell et al. (2011), they believe the benefit of shaving peak load will not last. The inefficient wealth transfers will leave incremental generation with a sub-normal return on equity, which means either that

- supply will exit or new supply will fail to enter, leading to a leftward shift in the supply curve compared to where it would have been otherwise
- the market will correct the problem by raising prices to a level sufficient to increase investment, putting an end to the transfers.

There is no other outcome. Investment in new supply will cease until the market returns to generation again to cover capacity costs.

For this study, I will run an agent-based model to simulate market dynamics of electricity market after the door is open to price responsive load. Particularly, the conventional generators' investment decisions on new capacity are examined so that this is a long-term study. A key question being asked to study investment problem is what information the agents take into investment decision making. Among many work in answering this question, the study by Bushnell and Ishii (2007) creates a flexible framework to study the dynamics of investment decisions with strategic short-term bidding. The investment decisions used by Bushnell and Ishii (2007) is forward looking, which requires generators to predict its investment decisions on future market environment and find the best path to maximize its own predicted current revenue. Given every generators makes its optimal investment decisions, a Nash-Equilibrium is reached. The discussion of investment decisions are beyond the scope of this study. Also, agent-based simulation is not seeking for the Nash-Equilibrium, but only mimics each agent's behavior.

The rules for generator agents' capacity investment decisions are back-ward looking. If they can not gain enough revenue from energy market to compensate the capacity cost, they will not invest 100 percent to replace retired capacity. This simple rule-of-thumb lead generator agent to make investment decision. The detail of experiment design can be found in the following subsection.

5.3.1 Experiment Design

5.3.1.1 Experiment Flow

As briefly talked in last section, the key assumption of this experiment is that investment decision is backward-looking, which means that generators make myopic investment decisions using only the past information. Particularly, it is assumed that generators investment decisions follows the rule in Equation 5.11

$$Cap_i^{t+1} = (90\% + 10\% \times \frac{R_i^t}{c_i \times Cap_i^t}) \times Cap_i^t \tag{5.11}$$

where Cap_i^t is generator i's generation capacity at period t. c_i is investment cost per MW of capacity for generator i, which is kept constant through the experiment. R_i^t is the capacity revenue collected by generator i from energy market at period t. By Equation 5.11, for every period 10 percent of capacity will be retired and need to be replaced by new investment. The investment decision is determined by the revenue/cost ratio. The new installed capacity exceeds retired capacity if capacity revenue is larger than capacity cost, and vice versa.

Figure 5.7 shows the main flow diagram for this experiment and 5.8 shows the sub-flow diagram for two processes as appear in the dashed table of main flow diagram. The experiment starts with the initialization as shown in 5.8a. This process formulates a power market in equilibrium when there is no demand response. The market is cleared using generators supply curve, load profile and grid network. Generators calculate capacity revenues from participating in the energy market, which equals the difference between payment received from ISO and operational cost. It is assumed that capacity revenue could just cover capacity investment cost so that there is no need for a capacity market to guarantee the return of capacity investment. So that capacity cost per MW c_i is be calculated.

Also, it is assumed that load growth rate equals zero so that the system is in steady state. The power market can be thought of compared with a steadily growing reference so that the load growth can be thought of as zero. To release this assumption will not hurt the main conclusions of this simulation model, but will add unnecessary details.

After the initialization, demand response is taken into the market and the equality between

capacity revenue and capacity cost is broken. Generators capacity starts to evolve corresponding to capacity revenue change.

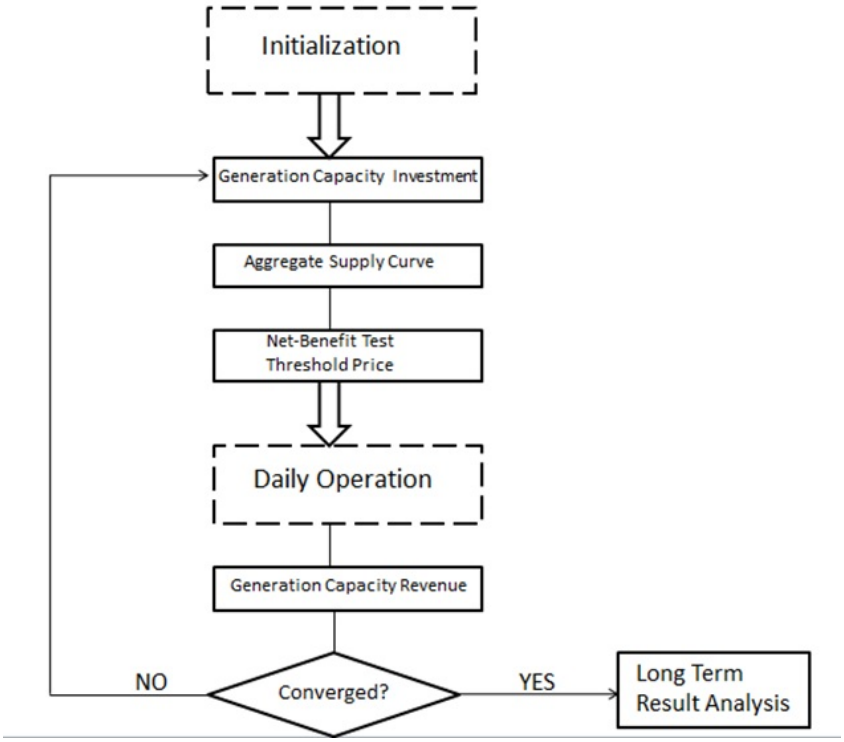

Figure 5.7: Main Flow Diagram

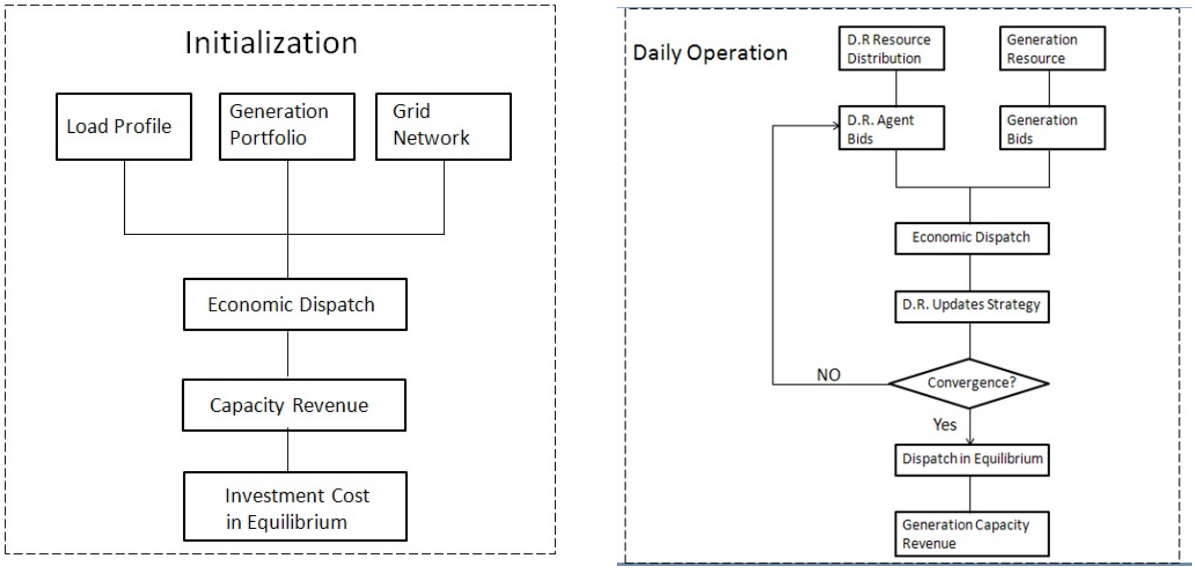

(a) Initialization

(b) Daily Operation

Figure 5.8: Experiment Flow Diagram

5.3.1.2 Demand and Supply Agents

In this experiment, the transmission grid and generators location follow that in the simulation framework. So, in this test cast there are 5 buses, 5 GenCos, and 3 LSEs. GenCos and LSEs are located at the buses as before.

However, transmission capacity and generation portfolio are modified to fit into this experiment design. In this experiment, there is no transmission line capacity limit. Because of this convenience, an aggregated supply curve can be formulated. Also, the generator's operation cost parameter are modified to fit into an exponential curve, which is used to estimate the aggregated supply curve in the following experiment. The generation cost parameter can be found in Figure 5.9 and Table 5.4.

GenCo's Operation Cost

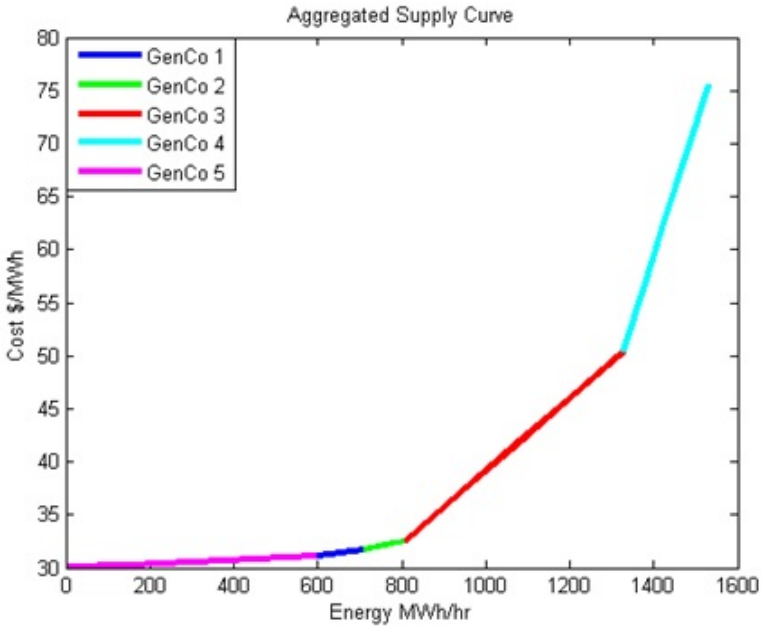

Figure 5.9: Aggregated Supply Curve

Table 5.4: GenCo's Supply Curve Parameters, $MC = a \cdot x + b$ where $0 < x < capacity$

GenCo	**b**	**a**	**capacity**
Gen 1	31.10	0.0055	110
Gen 2	31.71	0.0084	100
Gen 3	32.55	0.0344	520
Gen 4	50.43	0.1252	200
Gen 5	30.00	0.0018	600

At each iteration, each generator's capacity varies as new investment changes relative to retired capacity. The new estimated aggregated supply curve is formulated by using the information from each generator's new supply curve. Firstly, the each generator's new supply curve is discretized by chopping supply curve into a series of step functions as a pair of $\{c_i^j, q_i^j\}$. Then the pairs from al the generators are collected and sorted according to the cost order. The quantity q_i^j is then replaced by accumulated quantity Q_k with associated cost $C_k = c_i^j$, *where*

the accumulated quantity is defined as $Q_k = \sum_{c_i^j < C_k} q_i^j$. The data pairs C_k, Q_k are then fitted into exponential curve as follow:

$$C = \theta_1 + \theta_2 * exp^{theta_3 \times Q_k}$$

Using estimated parameters $\{\theta_1, \theta_2, \theta_3\}$, the point with elasticity of 1 can be found and the threshold price TP can be found. This whole process follows the FERC order 745 and will be implemented in ISOs market operation.

All the loads are located on the load buses. LSEs bid the fixed load profile into energy market. DR Providers are formulated as sperate agents that bid demand response offers into energy market. DR Providers are modeled as agents with interruptible load Q_d and load reservation value C_d. DR Provider d bids the interruptible load Q_d into energy market at the price $B_k = C_k - r$. This is because interruptible's opportunity cost is the payment from ISO plus saved retail cost. Therefore, DR Provider has incentive to bid into energy market with bids less than their load reservation value.

Suppose distribution of all DR Provider's reservation value for electricity follows a normal distribution, $C_d \sim N(\mu, \sigma^2)$, as shown in Figure 5.10. The parameters for this distribution is listed in Table 5.5. Therefore, total quantity of DR bids can be retrieved from the distribution of load reservation value. As shown on Figure 5.10, with paying DR Provider full LMP, total amount of bids from DR is the area $A1$ plus $A2$ because DR Providers with load reservation value $B + r$ have incentive to take the price of B.

$$\begin{aligned} &Q = V \times (F_{\mu,\sigma^2}(B + r) - F_{\mu,\sigma^2}(r) \\ &\textit{where } V \textit{ is the total volume of interruptible load} \end{aligned} \tag{5.12}$$

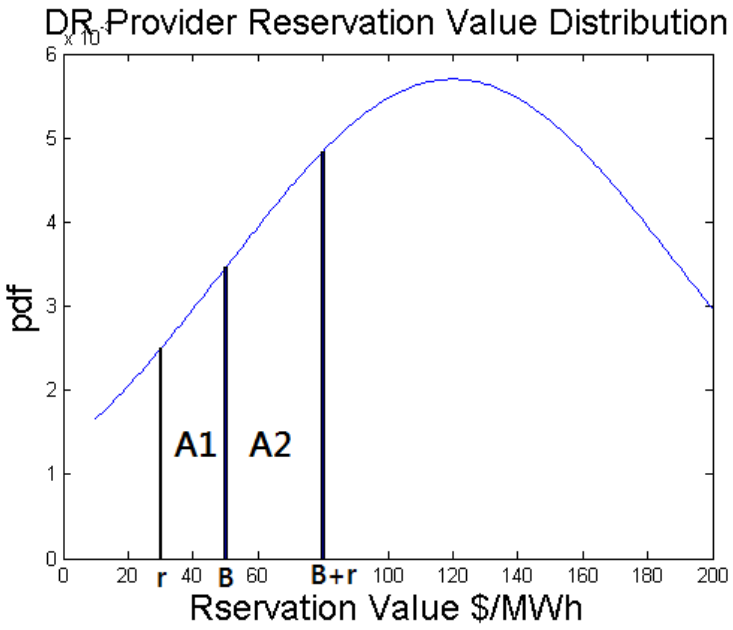

Figure 5.10: DR Cost Distribution

Table 5.5: Load Reservation Value Distribution Parameters

Mean μ	**Variance** σ^2	**Retail Rate** r	**DR Volume** V
150 $\$/MWh$	70 $(\$/MWh)^2$	30 $\$/MWh$	300 MW

5.3.2 Simulation Results and Analysis

Simulation runs with two cases, paying DR Providers with full LMP, versus paying DR Providers with $LMP - r$. In both of the two cases, simulation stops at reaching a new equilibrium.

Figure 5.11 shows the simulation results for the first case of paying DR Providers full LMP. The northwest graph illustrates the evolvement path of generators capacity. Clearly, all the five generators experienced a loss of generation capacity at the beginning stage of DR penetration. This is because wholesale price is lowered when the market is open to demand response. The southeast graph of Figure 5.12 shows a deep drop of load weighted price. The southeast graph of Figure 5.11 shows the hourly price at different stages of this simulation. The peak hour

price is shaved to be flat, and much lower than the benchmark case. The off-peak hour price does not change because the LMP is lower than the threshold price, as shown on the southwest graph of Figure 5.11, and therefore DR bids are not dispatched. On the other hand, due to the penetration of demand response, the dispatched power output of conventional generators drops, which is illustrated on the northeast graph of Figure 5.11. As both price and dispatched quantity drop, generators' capacity revenue from energy market shrinks, leading to a universal drop of generation capacity.

As conventional generators' capacity drops, there is not enough generation resource to serve the load and the low wholesale price can not be sustainable. The southeast graph of Figure 5.12 shows that wholesale price gradually pick up. The southeast graph of Figure 5.11 also shows that both peak and off-peak hour price rises up. It is interesting that at iteration year 19, peak-hour price is set by other conventional generators. In another word, DR Provider becomes inframarginal and more expensive generators are called to serve peak load. But in the off-peak hour, DR Provider becomes marginal unit which sets wholesale price at threshold price. This is because without DR, conventional generators can not keep wholesale price lower than DR's threshold price. Therefore, both the peak and off-peak hour price increases as conventional generators withdraw from the market.

The northwest graph of Figure 5.11 shows that the retreat of conventional generators slows down gradually. Particularly, generator 3's capacity even increases. In fact, as shown on the northeast graph of Figure 5.11, the average output of generator 3 increases even before its capacity starts to pick up. In contrast, baseload generator 1's capacity and output has exactly the same shape. This is because generator 1 has the lowest operational cost and will be dispatched to the full capacity. Generator 3 has a higher operational cost and is not dispatched to the full capacity. As cheapest resource is retreating from the market and DR can not cover all the remaining load, the more expensive generator 3 is dispatched at a higher rate. With the increase of dispatched output, generator 3 gets a higher revenue from energy market and has incentive to invest more in capacity. Northwest graph of Figure 5.11 shows that at the new equilibrium, generator 3's capacity overpasses that of generator 5.

Both southeast graphs on Figure 5.11 and 5.12 illustrate that at the new equilibrium,

wholesale price is lower than the original equilibrium. This is because DR has penetrated into energy market, which replaces other conventional generators' capacity. If there were a higher a price in the new equilibrium, it would support a higher total capacity of conventional generators. This conflict means that the new equilibrium is not reached.

Figure 5.12 also summarizes some criteria to judge the process of introducing demand response by paying full LMP. The southwest graph illustrates the total cost to serve system load. The total cost is defined as the sum of generator operational cost, generator capacity cost and DR Provider load reduction cost. Clearly, this graph shows a increase of total cost to serve an unchanged system load.

The northeast graph shows that load customers' payment, in fact, is also steadily increasing as compared with benchmark case. Load customers payment drops only in the first year, when the generation portfolio is not changed. This decrease of payment is guaranteed by ISO's net-benefit test. But this net-benefit test only examines the payment when generation capacity is fixed. In a longer term, withdraw of generation capacity already raises wholesale price to a high level. The short-term net-benefit test can not capture the effect of a long-term change.

As a comparison, the second case of paying DR Provider of LMP-r is also simulated. Figure 5.13 and 5.14 illustrates the simulation results. It can be seen that, market evolvement follows a similar pattern as that of the first case. But the impact on market is much less. Northwest graph of Figure 5.14 shows a much lower penetration level of demand response. This is because by paying DR the LMP-r, much less load customers have incentive to curtail their load. Generator's capacity and output is mush less affected by demand response penetration.

However, the northeast and southwest graphs of Figure 5.14 shows different results. In the second case, load customer's payment is less than that of the benchmark, which means that load customers are better off. Also the second case, the total cost to serve system load decreases. This result is not surprising because by paying DR Providers the price LMP-r, correct price information is passed to load customers.

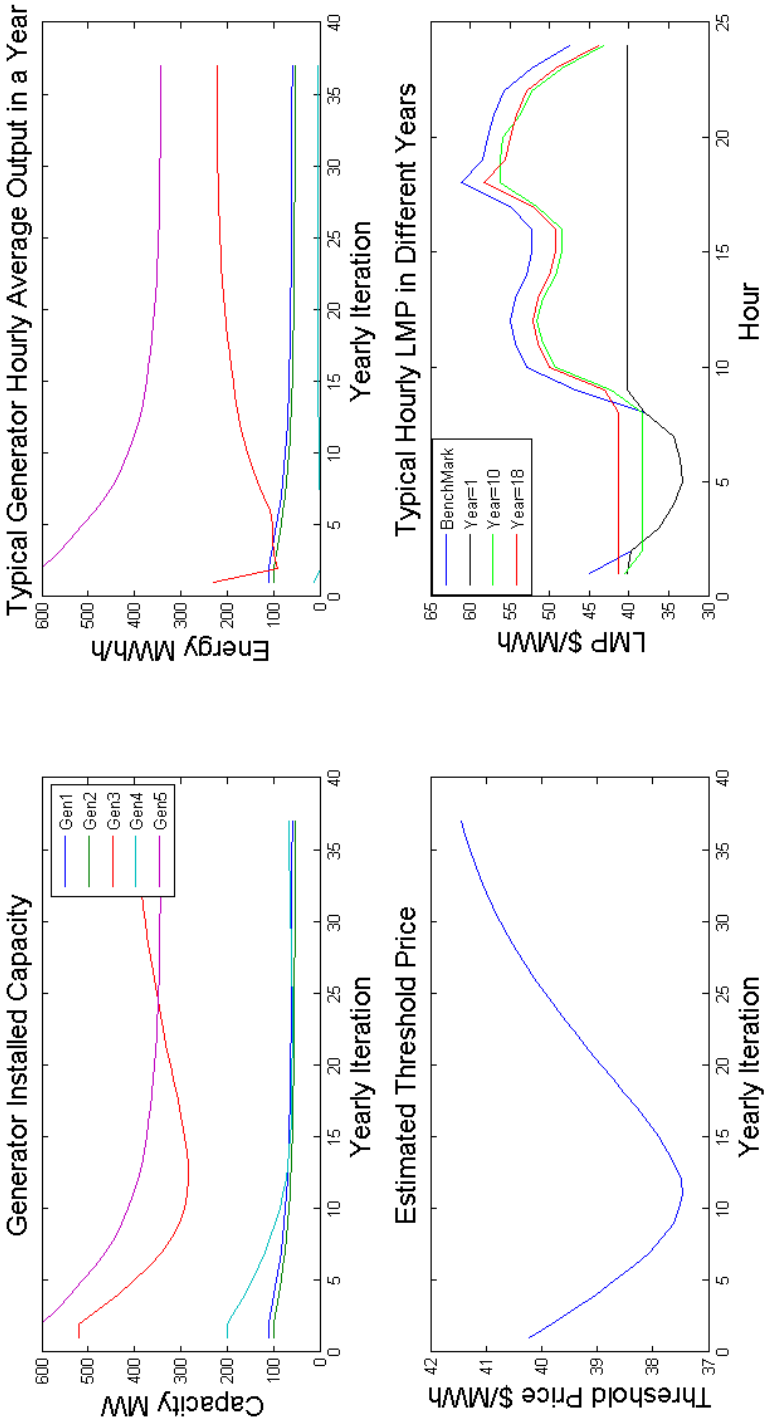

Figure 5.11: Simulation Results for Full LMP Case

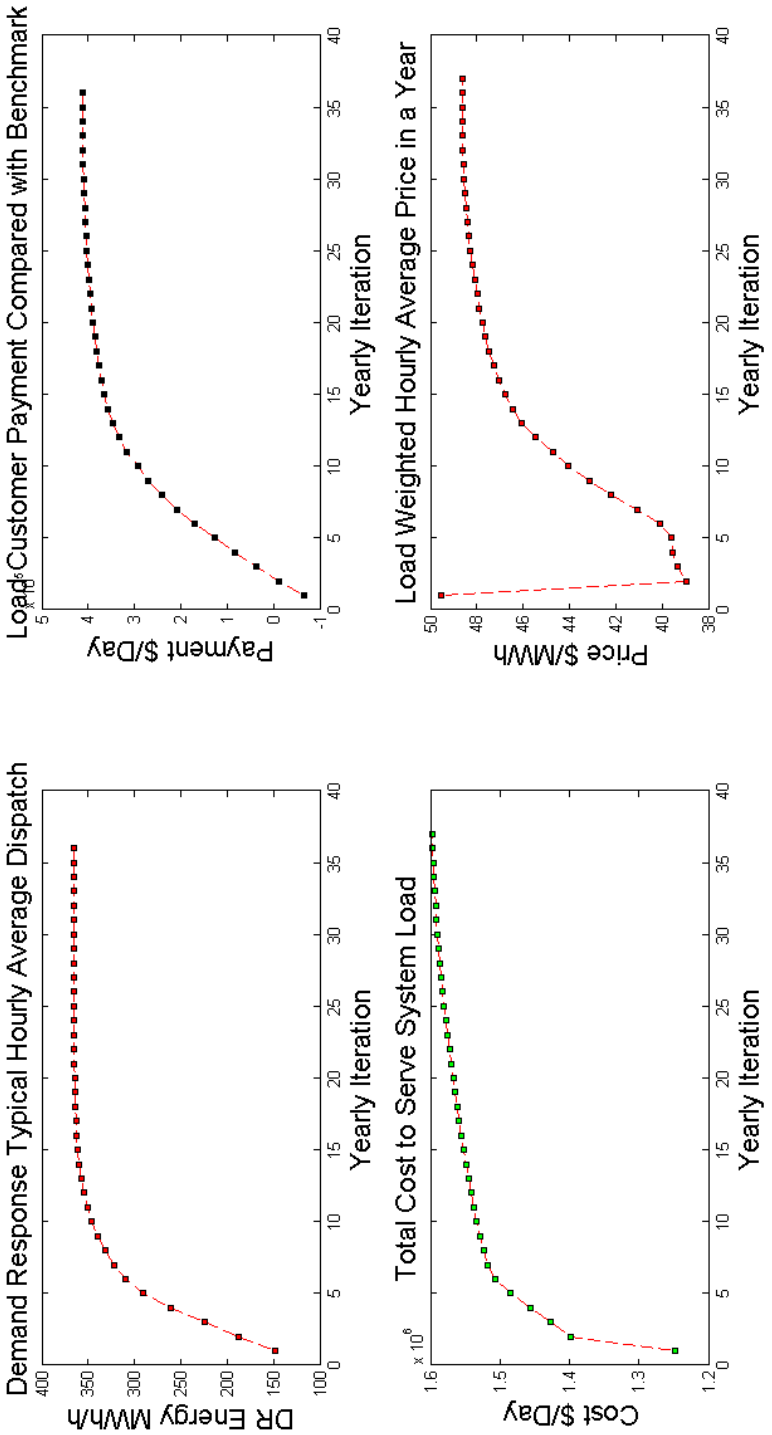

Figure 5.12: Simulation Results for Paying LMP Case (Cont)

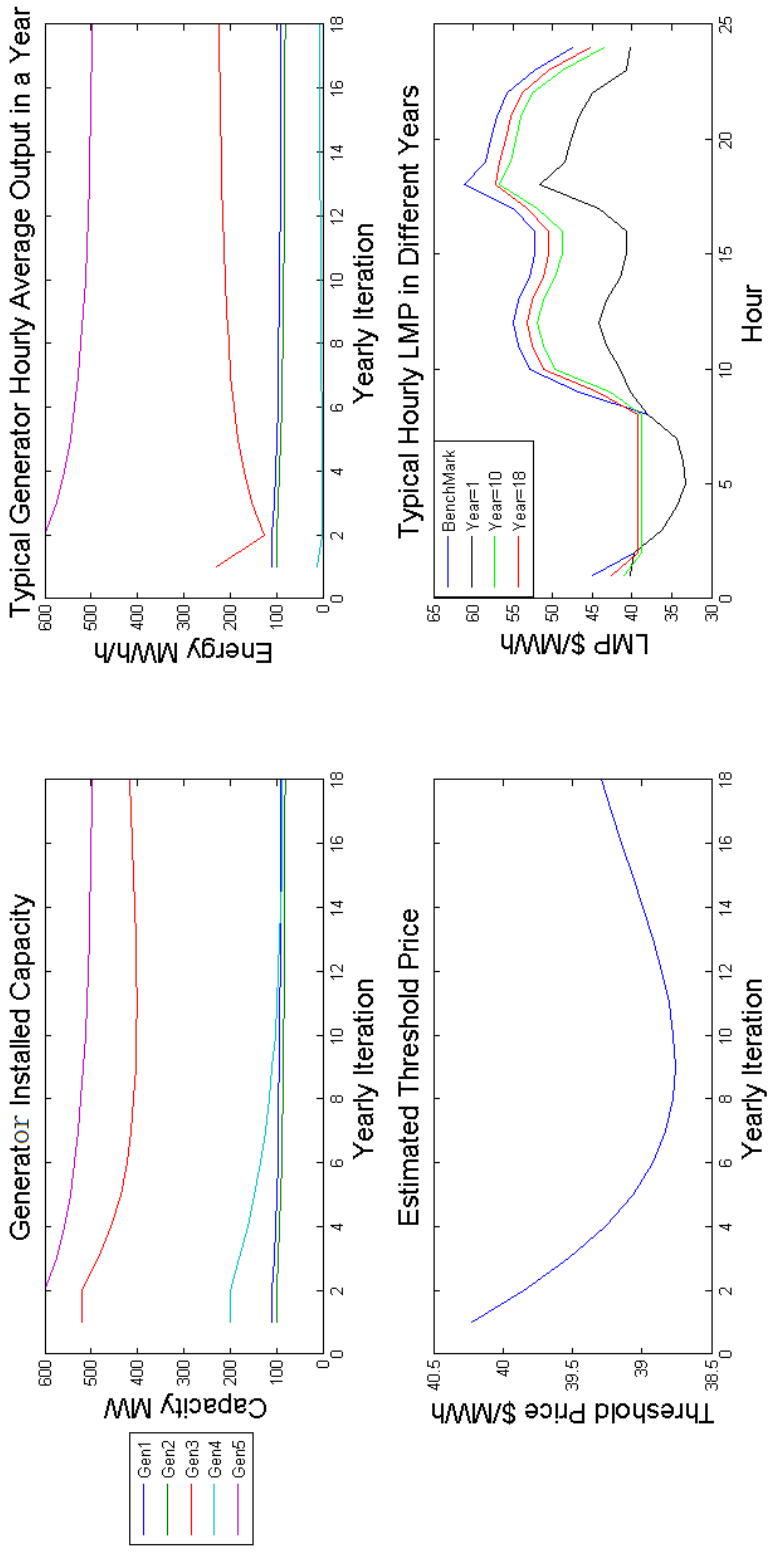

Figure 5.13: Simulation Results for Paying LMP-r Case

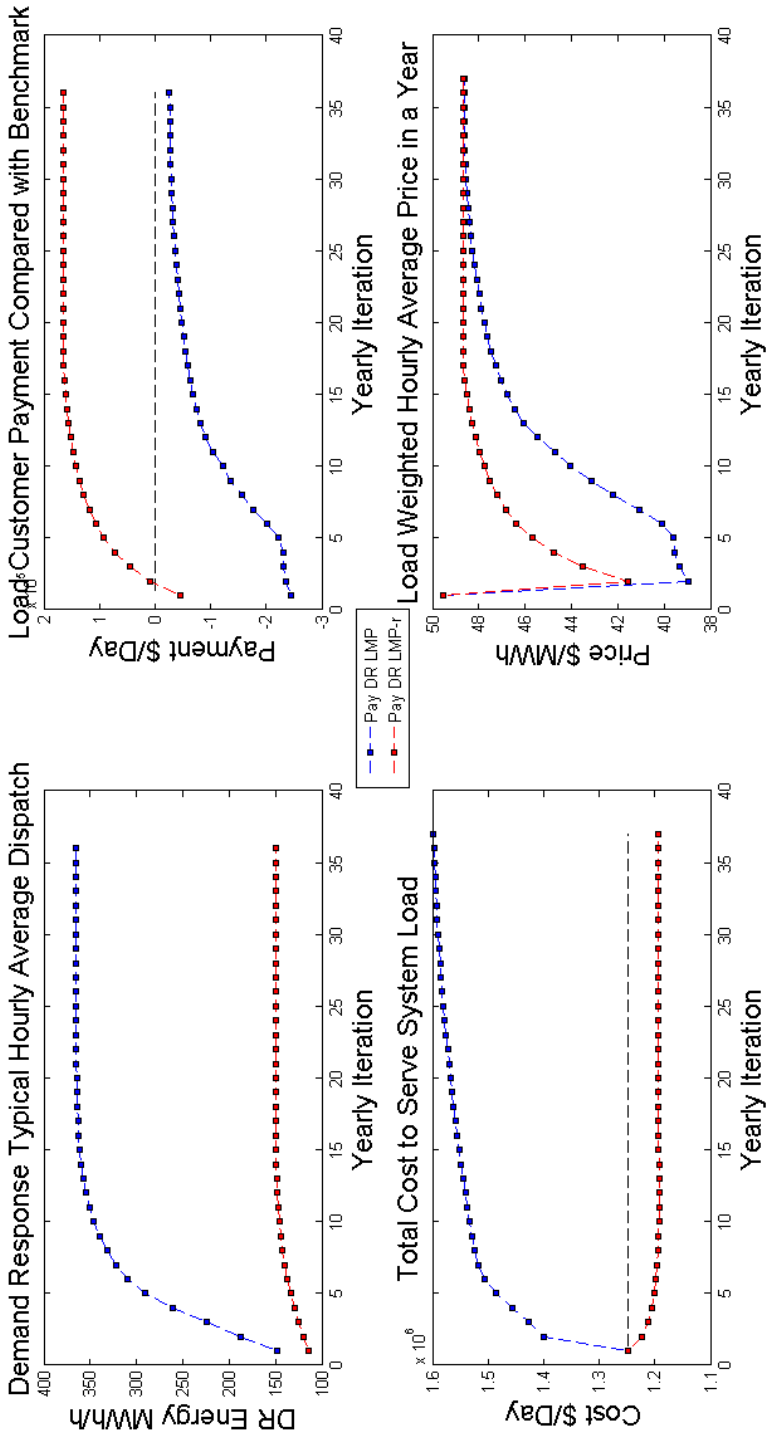

Figure 5.14: Comparison of Simulation Results of Two Cases

5.4 Conclusions

In this chapter, the potential impact of FERC order 745 is analyzed using an agent-based model. The three most outstanding features of FERC order 745 are paying customers full LMP, baseline estimation and net-benefit test. The first two features direct ISO how to pay DR Providers for the load reduction. The third feature states the underlying reason to implement price responsive load program. Without carefully examining the potential effect as caused by this FERC order 745, that may bring unexpected damage and disorder to current power market system.

Both a short-term and long-term study have been conducted in this chapter. The short-term study focuses on the baseline inflation problem, which involves a adverse-selection and moral-hazard issues. The simulation shows current baseline forecast methods can not well capture load customers true consumption level since people may react to the rules and intentionally inflate their baseline estimation. Particularly, load customers appear to bid all capacity at the low load state to get extra payment but withhold capacity at high load state to inflate baseline estimation.

The long-term study inspect the issues brought by double-payment and concept of net-benefit test. The simulation result shows that paying load customers full LMP will force more efficient generation out of the market, leading to a increase of total cost to serve system load. The underlying logic of lowering load customers electricity payment also fails in the long-term. The net-benefit test can not capture the long-term effect caused by retreat of conventional generators.

Both of the two studies suggest that current FERC order 745 may, at least, neglect some important issues that can cause efficiency loss. Paying load customers by LMP-r can induce the right amount of demand response resulting in a better result in terms of both customer payment and total cost. But paying load customers by LMP-r still can not solve the short-term baseline inflation problem. All these suggest that passing dynamic wholesale price to load customers be a better choice to connect wholesale and retail electricity markets.

CHAPTER 6. TEST OF WHOLESALE POWER MARKET BUYERS STRATEGIC BEHAVIOR UNDER DIFFERENT MARKET CLEARING RULES

6.1 Introduction

In this Chapter, focus will be given to wholesale power buyers, LSEs, potential strategic behavior in a two-settlement market. Even though LSE does not serve price-sensitive load customers, it still has incentive to submit price-sensitive bids into day-ahead market. The reason for LSE to submit price-sensitive bids is that if day-ahead price is too expensive, they would rather wait until the real-time market.

Except this natural reason for price-sensitive bids, LSE with monopsony power intentionally bid low into day-ahead market to lower day-ahead price. Borenstein et al. (2008) discussed LSEs strategic behavior during California electricity crisis. During the crisis, LSEs have strong incentive to control their procurement cost. Figure 6.1 illustrates how big LSE exerts market power. LSE is serving a fixed load $Q_f + Q_d$ which is out of control of LSE. If LSE only submits load Q_f into day-ahead market, the cleared day-ahead price P_{da} will be lower than the would-be day-ahead price P_{da}^*. Then LSE's total procurement cost for serving a fixed load $Q_f + Q_d$ will be

$$C = P_{da} \times Q_f + P_{rt} \times Q_d$$

Real-time price P_{rt} is not affected by LSE day-ahead market bidding given fixed load and supply function. Therefore, LSE could lower its total procurement cost C if it bids low in the day-ahead market and lowers clear price P_{da}.

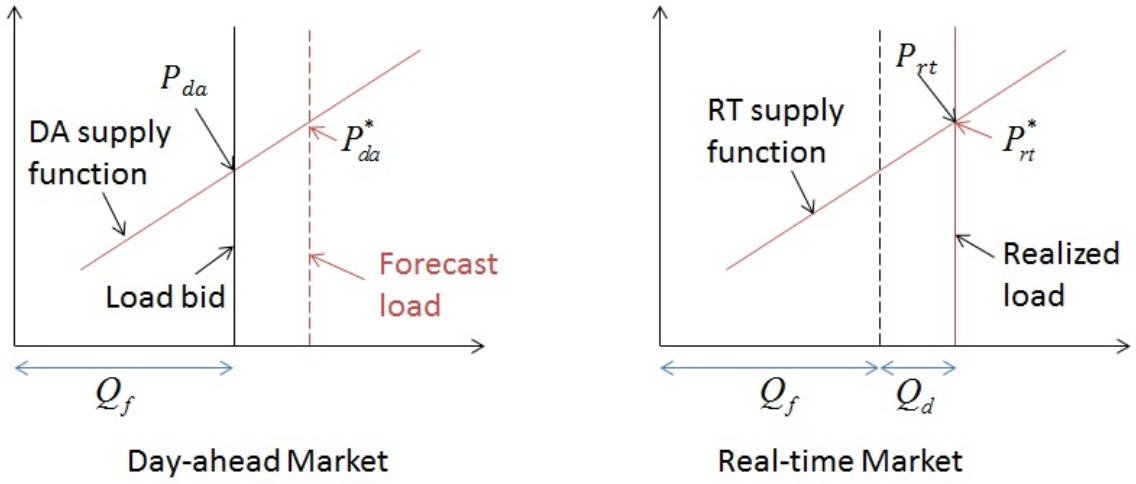

Figure 6.1: LSE Strategic Trading During California Crisis

As discussed in Borenstein et al. (2008), price spread between forward market and spot market is not eliminated by traders' arbitrage behavior. Reasons of power market inefficiency can be attributed to the institutional barriers and traders lack of appropriate information.

Price convergence between day-ahead and real-time market has been given big attention of ISO's market power mitigation department. Figure 6.2 illustrates that the DA-RT price difference concentrates in a a reasonable range. The price difference has a symmetric distribution, different from the low DA price pattern as appeared in California electricity crisis. This chapter tries to reexamine the current two-market structure and investigates its impact on big LSE's strategic behavior.

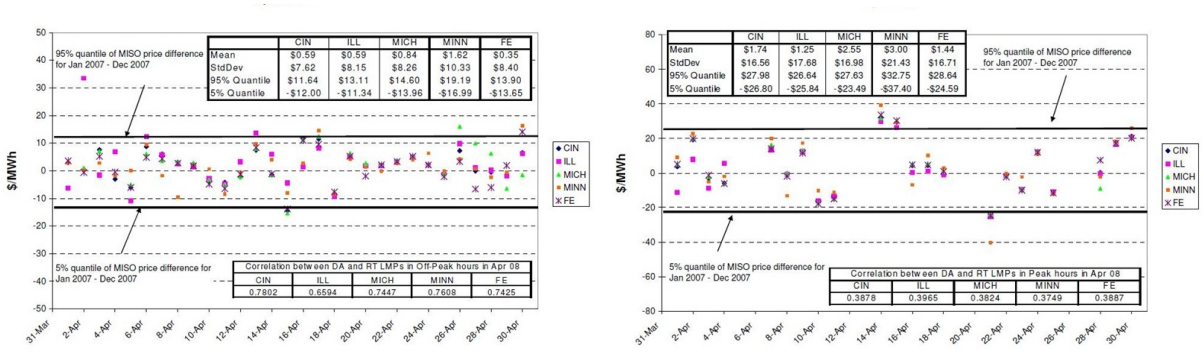

(a) Off-Peak Hours

(b) Peak Hours

Figure 6.2: Hourly DA-RT Price Spread within MISO Footprint

6.2 Two-Settlement and Reliability Commitment

Due to the purpose of this study, it is worthwhile to reexamine the two-settlement system as adopted by most ISOs or RTOs. Day-ahead market is a pure financial market, where LSEs, GenCos, and other traders trade power. Although GenCos are required to keep the supply curve unchanged when it goes to real-time market. There is no such requirement for LSE, leaving LSE large space to change their bidding curve. Day-ahead market plays a hedge function for market participants to avoid exposing to more volatile real-time price.

But the physical resource commitment function is separated from day-ahead market. This commitment decision is taken as an irreversible process because it takes a long time and cost to change the status of a generator unit (hot, warm, stand-by, cold). ISO's main task is to guarantee there are enough resource to meet real-time load. If the demand/supply balance can not keep, the system has risk to collapse. Because the power buyer does not have the obligation to keep system wide reliability. Therefore, ISO runs unit commitment using load forecast of itself, which is known as "reliability assessment commitment" (RAC). Again, this process is a pure physical process and does not generate price signal.

When it goes to operating day, the real-time market has both financial and physical functionality. The market is cleared using current on-line resources (hot, warm units). The available units in the real-time is a subset of that in day-ahead market. So, the price volatility is much

higher than day-ahead market. A summary of this process can be found in Figure 6.3.

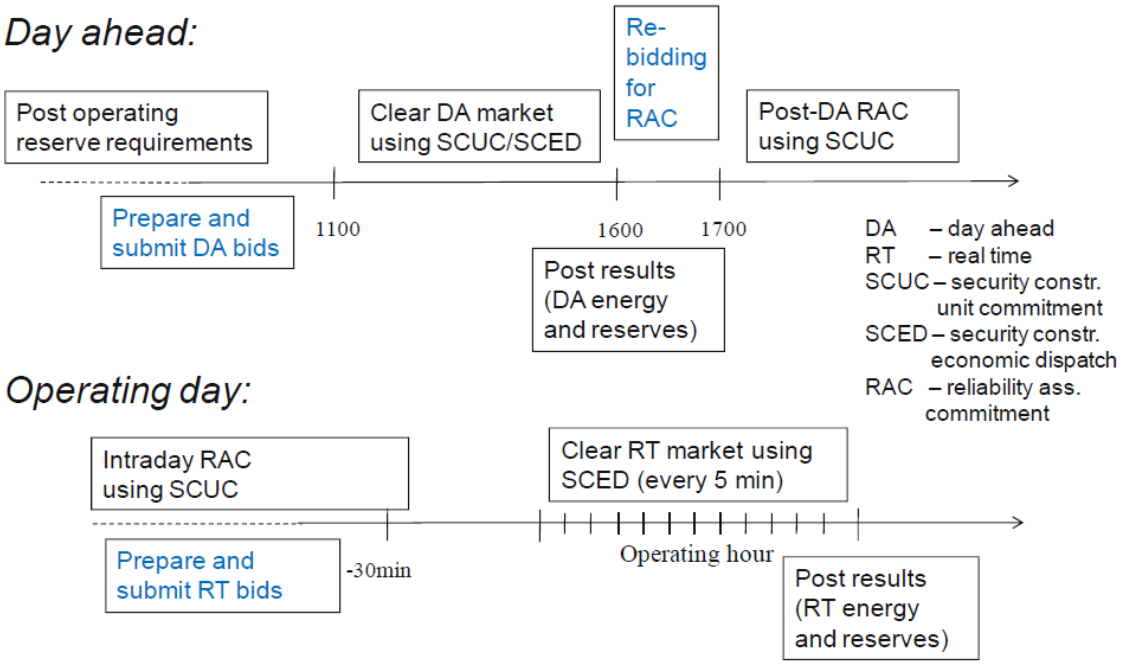

Figure 6.3: Market Operation Line for MISO

In this study, three different market clear rules are compared, as listed in Table 6.1. The "No UC" rule means that ISO does not make unit commitment decisions and will keep all the generators ready to use in the real-time market. The "BUC" rule means bid-based unit commitment. By this name, ISO runs unit commitment using LSE's demand bids. The "RAC" rule means that ISO runs unit commitment using its own load forecast.

Figure 6.4 through 6.6 illustrates how the three rules work. Particularly, for each rule, LSE's bids have different effect on supply curve. Clearly, LSE bids do not affect supply curve since generation resources do not need to be committed. In the Bid-based Unit Commitment case, LSE bids affect both day-ahead and real-time market. LSE will reduce on-line resource if LSE bids low. In the Reliability Assessment Commitment case, LSE bids can only affect day-ahead supply function but has no effect on the real-time supply function. These rule differences give LSE different incentives to exert market power.

Table 6.1: Market Clearing Rules Comparison

	No UC	**BUC**	**RAC**
Functionality	Only Financial Function	Both Financial and Physical Function	Seperate Financial and Physical Function
Effect of LSE Bids on Supply	No Impact	DA and RT Supply Function	Only DA Supply Function
Reliability	No Guarantee	Not Fully Guaranteed	Guaranteed
Load Used to Clear Market	Bid	Bid	Bid for Financial Purpose, Load Forecast for Physical Purpose
Market Performance		To Be Studied	

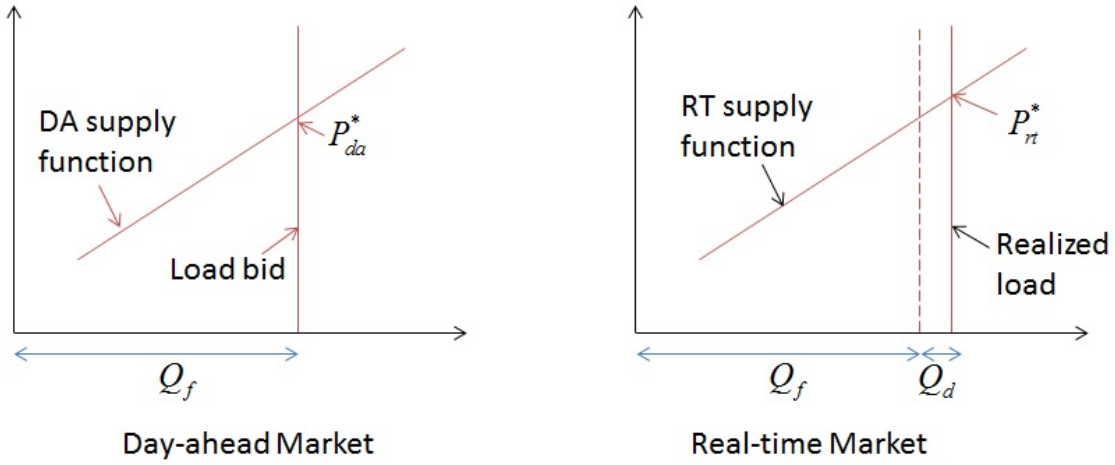

Figure 6.4: No Unit Commitment

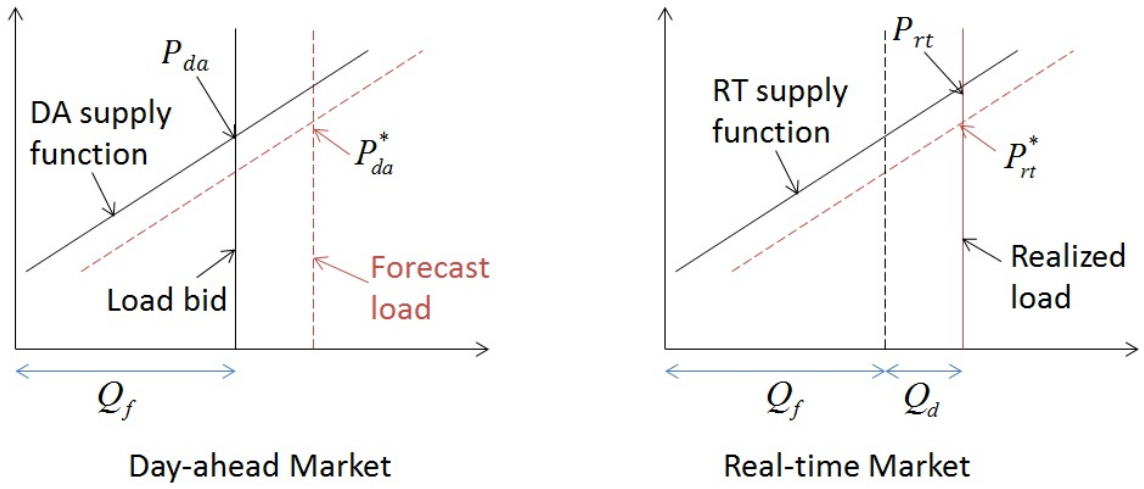

Figure 6.5: Bid-based Unit Commitment

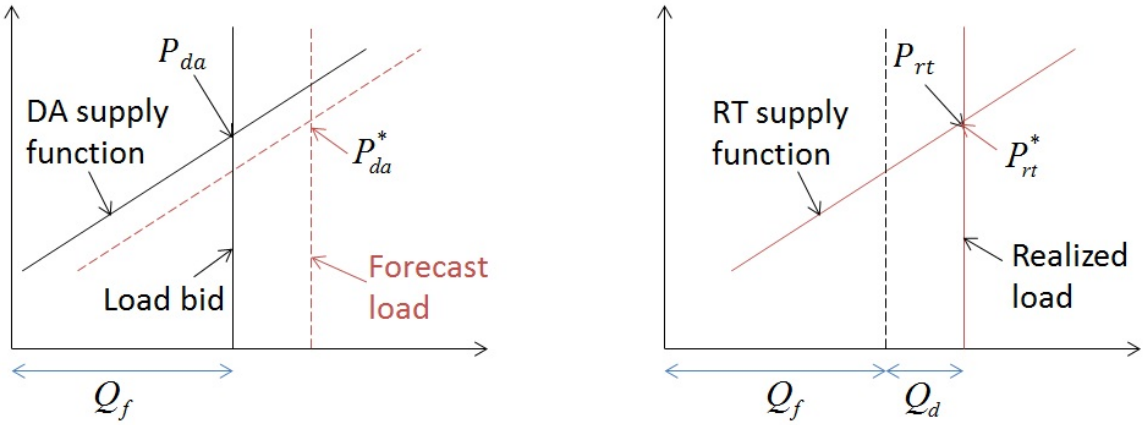

Figure 6.6: Reliability Assessment Commitment

6.3 Experiment Setup

This section talks about the experiment set up and gives tables of parameter values.

6.3.1 Unit Commitment and Implementation

The unit commitment function of the simulation framework is turn on to run this experiment. Day-ahead market is cleared using two steps. The first step solves a mixed-integer optimization problem as shown from equation (6.1) to (6.9). This steps comes out with a (0,1) decisions for each generator to indicate if this generator will be used for next step.

$$\min_{i,t} \sum_t \sum_i z_{it}F_{it} + \sum_t \sum_i g_{it}C_{it} + \sum_t \sum_i y_{it}S_{it} + \sum_t \sum_i x_{it}H_{it} + \sum_t \sum_i d_{it}B_{it} \quad (6.1)$$

subject to:

$$\begin{aligned}
\text{power balance} \quad & \textstyle\sum_i g_{it} = D_t = \sum_i d_{it} \quad \forall t, && (6.2)\\
\text{reserve} \quad & \textstyle\sum_i r_{it} \geq SD_t \quad \forall t, && (6.3)\\
\text{min generation} \quad & g_{it} \geq z_{it}MINi \quad \forall i,t, && (6.4)\\
\text{max generation} \quad & g_{it} + r_{i,t} \leq z_{it}MAXi \quad \forall i,t, && (6.5)\\
\text{ramp rate pos limit} \quad & g_{it} \leq g_{it-1} + MxInc_i \quad \forall i,t, && (6.6)\\
\text{ramp rate neg limit} \quad & g_{it} \geq g_{it-1} - MxDec_i \quad \forall i,t, && (6.7)\\
\text{start if-then-on} \quad & z_{it} \leq z_{it-1} + y_{it} \quad \forall i,t, && (6.8)\\
\text{normal line flow limit} \quad & \textstyle\sum_i r_{it} \geq SD_t \quad \forall k,t, && (6.9)
\end{aligned}$$

The second step solves a DC optimization of power flow problem, as shown from equation (6.10) to (6.16). All the generator k is the committed generator from step 1. In this step, the LMP, power line flow, and power dispatch results are solved.

$$\min_{P_{gk}} \sum_{k \in \{commited\, generator\, buses\}} s_{gk}P_{gk} \quad (6.10)$$

subject to:

$$\begin{aligned}
\text{power injection equation} \quad & \underline{P} = \underline{B}' \cdot \underline{\theta} && (6.11)\\
\text{line flow equation} \quad & \underline{P}_B = (\underline{D} \cdot \underline{A} \cdot \theta), && (6.12)\\
\text{line flow limit} \quad & -\underline{P}_{B,max} \leq \underline{P}_B \leq \underline{P}_{B,max}, && (6.13)\\
\text{generator capacity limit} \quad & 0 \leq P_{gk} \leq P_{gk,max}, \forall k \in \{generatorbuses\} && (6.14)\\
\text{real-time load} \quad & P_{dk} = P_{dk}^{rt}, \forall k \in \{loadbuses\} && (6.15)\\
\text{power injection} \quad & P_k = P_{gk} - P_{dk}, k = 1, \ldots, N && (6.16)
\end{aligned}$$

For the bids-based unit commitment, d_{it} in equation (6.2) uses LSEs demand bids. For the reliability assessment commitment, the day-ahead market commitment is solved using LSEs bids. The real-time market commitment is solved using ISO's load forecast.

6.3.2 Environment and Agents

This study uses a 4 bus, 5 lines, 3 GenCo, 2LSE topology. The parameters of this grid can be found on Figure 6.7. The parameters of GenCos supply function and LSE load profile can be found in Table 6.2.

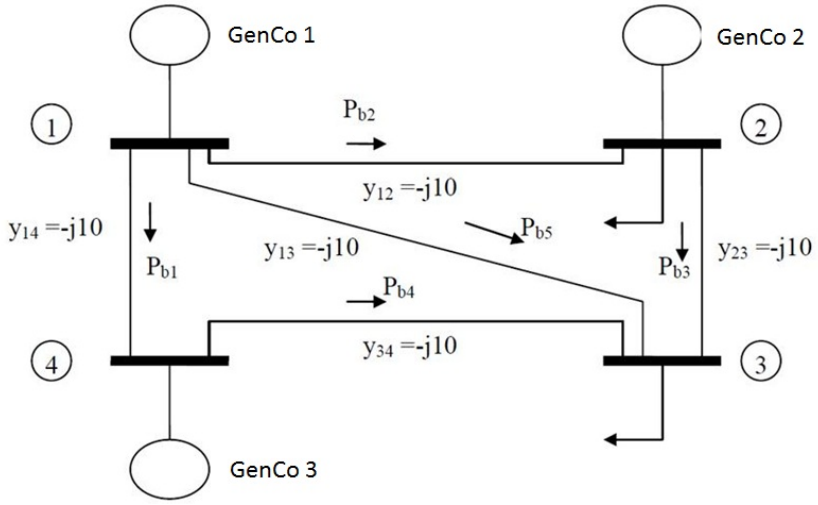

Figure 6.7: Grid Network for Experiments (standard IEEE 4 bus test case)

Table 6.2: Experiment Parameter Settings

	GenCo 1	**GenCo 2**	**GenCo 3**	**LSE 1**	**LSE 2**
GenCo True Capacity					
Lower Capacity Limit	0.5	0.375	0.48		
Upper Capacity Limit	2	1.5	2.2		
LSE True Load				2.6	0.6
GenCo True Cost					
Supply Offer Slope	52	100	80		
Supply Offer Ordinate	1289.6	1211	1289.6		
LSE Strategic Action					
Fixed Load Bid				X	0.6
Load Maximum				2.6	Y
Demand Bid Slope				-50	-100
Demand Bid Ordinate				1300	1400

6.3.3 Fictitious Play

In game theory, fictitious play is a learning rule first introduced by G.W. Brown (1951). In it, each player presumes that her/his opponents are playing stationary (possibly mixed) strategies. At each round, each player thus best responds to the empirical frequency of play of his opponent. Such a method is of course adequate if the opponent indeed uses a stationary strategy, while it is flawed if the opponent's strategy is non stationary. The opponent's strategy may for example be conditioned on the fictitious player's last move.

In this experiment, only LSEs are modeled as intelligent players. Their strategic variables are the demand bids, as shown in red character on Table 6.2.

This experiment employs a sequential fictitious game structure. The game flow is shown on Figure 6.8.

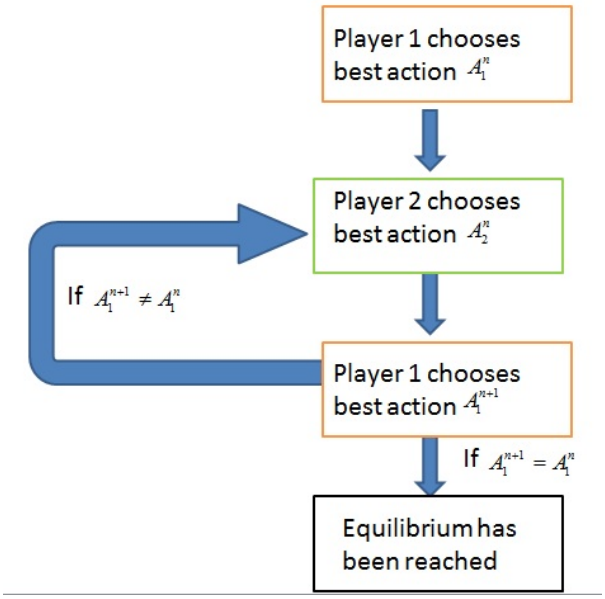

Figure 6.8: Sequential Alternative Strategic Behavior

6.4 Experiment Result

6.4.1 Overview of LSE Procurement Cost

LSE's procurement cost is illustrated on Figure 6.9.

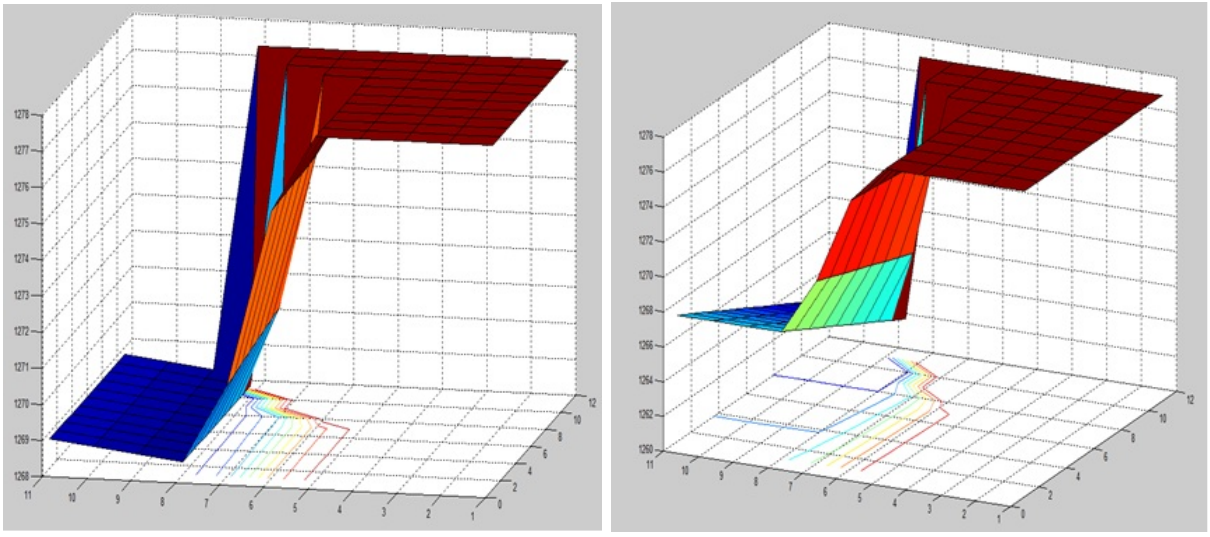

(a) LSE 1 Procurement Cost

(b) LSE 2 Procurement Cost

Figure 6.9: Baseline Estimate with BIP=30

Figure 6.10 shows the simulation result of this fictitious play. Without UC, the LSE 1 bids at a load level at 1.9, lower than the true load of 2.6. LSE 2 bids at 0.7, higher than the true load level of 0.6.

Figure 6.11 illustrates the benefit change of the players along the simulation path. At the new equilibrium, both of the two LSEs are better off in terms of lower procurement cost. But both the two GenCos collect less money from the energy market.

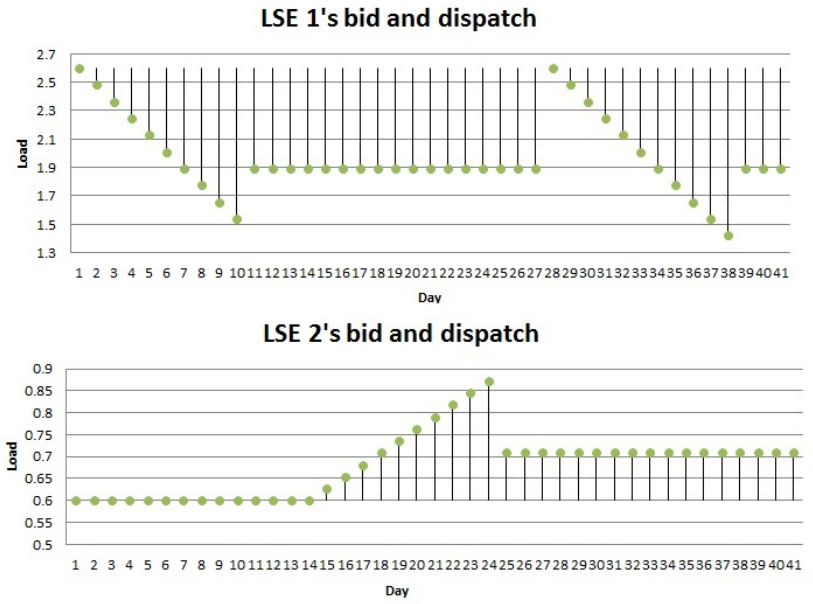

Figure 6.10: LSE Bidding Without Unit Commitment

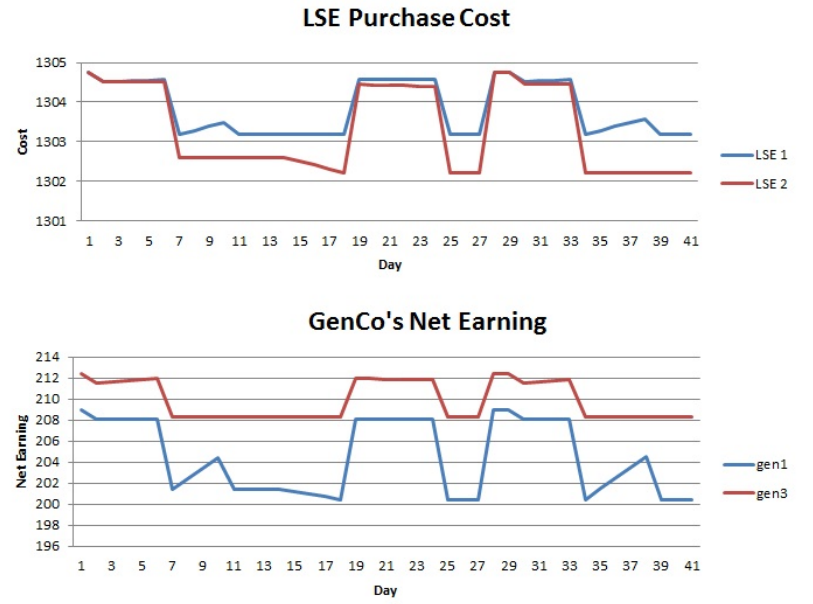

Figure 6.11: Net Earnings without Unit Commitment

Figure 6.10 shows the simulation result of this fictitious play. Without UC, the LSE 1 bids at a load level at 2.5, very close to the true load of 2.6. LSE 2 bids at 0.68, higher than the

true load level of 0.6.

Figure 6.11 illustrates the benefit change of the players along the simulation path. At the new equilibrium, neither LSEs procurement cost or GenCos net earning has big change.

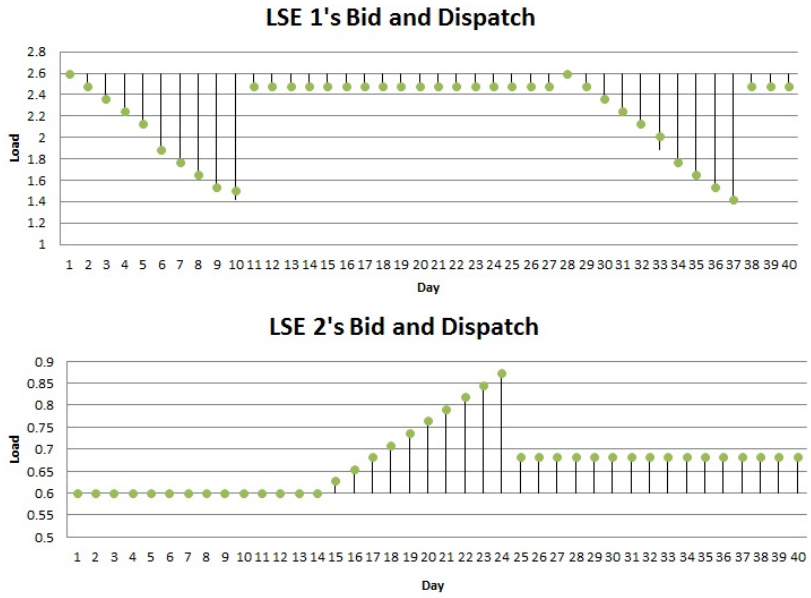

Figure 6.12: LSE Bidding with Bid-Based Unit Commitment

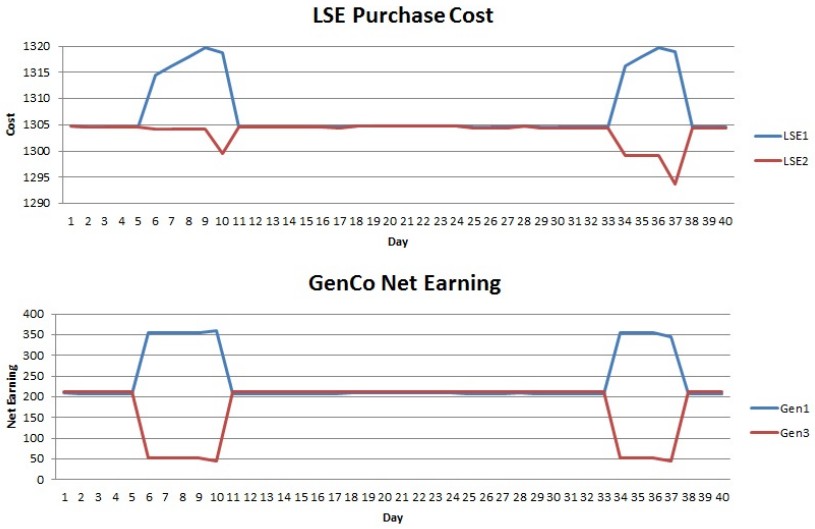

Figure 6.13: Net Earnings with Bid-Based Unit Commitment

Figure 6.10 shows the simulation result of this fictitious play. Without UC, the LSE 1 bids at a load level at 2.25, lower than the true load of 2.6. LSE 2 bids at 0.87, higher than the true load level of 0.6.

Figure 6.11 illustrates the benefit change of the players along the simulation path. At the new equilibrium, neither LSEs procurement cost or GenCos net earning has big change.

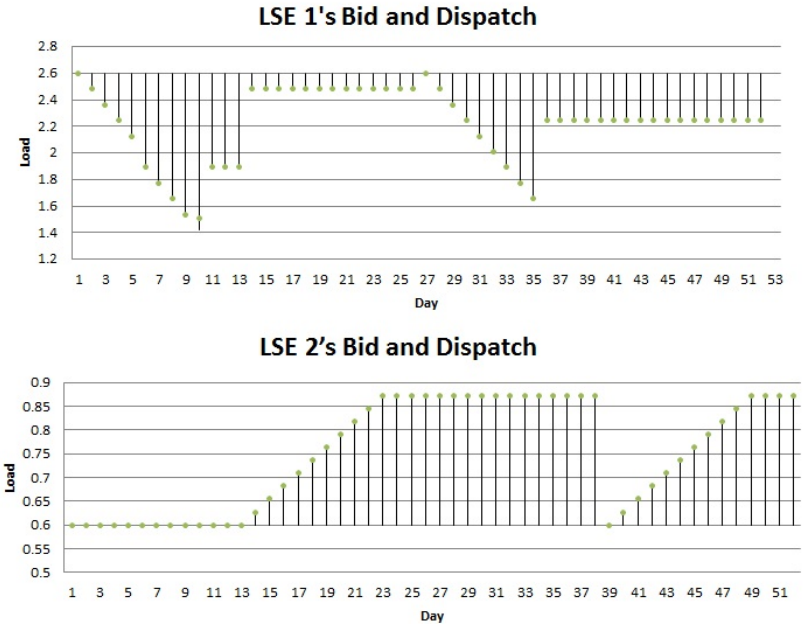

Figure 6.14: LSE Bidding with RAC

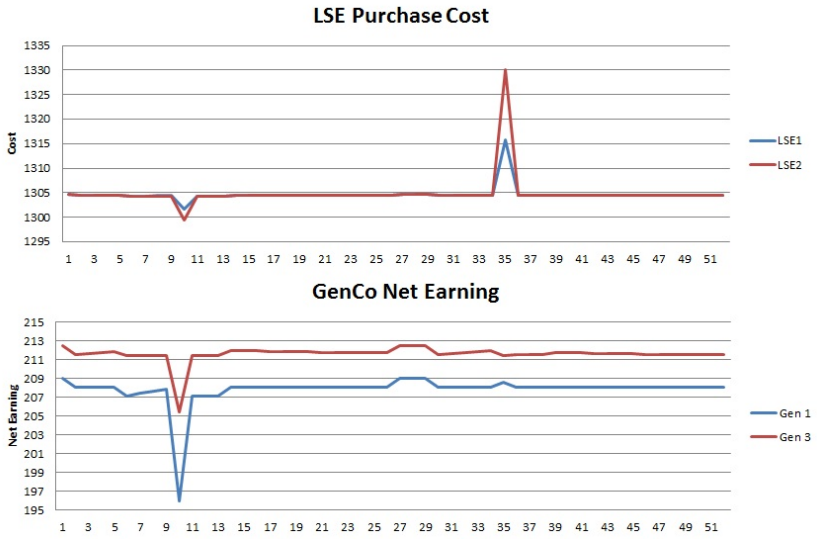

Figure 6.15: Net Earnings with RAC

6.5 Conclusions

In this experiment, three market clear rules are examined in terms of LSE's strategic behavior. The simulation result shows that in the no-UC situation, the LSEs have the strongest incentive to deviate from their true load. The Bids-based commitment does the best in dampening LSEs strategic behavior incentives. This is because LSEs bids affect both the DA and RT supply function. Their load withholding behavior will not reduce price too much. In the reliability assessment commitment case, LSEs have moderate incentives to withhold their load. This is because LSEs strategic behavior is not penalized by the high real-time price.

CHAPTER 7. Conclusions

U.S. restructured wholesale power markets are large-scale systems encompassing physical constraints, administered rules of operation, and strategic human participants. The complexity of these systems makes it difficult to model and study them using standard analytical and statistical tools. To compensate this gap, this study develops and uses an agent-based simulation framework to systematically investigate the performance of these markets through intensive computational experiments.

Using this simulation framework, the study examines many issues of the restructured power market. The main focus of this study is demand response, one of the three top initiatives of FERC. The other two FERC top initiatives are smart grid and renewable energy, both of which are also closely related with demand response. Without smart grid technology, final consumers can not observe or respond to wholesale market operation condition. Demand response, on the other hand, is taken as an important resource to compensate intermittency of renewable energy. Without demand response, the low demand elasticity induces generators to play games in the wholesale market. Without demand response, expensive peaker units are needed to satisfy the less frequent events of spike load. Though saying benefits of demand response, this industry also worries about the uncertainty and volatility brought by demand response. It is dangerous to implement demand response without carefully inspecting potential problems of rules design and market participant's response.

The primary objective of this study is to gain a better understanding of the market performance with incorporating demand response through different approaches. One approach is to pass dynamic wholesale price to the final consumer, either day-ahead price or real-time price. The other approach is to let demand bids into wholesale market and performs like generation resource. This study investigates both of the two approaches and examines the effect

of asymmetric information on market performance.

The main contributions of the dissertation can be summarized as follow:

1. Explanation for observed profit pattern in the beef industry
    - Explanation for different profit patterns of beef industry's two sectors.
    - Support for "Ricardian Rent Pass-Through" assumption.
2. New simulation framework for studying power market
    - DCOPF, and UC algorithm used for wholesale market operation.
    - Two-settlement wholesale market
    - Q-Learning algorithm that can be used by agents
    - Detailed load model that simulates energy generation process
    - New market rules for demand response program
    - Generation capacity investment and evolvement
3. Integrating retail and wholesale power market with dynamic price
    - DA market deviates from RT market without LSE learning
    - DA market converges with RT market with LSE learning
    - LSE achieves maximum profit with learning ability
    - Design of learning consumers that respond to real-time price
    - Price volatility decreases with the number of agents and increases with removing forecast methods
4. Critique of new market rules for demand response
    - The design of baseline induces consumer to strategically behave
    - Baseline estimation method can not eliminate estimation error
    - Under the FERC order, total cost to serve load increases
    - Under the FERC order, load customer payment increases

5. LSE strategic behavior under different market rules

    - LSE has incentive to avoid bidding all load into DA market
    - LSE bids could affect supply curve with UC rules
    - Bid-based UC works best to dampen LSEs strategic behavior

APPENDIX A. Deviation form of X,S and Q

With this deviation form, equation () can be written as

$$\begin{aligned} S^*_{t+\tau} &= (\alpha-\alpha)+(y^*_{t+\tau}-\overline{y})-\gamma[(q^*_{t+\tau}-\overline{q})+(m^*_{t+\tau-1}-\overline{m})] \\ &= u^{y*}_{t+\tau+1}-\gamma[Q^*_{t+\tau}(1+r)+u^{m*}_{t+\tau+1}] \end{aligned}$$

The deviation form of () is $Q^*_{t+\tau}=\beta^\tau Q_t+\sum_{i=1}^{\tau}\beta^\tau u^{h*}_{t+\tau-i}$. Substitute this into the equation above, we can get:

$$S^*_{t+\tau}=u^{y*}_{t+\tau+1}-\gamma[(\beta^\tau Q_t+\sum_{i=1}^{\tau}\beta^\tau u^{h*}_{t+\tau-i})(1+r)+u^{m*}_{t+\tau+1}] \tag{A.1}$$

Also rewrite the inter-temporal budget constraint () in deviation form: $X_t=\sum_{\tau=0}^{\infty}S^*_{t+_t}/(1+g)^{\tau+1}$. Then substitute equation (A.1) into this budget constraint, which implies:

$$\begin{aligned} X_t &= -\frac{\gamma(1+r)}{1+g-\beta}Q_t+\sum_{\tau=0}^{\infty}v^*_{t+\tau}/(1+g)^{\tau+1} \qquad (A.2)\\ \text{where} v^*_{t+\tau} &= u^{y*}_{t+\tau+1}-\gamma u^{m*}_{t+\tau+1}-\frac{(1+r)\gamma\beta u^*_{t+\tau}}{1+g-\beta} \end{aligned}$$

From this, we can solve for Q_t in terms of X_t and u^{i*}_t:

$$Q_t=\frac{1+g-\beta}{\gamma(1+r)}[-X_t+\sum_{\tau=0}^{\infty}v^*_{t+\tau}/(1+g)^{\tau+1}] \tag{A.3}$$

Then insert equation (A.3) into the deviation form of equation(2.13), we can express S_t in terms of X_t and u^{i*}_t:

$$\begin{aligned} S_t &= u^{y*}_{t+1}-\gamma Q_t(1+r)-\gamma u^{m*}_{t+1} \qquad (A.4)\\ &= (1+g-\beta)X_t-(1+g-\beta)\sum_{\tau=0}^{\infty}v^*_{t+\tau}/(1+g)^{\tau+1}+u^{y*}_{t+1}-\gamma u^{m*}_{t+1} \end{aligned}$$

Finally, substitute equation () into the deviation form of equation (), we can get the cattle stock's path:

$$\begin{aligned} X_{t+1} &= (1+g)X_t - S_t \\ &= \beta X_t + (1+g-\beta)\sum_{\tau=0}^{\infty} v^*_{t+\tau}/(1+g)^{\tau+1} - u^{y*}_{t+1} + \gamma u^{m*}_{t+1} \end{aligned} \tag{A.5}$$

APPENDIX B. Reduced Form of X, S, and Q

This appendex is used to show the derivation of X, S, and Q.

$$
\begin{aligned}
X_t &= \sum_{\tau=0}^{\infty}(u_{t+\tau+1}^{y*} - \gamma[(\beta^{\tau}Q_t + \sum_{i=1}^{\tau}\beta^{\tau}u_{t+\tau-i}^{h*})(1+r) + u_{t+\tau+1}^{m*}])/(1+g)^{\tau+1} \\
&= -\sum_{\tau=0}^{\infty}(\frac{\beta}{1+g})^{\tau}\frac{\gamma(1+r)}{1+g}Q_t + \sum_{\tau=0}^{\infty}(u_{t+\tau+1}^{y*} - \gamma u_{t+\tau+1}^{m*} - \frac{(1+r)\gamma\beta u_{t+\tau}^{*}}{1+g-\beta})/(1+g)^{\tau+1} \\
&= -\frac{1}{1-\frac{\beta}{1+g}}\frac{\gamma(1+r)}{1+g}Q_t + \sum_{\tau=0}^{\infty}v_{t+\tau}^{*}/(1+g)^{\tau+1} \\
&= -\frac{\gamma(1+r)}{1+g-\beta}Q_t + \sum_{\tau=0}^{\infty}v_{t+\tau}^{*}/(1+g)^{\tau+1} \\
\text{where } v_{t+\tau}^{*} &= u_{t+\tau+1}^{y*} - \gamma u_{t+\tau+1}^{m*} - \frac{(1+r)\gamma\beta u_{t+\tau}^{*}}{1+g-\beta}
\end{aligned}
\tag{B.1}
$$

$$
\begin{aligned}
Q_t &= \frac{1+g-\beta}{\gamma(1+r)}[-X_t + \sum_{\tau=0}^{\infty}(u_{t+\tau+1}^{y*} - \gamma u_{t+\tau+1}^{m*} - \frac{(1+r)\gamma\beta u_{t+\tau}^{h*}}{1+g-\beta})/(1+g)^{\tau+1}] \\
&= \frac{1+g-\beta}{\gamma(1+r)}[-X_t + \sum_{\tau=0}^{\infty}(\frac{\rho_y}{1+g})^{\tau+1}u_t^y - \gamma\sum_{\tau=0}^{\infty}(\frac{\rho_m}{1+g})^{\tau+1}u_t^m] - \frac{\beta}{\rho_h}\sum_{\tau=0}^{\infty}(\frac{\rho_h}{1+g})^{\tau+1}u_t^h \\
&= \frac{1+g-\beta}{\gamma(1+r)}[-X_t + \frac{1}{1-\frac{\rho_y}{1+g}}\frac{\rho_y}{1+g}u_t^y - \gamma\frac{1}{1-\frac{\rho_m}{1+g}}\frac{\rho_m}{1+g}u_t^m] - \\
&\quad \frac{\beta}{\rho_h}\frac{1}{1-\frac{\rho_h}{1+g}}\frac{\rho_h}{1+g}u_t^h \\
&= \frac{1+g-\beta}{\gamma(1+r)}[-X_t + \frac{\rho_y}{1+g-\rho_y}u_t^y - \frac{\gamma\rho_m}{1+g-\rho_m}u_t^m] - \frac{\beta}{1+g-\rho_h}u_t^h
\end{aligned}
\tag{B.2}
$$

$$
\begin{aligned}
S_t &= \rho_y u_t^y - \gamma(1+r)\frac{1+g-\beta}{\gamma(1+r)}[-X_t + \frac{\rho_y}{1+g-\rho_y}u_t^y - \frac{\gamma\rho_m}{1+g-\rho_m}u_t^m] \qquad \text{(B.3)}\\
&\quad +\gamma(1+r)\frac{\beta}{1+g-\rho_h}u_t^h - \gamma\rho_m u_t^m\\
&= (1+g-\beta)X_t + \frac{\rho_y(1+g-\rho_y)-\rho_y(1+g-\beta)}{1+g-\rho_y}u_t^y -\\
&\quad \gamma\frac{\rho_m(1+g-\rho_m)-\rho_m(1+g-\beta)}{1+g-\rho_m}u_t^m + \frac{\beta\gamma(1+r)}{1+g-\rho_h}u_t^h\\
&= (1+g-\beta)X_t + \frac{\rho_y(\beta-\rho_y)}{1+g-\rho_y}u_t^y - \gamma\frac{\rho_m(\beta-\rho_m)}{1+g-\rho_m}u_t^m + \frac{\beta\gamma(1+r)}{1+g-\rho_h}u_t^h
\end{aligned}
$$

$$
\begin{aligned}
X_{t+1} &= (1+g)X_t - [(1+g-\beta)X_t + \frac{\rho_y(\beta-\rho_y)}{1+g-\rho_y}u_t^y - \gamma\frac{\rho_m(\beta-\rho_m)}{1+g-\rho_m}u_t^m \qquad \text{(B.4)}\\
&\quad +\frac{\beta\gamma(1+r)}{1+g-\rho_h}u_t^h]\\
&= \beta X_t - \frac{\rho_y(\beta-\rho_y)}{1+g-\rho_y}u_t^y + \gamma\frac{\rho_m(\beta-\rho_m)}{1+g-\rho_m}u_t^m - \frac{\beta\gamma(1+r)}{1+g-\rho_h}u_t^h
\end{aligned}
$$

APPENDIX C. Reduced Recursive Form of Cow-Calf Return

In this appendex, a clear form of cow-calf return's recursive form will be derived.

First, from equation(),we can solve for X_t:

$$X_t = -\frac{\gamma(1+r)}{1+g-\beta}R_t^r - \frac{\gamma(1+r)}{1+g-\beta}\frac{1+g+\beta-\rho_h}{1+g-\rho_h}u_t^h + \frac{\rho_y}{1+g-\rho_y}u_t^y - \frac{\gamma\rho_m}{1+g-\rho_m}u_t^m$$

Then forward cow-calf operator's return () for one period as follow:

$$\begin{aligned} R_{t+1}^r &= \frac{1+g-\beta}{\gamma(1+r)}[-X_{t+1} + \frac{\rho_y}{1+g-\rho_y}u_{t+1}^y - \frac{\gamma\rho_m}{1+g-\rho_m}u_{t+1}^m] \\ &\quad -\frac{(1+g+\beta-\rho_h)}{1+g-\rho_h}u_{t+1}^h \\ &= \frac{1+g-\beta}{\gamma(1+r)}[-X_{t+1} + \frac{\rho_y}{1+g-\rho_y}(\rho_y u_t^y + \varepsilon_{t+1}^y) \\ &\quad -\frac{\gamma\rho_m}{1+g-\rho_m}(\rho_m u_t^m + \varepsilon_{t+1}^m)] - \frac{(1+g+\beta-\rho_h)}{1+g-\rho_h}(\rho_h u_t^h + \varepsilon_{t+1}^h) \\ &= \frac{1+g-\beta}{\gamma(1+r)}[-X_{t+1} + \frac{\rho_y^2}{1+g-\rho_y}u_{t+1}^y - \frac{\gamma\rho_m^2}{1+g-\rho_m}u_{t+1}^m] - \\ &\quad \frac{(1+g+\beta-\rho_h)\rho_h}{1+g-\rho_h}u_{t+1}^h + \Psi_{t+1} \\ \text{where } \Psi_{t+1} &= \frac{1+g-\beta}{\gamma(1+r)}[\frac{\rho_y}{1+g-\rho_y}\varepsilon_{t+1}^y - \frac{\gamma\rho_m}{1+g-\rho_m}\varepsilon_{t+1}^m] \\ &\quad -\frac{(1+g+\beta-\rho_h)}{1+g-\rho_h}\varepsilon_{t+1}^h \end{aligned} \tag{C.1}$$

Then substitute equation () into equation (), the returns for cow-calf operators can be

recursively expressed as:

$$
\begin{aligned}
R^r_{t+1} &= \frac{1+g-\beta}{\gamma(1+r)}[-\beta X_t + \frac{\rho_y(\beta-\rho_y)}{1+g-\rho_y}u^y_t - \gamma\frac{\rho_m(\beta-\rho_m)}{1+g-\rho_m}u^m_t + \frac{\beta\gamma(1+r)}{1+g-\rho_h}u^h_t \\
&\quad + \frac{\rho^2_y}{1+g-\rho_y}u^y_t - \frac{\gamma\rho^2_m}{1+g-\rho_m}u^m_t] - \frac{(1+g+\beta-\rho_h)\rho_h}{1+g-\rho_h}u^h_t + \Psi_{t+1} \\
&= \frac{1+g-\beta}{\gamma(1+r)}[-\beta X_t + \frac{\rho_y\beta}{1+g-\rho_y}u^y_t - \frac{\gamma\rho_m\beta}{1+g-\rho_m}u^m_t] + \\
&\quad \frac{\beta(1+g-\beta)-(1+g+\beta-\rho_h)\rho_h}{1+g-\rho_h}u^h_t + \Psi_{t+1} \\
&= \frac{1+g-\beta}{\gamma(1+r)}[-\beta(-\frac{\gamma(1+r)}{1+g-\beta}R^r_t - \frac{\gamma(1+r)}{1+g-\beta}\frac{1+g+\beta-\rho_h}{1+g-\rho_h}u^h_t + \\
&\quad \frac{\rho_y}{1+g-\rho_y}u^y_t - \frac{\gamma\rho_m}{1+g-\rho_m}u^m_t) \\
&\quad + \frac{\rho_y\beta}{1+g-\rho_y}u^y_t - \frac{\gamma\rho_m\beta}{1+g-\rho_m}u^m_t] + \\
&\quad \frac{\beta(1+g-\beta)-(1+g+\beta-\rho_h)\rho_h}{1+g-\rho_h}u^h_t + \Psi_{t+1} \\
&= \beta R^r_t + (\frac{(1+g+\beta-\rho_h)}{(1+g-\rho_h)}(\beta-\rho_h) + \frac{\beta(1+g-\beta)}{1+g-\rho_h})u^h_t + \Psi_{t+1}
\end{aligned}
\tag{C.2}
$$

In sum, the recursive form for R^r_t can be written as

$$
\begin{aligned}
R^r_{t+1} &= \beta R^r_t + \lambda u^h_t + \Psi_{t+1} \\
\text{where } \lambda &= \frac{(1+g+\beta-\rho_h)}{(1+g-\rho_h)}(\beta-\rho_h) + \frac{\beta(1+g-\beta)}{1+g-\rho_h}
\end{aligned}
\tag{C.3}
$$

APPENDIX D. Counterpart in Rosen (1994)

The counterpart of equation () in Rosen (1994) is summarized as:

$$\begin{aligned}
Q_t &= \frac{1+g-\beta}{\gamma}[-X_t + \sum_{\tau=0}^{\infty} v^*_{t+\tau}/(1+g)^{\tau+1}] \\
S_t &= (1+g-\beta)[X_t - \sum_{\tau=0}^{\infty} v^*_{t+\tau}/(1+g)^{\tau+1}] + u^y_t - \gamma u^m_t \\
X_{t+1} &= \beta X_t + (1+g-\beta)\sum_{\tau=0}^{\infty} v^*_{t+\tau}/(1+g)^{\tau+1} - u^y_t + \gamma u^m_t \\
where\ v^*_{t+\tau} &= u^{y*}_{t+\tau} - \gamma u^{m*}_{t+\tau} - \frac{\gamma\beta u^*_{t+\tau}}{1+g-\beta}
\end{aligned}$$

The counterpart of equations (2.22)-(2.24) in Rosen (1987) is summarized as:

$$\begin{aligned}
Q_t &= \frac{1+g-\beta}{\gamma}[-X_t + \frac{u^y_t}{1+g-\rho_y} - \frac{\gamma u^m_t}{1+g-\rho_m}] - \frac{\beta u^h_t}{1+g-\rho_h} \\
S_t &= (1+g-\beta)X_t + \frac{(\beta-\rho_y)}{1+g-\rho_y}u^y_t - \gamma\frac{(\beta-\rho_m)}{1+g-\rho_m}u^m_t + \frac{\beta\gamma}{1+g-\rho_h}u^h_t \\
X_{t+1} &= \beta X_t - \frac{\beta-\rho_y}{1+g-\rho_y}u^y_t + \gamma\frac{\beta-\rho_m}{1+g-\rho_m}u^m_t - \frac{\beta\gamma}{1+g-\rho_h}u^h_t
\end{aligned}$$

Bibliography

(2009). Ercot launches financial settlement process for smart meters.

(2009). Report to the 81st texas legislature. scope of competition in electric markets in texas.

(2011). Ames wholesale power market test bed homepage. www.econ.iastate.edu/tesfatsi/amesmarkethome.html.

(2011). Gridlab-d, power distribution simulation software. www.gridlabd.org.

Aadland, D. (2004). Cattle cycles, heterogeneous expectations and the age distribution of capital. *Journal of Economic Dynamics and Control*, 28:1977–2002.

Aadland, D. (2005). The economics of cattle supply. Utah State University, Department of Economics, Working Papers: 2000-11.

Aadland, D. and BAILEY, B. (2001). Short-run supply responses in the u.s. beef-cattle industry. *American Journal of Agricultural Economics*, 83:826–839.

Baak, S. (1999). Tests for bounded rationality with a linear dynamic model distorted by heterogeneous expectations. *Journal of Economic Dynamics and Control*, 23:1517–43.

Berger, U. (2007). Browns original fictitious play. *Journal of Economic Theory*, 135.

Borenstein, S. (2006). Customer risk from real-time retail electricity pricing: Bill volatility and hedgability. NBER Working Paper No. 12524.

Borenstein, S. and Bushnell, J. (2000). Electricity restructuring: Deregulation or reregulation? *Regulation*, 23.

Borenstein, S., Bushnell, J., K. C., and Wolfram, C. (2008). Inefficiencies and market power in financial arbitrage: A study of californias electricity markets. *The Journal Of Industrial Economics*, LVI:0022–1821.

Borenstein, S. and Holland, S. (2005). On the efficiency of competitive electricity markets with time-invariant retail prices. *Rand Journal of Economics*, 36.

Borenstein, S., Jaske, M., and Rosenfeld, A. (2002). An equilibrium model of investment in restructured electricity marketsdynamic pricing, advanced metering and demand response in electricity markets. Center for the Study of Energy Markets Working Paper 105.

Botterud, A. and Wang, J. (2010). Wind power forecasting and electricity market operations. In *Proc. IEEE PES Gen. Meet.*

Brennan, T., Palmer, K., and Martinez, S. (2001). Implementing electricity restructuring: Policies, potholes, and prospects. Discussion Paper 01-62, Resources for the Future.

Brown, G. (1951). *Iterative Solutions of Games by Fictitious Play.* New York: Wiley.

Bushnell, J., Harvey, S. M., Hobbs, B., and Stoft, S. (2011). Opinion on economic issues raised by ferc order 745, demand response compensation in organized wholesale energy markets. Market Surveillance Committee of the California ISO.

Bushnell, J., Hobbs, B., and Wolak, F. A. (2009). When it comes to demand response, is ferc its own worst enemy? *The Electricity Journal*, 22:9–18.

Bushnell, J. and Ishii, J. (2007). An equilibrium model of investment in restructured electricity markets. Center for the Study of Energy Markets Working Paper 164.

Centolella, P. (2010). The integration of price responsive demand into regional transmission organization (rto) wholesale power markets and system operations. *Energy*, 35.

Chavas, J.-P. (2000). On information and market dynamics: The case of the us beef market. *Journal of Economic Dynamics and Control*, 24:833–853.

Du, X., Henness, D. A., and Edwards, W. (2007). Determinants of iowa cropland cash rental rates: Testing ricardian rent theory. Department of Economics, Iowa State University, Working paper. 07-WP 454.

Federal Energy Regulatory Commission (2003). White paper on bulk power market design, Docket No. RM01-12-000.

Foster, K. and Burt, O. (1992). A dynamic model of investment in the us beef-cycle indunstry. *Journal of Business and Economics Statistics*, 10:419–26.

Jarvis, L. (1974). Cattle as capital goods and ranchers as portfolio managers: An application to the argentine cattle sector. *The Journal of Political Economy*, 82:489–520.

Joskow, P. and Tirole, J. (2006). Retail electricity competition. *Rand Journal of Economics*, 37.

Joskow, P. L. (2006). Competitive electricity markets and investment in new generating capacity. AEI-Brookings Joint Center Working Paper No. 06-14, available at `http://ssrn.com/abstract=902005`.

KEMA (2011). Ferc 745 baseline analysis. KEMA Consulting Group Report.

Kiesling, L. and Kleit, A. (2009). *Electricity Restructuring: The Texas Story.* American Enterprise Institute Press.

Kirwan, B. The incidence of u.s. agricultural subsidies on farmland rental rates.

Lally, J. (2002). Financial transmission rights: Auction example in financial transmission rights draft. (01-10-02), ISO New England, Inc., section 6.

LeBaron, B., Arthur, W., and Palmer, R. (1999). Time series properties of an artificial stock market. *Journal of Economic Dynamics and Control*, 23:1487–1516.

Lehtinen, A. and Kuorikoski, J. (2007). Computing the perfect model: Why do economists shun simulation? *Philosophy of Science*, 74:304–329.

Li, H. (2009). Dynamic performance of restructured wholesale power markets with learning generation companies: an agent-based test bed study. Dissertation, Department of Electric and Computer Engineering, Iowa State University.

Li, H. and Tesfatsion, L. (2009). The ames wholesale power market test bed: A computational laboratory for research, teaching, and training. IEEE Proceedings, Power and Energy Society General Meeting, Calgary, Canada.

Li, H. and Tesfatsion, L. (2009a). Iso net surplus extraction in restructured wholesale power markets. ISU Economics Working Paper No. 09015.

Macal, C. M. and M.J., N. (2010). Tutorial on agent-based modelling and simulation. *Journal of Simulation*, 4:151–162.

Ricardo, D. (1821). *On the Principles of Political Economy and Taxation (3rd. ed).* Cambridge: Cambridge University Press.

Roozbehani, M., Dahleh, M., and Mitter, S. (2011). Volatility of power grids under real-time pricing. IEEE Transactions on Power Systems, Submitted.

Rosen, S. (1994). Dynamic animal economics. *American Journal of Agricultural Economics*, 69:547–557.

Rosen, S., Murphy, K., and Scheinkman, J. (1994). Cattle cycles. *The Journal of Political Economy*, 102:468–492.

Rucker, R., Burt, O., and LaFrance, J. (1984). An econometric model of cattle inventories. *American Journal of Agricultural Economics*, 66:131–144.

Schelling, T. C. (1971). Dynamic models of segregation. *Journal of Mathematical Sociology*, 1:143–186.

Watkins, C. (1989). Learning from delayed rewards. Dissertation, Department of Computer Science, University of Cambridge, England.

Weidlich, A. and Veit, D. (2008). A critical survey of agent-based wholesale electricity market models. *Energy Economics*, 30:1728–1759.

Yu, N.-P. (2007). Modeling of suppliers learning behaviors in an electricity market environmen. Thesis, Department of Electrical Engineering.

Zhou, Z., Chan, W. K., and Chow, J. H. (2007). Agent-based simulation of electricity markets: A survey of tools. *Artificial Intelligence Review*, 28:305–342.